JEDEC STANDARD

Measurement and Reporting of Alpha Particle and Terrestrial Cosmic Ray-Induced Soft Errors in Semiconductor Devices

JESD89B

(Revision of JESD89A, October 2006)

SEPTEMBER 2021

JEDEC SOLID STATE TECHNOLOGY ASSOCIATION

NOTICE

JEDEC standards and publications contain material that has been prepared, reviewed, and approved through the JEDEC Board of Directors level and subsequently reviewed and approved by the JEDEC legal counsel.

JEDEC standards and publications are designed to serve the public interest through eliminating misunderstandings between manufacturers and purchasers, facilitating interchangeability and improvement of products, and assisting the purchaser in selecting and obtaining with minimum delay the proper product for use by those other than JEDEC members, whether the standard is to be used either domestically or internationally.

JEDEC standards and publications are adopted without regard to whether or not their adoption may involve patents or articles, materials, or processes. By such action JEDEC does not assume any liability to any patent owner, nor does it assume any obligation whatever to parties adopting the JEDEC standards or publications.

The information included in JEDEC standards and publications represents a sound approach to product specification and application, principally from the solid state device manufacturer viewpoint. Within the JEDEC organization there are procedures whereby a JEDEC standard or publication may be further processed and ultimately become an ANSI standard.

No claims to be in conformance with this standard may be made unless all requirements stated in the standard are met.

Inquiries, comments, and suggestions relative to the content of this JEDEC standard or publication should be addressed to JEDEC at the address below, or refer to www.jedec.org under Standards and Documents for alternative contact information.

Published by
©JEDEC Solid State Technology Association 2021
3103 North 10th Street
Suite 240 South
Arlington, VA 22201-2108

PRICE: Contact JEDEC

Printed in the U.S.A.

MEASUREMENT AND REPORTING OF ALPHA PARTICLE AND TERRESTRIAL COSMIC RAY INDUCED SOFT ERRORS IN SEMICONDUCTOR DEVICES

CONTENTS

MEASUREMENT AND REPORTING OF ALPHA PARTICLE AND TERRESTRIAL COSMIC RAY INDUCED SOFT ERRORS IN SEMICONDUCTOR DEVICES

CONTENTS (cont'd)

Annexes

Foreword

This standard defines the requirements and procedures for terrestrial soft error rate (SER) testing of integrated circuits and reporting of results. Both real-time (unaccelerated) and accelerated testing procedures are described. At terrestrial, Earth-based altitudes, the predominant sources of radiation include both cosmic-ray radiation, dominated by high- and low-energy neutron-induced reactions, and alpha-particle radiation from radioisotopic impurities in the package and chip materials. Other high energy particles, such as muons, are generated by cosmic rays and reach terrestrial altitudes. They are not considered in this standard at this point in time since there have been no significant soft error muon induced cross sections reported. An overall assessment of a device's SER is complete, ***only*** when an unaccelerated test is done under actual use conditions, ***or*** accelerated SER data for the alpha-particle component, the high-energy cosmic-radiation component, and if necessary, the thermal neutron component (see **7** for details) has been obtained and extrapolated to the use conditions.

Annexes D, E, F, G, H and J are informative; annexes A, B and C are normative.

Introduction

Soft errors are nondestructive functional errors induced by energetic particle strikes. Soft errors are a subset of single event effects (SEE), and include single-event upsets (SEU), single-bit upsets (SBU),multiple-bit upsets (MBU), single-event functional interrupts (SEFI), single-event transients (SET) that, if latched, become SEU, and single-event latchup (SEL) where the formation of parasitic bipolar action in CMOS wells induce a low-impedance path between power and ground, producing a localized high current condition (SEL can also cause latent and hard errors) if a thermal runaway condition is created). While there is variation on the exact use of these terms in the literature, Figure 1 shows how they are defined in this document (see **2** – Terms and definitions. For the components tested, all applicable SEE rates due to the different radiation types should be characterized.

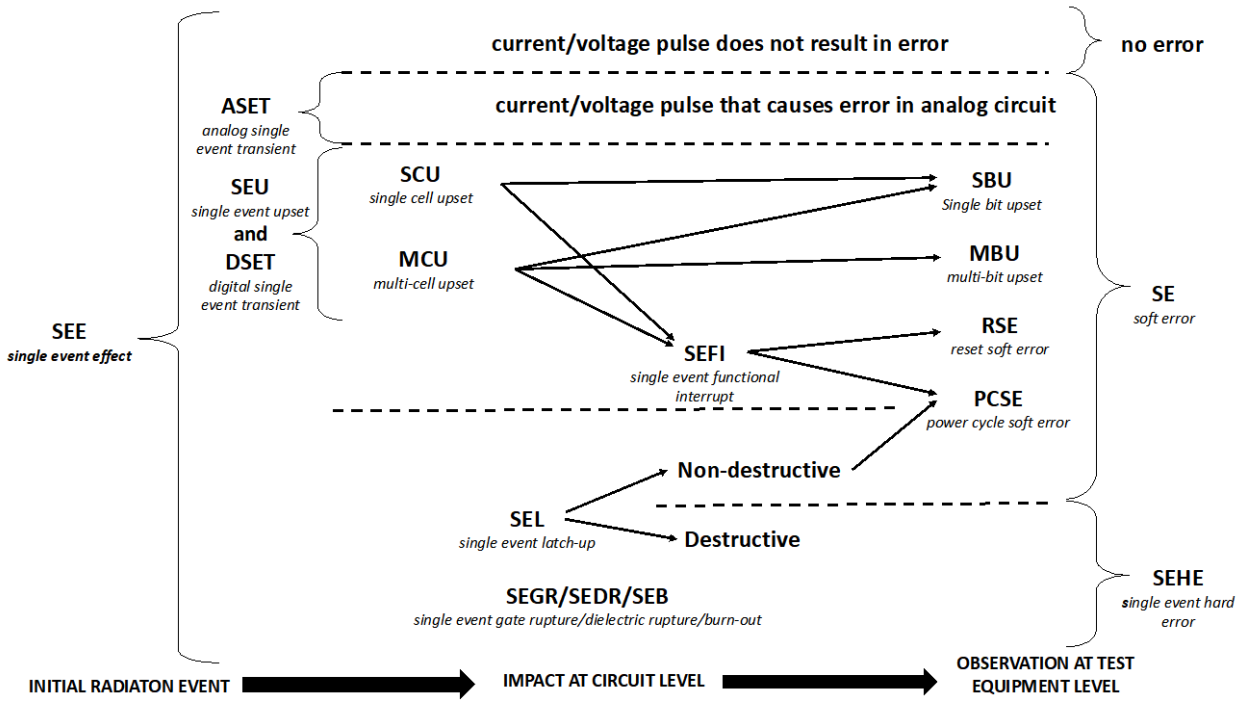

Figure 1 — Diagram of terms used to describe single event effects (SEE). More detailed definitions can be found in 2 Terms and definitions.

In general, soft errors may be induced by alpha particles emitted from radioactive impurities in materials nearby the sensitive volume, such as packaging, solder bumps, etc., and by highly ionizing secondary particles produced from the reaction of both thermal and high-energy neutrons with component materials.

There are two fundamental methods to determine a product's SER. One is to test a large number of actual production devices for a long enough period of time (weeks or months) until enough soft errors have been accumulated to give a reasonably confident estimate of the SER. This is generally referred to as a real-time or unaccelerated SER testing. Real-time testing has the advantage of being a direct measurement of the actual product SER requiring no intense radiation sources, extrapolations to use conditions, etc. (provided the test is performed in a building location similar to the actual use environment – see A.5). However, real-time testing does require a system capable of monitoring hundreds or thousands of devices in parallel, for long periods of time.

The other method commonly employed to allow more rapid SER estimations and to clarify the source of errors is accelerated SER testing. In accelerated SER testing, devices are exposed to a specific radiation source whose intensity is much higher than the ambient levels of radiation the device would normally encounter. Accelerated SER allows useful data to be obtained in a fraction of the time required by unaccelerated real-time testing. Only a few units are needed and complete evaluations can often be done in a few hours or days instead of weeks or months. The disadvantages of accelerated SER are that the results must be extrapolated to use conditions and that several different radiation sources ***must*** be used to ensure that the estimation accounts for soft errors induced by both alpha particle and cosmic-ray generated neutron events.

MEASUREMENT AND REPORTING OF ALPHA PARTICLE AND TERRESTRIAL COSMIC RAY INDUCED SOFT ERRORS IN SEMICONDUCTOR DEVICES

(From JEDEC Board ballot JCB-20-11, formulated under the cognizance of the JC-13.4 Subcommittee on Radiation Hardness: Assurance and Characterization.)

1 Scope

This standard specification covers soft errors due to alpha particles and terrestrial neutrons generated by cosmic rays. 2 covers terms and defintions. 3 covers test methods and issues common to all test types. 4 covers real-time or unaccelerated measurements, 5 covers accelerated soft error rate test procedures related to alpha particles, 6 covers accelerated soft error rate test procedures related to high-energy neutron reactions (>1 MeV), and 7 covers test procedures for thermal neutron reactions with ^{10}B.

This standard defines the requirements and procedures for terrestrial soft error rate (including real-time and accelerated) testing of integrated circuits and a standardized methodology for reporting the results of the tests.

The procedures apply to components including memory and logic. System behavior, including effects like Silent Data Corruption (SDC) and Detectable but Uncorrectable Errors (DUE), is beyond the scope of this standard.

NOTE This standard applies to electronic devices in a terrestrial environments (i.e., ~ 0 to 4,000 meters). Other environments (such as avionics or medical-radiation therapy) are outside the scope of this standard.

1.1 Related Documents

Testing with accelerated radiation sources can introduce damage mechanisms that interfere with the soft error measurements covered in this standard. The user should familiarize themselves with the following documents and eliminate or minimize these sources of interference:

- **JESD57** Test Procedures for the Measurement of Single-Event Effects in Semiconductor Devices from Heavy Ion Irradiation
- **JESD234** Test Standard for the Measurement of Proton Radiaton Single Event Effects in Electronic Devices

In addition, the following document provides more information on destructive effects from terrestrial radiation and accelerator environments:

- **JEP151** Test Procedure for the Measurement of Terrestrial Cosmic Ray Induced Destructive Effects in Power Semiconductor Devices
- **MIL-HDBK-814** Ionizing Dose and Neutron Hardness Assurance Guidelines for Microcircuits and Semiconductor Devices, 1994

And measurement of alpha flux is covered in the following:

- **JESD221** Alpha Radiation Measurement in Electronic Materials

1.1 Related Documents (cont'd)

The following sources are additional information on device irradiation:

- **ASTM F1192** Standard Guide for the Measurement of Single Event Phenomena (SEP) Induced by Heavy Ion Irradiation of Semiconductor Devices
- **ASTM E262-03** Standard Method for Determining Thermal Neutron Reaction and Fluence Rates by Radioactivation Techniques
- **MIL-STD-883J** Method 1017.3 Neutron Irradiation

Warning: These tests may involve hazardous materials, operations, and equipment. It is the responsibility of the user of this test method in consultation with radiation safety personnel to establish the appropriate safety and health practices and to determine the applicability of regulatory limitations prior to use.

2 Terms and definitions

ATE: Automated test equipment.

bit: Logical representation of a binary digit (i.e., zero or one)

cell: Either a combinatorial cell or a storage cell. Combinatorial cell is a circuit element that performs a combinatorial function within logic (e.g., XOR, NOR, NAND, etc.) Storage cell is a circuit element that stores one or more bits (e.g., DRAM, SRAM, multi-level FLASH, register, latch, flip flop, etc.)

component: A packaged die or integrated circuit (IC). A component is comprised of transistors, circuit nodes, interconnects, packaging, etc.

NOTE This may be either a test vehicle (i.e., test chip) or an actual IC product.

collected charge: The charge collected by a particular circuit node during the passage of a particle.

NOTE The collected charge is dependent on multiple design and manufacturing parameters: device geometry and design, circuit layout, particle mass, energy and trajectory, the density and type of material in the sensitive volume and the substrate material.

critical charge: The minimum amount of collected charge that will cause a device node to change state and result in a single event upset (SEU).

device, electronic: synonymous with component or microcircuit

differential flux: Flux per unit of energy, denoted as $d\dot{\Phi}/dE$.

NOTE 1 Differential flux is usually expressed in particles per unit area per unit energy per unit time, e.g., n/(cm² MeV hr).

NOTE 2 Spectral flux density is used in other publications and is synonymous with differential flux in this standard.

DUT: Device under test. In this instance, device is defined as a product IC or test chip.

ECC: Error correction code, sometimes called error detection and correction (EDAC).

fault coverage: The percentage of possible faults detected by a set of test vectors.

FIT: Failure in time; the number of failures per 10^9 device-hours.

fluence (of particle radiation incident on a surface): The total amount of particles incident on a surface in a given period of time, divided by the area of the surface and represented by the upper-case symbol Φ in this standard.

NOTE This fluence is usually expressed in particles per unit area (e.g., n/cm^2). Fluence is the product of flux multiplied by exposure time.

2 Terms and definitions (cont'd)

flux: The time rate of flow of particles incident on a surface, divided by the area of that surface, and represented by the symbol $\dot{\Phi}$ in this standard. It is the time rate of change of the fluence Φ: $\dot{\Phi} = d\Phi/dt$.

NOTE 1 Flux is usually expressed in particles per unit area, per unit time (e.g., n/cm^2h).

NOTE 2 The term "flux" is used in this standard whereas other standards might use the term "flux density" for the same meaning.

glitch: Any spurious voltage or current pulse in a circuit that occurs from a radiation event or electrical noise.

hard error: An irreversible change in operation that is typically associated with permanent damage to one or more elements of a device or circuit gate oxide rupture, single event burn-out and destructive latch-up.

NOTE The error is "hard" because the data is lost and the component or device is non-functional, even after power reset and re-initialization.

multiple-bit upset (MBU): A single event that induces upset of multiple-cells where two or more of the upsets occur in the same logical word (or frame/column/sector, etc. for FPGAs).

NOTE An MBU is a logical manifestation of a single event.

multiple-cell upset (MCU): A single event that induces several cells (e.g., memory cells or flip-flops) in an IC to flip their state at one time.

NOTE 1 The induced errors are usually, but not always, physically adjacent. This does not imply logical adjacency, since this will depend on how cells are placed and routed (interleaved).

NOTE 2 MCUs can manifest themselves logically as MBUs, multiple SBUs or a combination of the two.

power cycle soft error (PCSE): a single event effect that is not corrected by repeated reading or writing but can be corrected by removal and reapplication of power.

NOTE Non-destructive single event latch-up and SEFIs are power cycle soft errors.

process: A combination of people, procedures, methods, machines, materials, measurement equipment, and/or environment for specific work activities to produce a given product or service.

NOTE For the purposes of this standard the process is specifically the manufacturing steps and methodologies used to fabricate a component.

product: A component or service sold to satisfy a particular customer application.

NOTE For the purposes of this standard a product is a complete integrated circuit sold to satisfy a particular customer application.

2 Terms and definitions (cont'd)

radiation: Energy emitted in the form of electromagnetic waves or moving nuclear particles capable of causing direct or indirect ionization. Examples include protons, electrons, alpha particles and neutrons.

NOTE For purposes of this standard the primary radiation of concern is ionizing and includes protons, electrons, alpha particles, and nuclear reaction products.

real-time soft error rate (RTSER): Soft error rate measurement technique in a naturally occurring alpha particle and neutron environment using a large number of devices to obtain a statistically significant error count. This is in contrast to an accelerated SER test in which an intense radiation source is used on a single, or small number of devices. RTSER error counts can be increased by using a higher neutron flux at higher altitudes, but for the purposes of this specification, the term "accelerated test" is reserved for intense radiation sources that do not occur in natural terrestrial environments. System SER (SSER) is another term that is often used and is considered synonymous with RTSER.

reset soft error (RSE): an SEU that requires re-writing to the device configuration registers in order to return to normal operation without a power cycle operation. This reset can also be considered a reconfiguration (e.g., FPGA) or reprogramming.

sensitive volume: A region, or multiple regions, that will cause an SEE.

NOTE The sensitive volume is determined by the angle of the incident radiation, the mass and energy of the incident particles, and the density and type of material in the volume being penetrated by the incident radiation.

single bit upset (SBU): an SEU in which the observed error is a single logical or data bit.

NOTE The actual SEU can be an MCU, but if the cells are multiplex into different words, then the MCU will appear as multiple SBUs.

single cell upset (SCU): an SEU where only one cell or logic element (latch, flip flop, etc.) is upset (compare to MCU).

single-event burnout (SEB): An event in which a single energetic particle strike induces a localized high-current state in a device, resulting in catastrophic failure.

single-event dielectric rupture (SEDR): An event in which conducting path is created in a dielectric material from a single energetic particle strike.

single-event effect (SEE): An event initiated by a particle strike that causes a transient voltage or current pulse. Various types of SEE are shown in Figure 1.

2 Terms and definitions (cont'd)

single-event functional interrupt (SEFI): A single event effect (SEE) that causes the component to reset, lock-up, or otherwise malfunction in a detectable way, but does not result in permanent damage (i.e. hard error).

NOTE A SEFI is often associated with an SBU/MBU in a control bit or register , whereas an SEL is caused by the turn-on of a parasitic thyristor. Many SEFI events can be cleared with a component reset operation (see RSE). In cases where resetting some configuration registers requires a complete power cycle of the device, it can be difficult to distinguish between a SEFI and an SEL. A SEFI event does not nesessarily result in an extended increase in operational current like a high current SEL.

single-event gate rupture (SEGR): An event in which a single energetic particle strike results in a breakdown and subsequent conducting path through the gate oxide of a MOSFET.

NOTE An SEGR is manifested by an increase in gate leakage current and can result in either the degradation or the complete failure of the device.

single event hard error (SEHE): A hard error caused by a single event radiation strike.

single-event latch-up (SEL): An abnormal current state in a circuit caused by the passage of a single energetic particle inducing a parasitic thyristor to turn on and remain in a fixed state regardless of inputs, until the device is power cycled.

NOTE 1 Some SEL events result in a measureable current increase (e.g., latch-up of an IO circuit). Some SEL events may result in a difficult to detect increase in current (micro-SEL) compared to the quiescent current of the entire component (e.g., latch-up of memory cells within a common well).

NOTE 2 A high current SEL may cause permanent damage to the component and result in a hard error. Micro-SEL events are typically non-destructive due to the low current draw and can be cleared by power cycling.

single event transient (SET): A time dependent radiation induced spurious current or voltage signal on a circuit node. A digital SET (DSET) occurs when an SET in a combinational logic gate (along data or control paths) propagates and is latched to create an error (SEU) in the output of a sequential element. An analog SET (ASET) is a spurious signal in an analog circuit (e.g., a spurious signal on an IO pin, etc.) that causes an erroneous output.

NOTE Not all SETs will result in an upset or soft error. SETs propagating along data and control paths can be masked and never become a latched SEU (logic masking, electrical and temporal masking).

single-event upset (SEU): An error in a circuit that is not permanent (i.e. not a hard error) caused by a state change of a latch, flop, memory cell or other bistable element from a single energetic particle strike. The energetic strike can occur directly on the circuit element or propagate to that circuit (see SET).

NOTE In many documents and publications, SEU is used to include other soft errors, such as SEFI and SEL.

single-event upset (SEU) cross-section: the number of events per unit fluence. For device SEU cross-section, the dimensions are area per device. For bit SEU cross-section, the dimensions are area per bit.

single-event upset (SEU) rate: the rate at which single event upsets occur.

2 Terms and definitions (cont'd)

soft error: An erroneous output signal from a circuit that can be corrected by performing one or more normal functions of the device (e.g., retrying operation, rewriting data, power cycling, etc.) In many documents and publications, soft error is synonymous with SEU.

NOTE 1 The term refers to an error caused by radiation or electromagnetic noise (e.g., electromagnetic pulse from a nuclear event) and not to an error associated with a physical defect introduced during the manufacturing process. For the purposes of this standard, soft errors are considered to be single particle radiation induced events and not due to other sources, such as signal integrity or noise.

NOTE 2 The terms soft error and soft error rate (SER) have been adopted by the commercial IC industry while other terms, such as SEU, SEFI, etc.. are typically used by the avionics, space, automotive, functional safety and military electronics communities.

NOTE 3 The term "soft error" was first introduced (for DRAMs and ICs) by May and Woods of Intel in their April 1978 paper at the IRPS and the term "single event upset" was introduced by Guenzer, Wolicki and Allas of NRL in their 1979 NSREC paper (SEU of DRAMs by neutrons and protons).

soft error rate (SER): The rate at which soft errors occur.

storage element: A circuit or device that can be programmed to hold (or store) different states. For example, a DRAM cell, that can store charge (or not) on a capacitor. An SRAM cell or a flip-flop is another example.

test chip: A circuit or IC designed for the purpose of evaluating one or many device characteristics. For the purposes of this document, the characterization would be the soft error sensitivity of a particular process technology. But the test chip can incorporate other structures used to characterize different parameters, such as yield, speed, voltage margin, etc.

NOTE This test chip is not typically a product but is a dedicated component or section of an IC chip designed to be used to extrapolate to the SER of a product.

user: The individual using this standard to measure the soft error characteristics of a component or technology

3 Test equipment and software requirements

3.1 Test plan

A test plan shall be developed to support testing of each DUT type (if multiple types of devices are to be tested) and each type of test condition (i.e., temperature, voltage, frequency and test pattern). This test plan will serve as a guide for the procedures and decisions to be made during the irradiation period. In most cases, if the test plan cannot be followed exactly , adjustments must be made during the course of testing based on equipment performance, user observations and other factors that might not have been accounted for in the original plan.

In developing a test plan, the user should consider the following questions:

1) What are the single event effects that are of interest? And how can they be detected and classified?
2) What are the operating conditions of interest? What voltage, temperature, and frequency range is of interest (i.e., the entire datasheet specification, just nominal conditions or maximum stress conditions for soft errors)? What test patterns or program applications will be run? What device modes will be used (i.e., active vs standby as well any special automated selective power saving programs)?
3) What sources of radiation will be used (e.g., the natural terrestrial spectrum? or special high intensity sources?) And what is the test duration – hours, days, weeks? Note: For accelerated alpha and neutron testing covered in Sec 5, 6 and 7), it is possible that the devices will receive particle doses greater than that under normal lifetime conditions which could impact various electrical parameters (i.e., dose effects). These dose effects are beyond the scope of this standard and the user should refer to other standards listed in Sec 1.1. As a precaution to determine dose effects are not an issue, the user can do device characterization (e.g., threshold voltage, leakage current, maximum frequency, etc) before and after accelerated testing.
4) What is the minimum detectable soft error limit of interest in case no errors are seen (e.g., How much testing is required to determine that a DUT displays an SEL < 10 FIT @90% confidence level if no SEL events are observed?) or what level of statistical variation around a measured mean soft error rate is desired (e.g., Is a +/- 50% variation about the mean at a 60% confidence level acceptable)? The answer to these questions will help to determine the test time required.

The following examples show how these questions can be handled.

Example 1 – An SRAM for which the user wants to determine the average cell upset rate within an 80% confidence level (CL) upper bound and 20% CL lower bound. annex C.2 gives an example of a device with an average soft error rate of ~1257 FIT. Table C.3 shows that if device testing is only carried out for 450 hours on 3500 parts, the upper and lower limits are 2717 FIT and 975 FIT, or 1270 FIT (see Table C.1) +114%/-23%. If testing were extended to 2045 hours, then the results would be 1257 FIT +39%/-19%. If the user desired and even smaller variation, longer test times and/or more devices would be required.

Example 2 – A power controller where the user wants to confirm the SEL is <10FIT at a 90% CL using a neutron beam with an acceleration factor of 10^6. This usually implies that no SEL events will be observed at this low a FIT. Table C.2 shows the chi-squared values for error count and CL. For 0 errors and a 90% upper limit, $X^2 = 0.211$. Using the left side of Eq C.3 for a single device, the unaccelerated test time (T_r) would have to be $>10^7$ hr without any SEL events to satisfy <10 FIT, meaning >10 hr beam testing.

3.1 Test plan (cont'd)

Once these questions are addressed and the user has familiarized themselves with the appropriate radiation test sections (**4** through **7**), a test plan can be developed. If the soft error test campaign involves a remote site from the user's home location (e.g., particle beam facility or high altitude site for RTSER), it is highly recommended to make a site survey visit prior to creating a test plan in order to determine the details of the facility's support team, procedures, physical layout and infrastructure.

For beam and reactor facilities, the following questions should be addressed during the site survey visit:

- Is there special registration and training required by the facility prior to testing?
- If the facility runs 24hr a day, how does the user plan around the clock coverage?
- What are shielding materials to protect the test equipment and are they available at the facility or does the user need to bring them (espeecially thermal neutrons)?
- If other devices are on the DUT board and exposed to the beam, what precautions are taken (i.e., can these devices be put in a special position with respect to the beam or be shielded)? Where will equipment be placed and how will it be powered and accessed?
- How will communication between the various pieces of hardware be handled?
- Are there enough cables and are they long enough to connect all the equipment?
- What technique will be used to align the DUTs with the beam?
- Will one DUT be tested at a time? If multiple DUTs are exposed side by side, what is the beam uniformity across the exposure area? Or if the DUTs are mounted front to back, how will beam flux attenuation, energy dispersion and spallation effects be accounted for? (e.g., can the facility experts provide guidance or advice?)
- How will recording of results (both error logs and particle fluence) be managed?
- Is there a capability to analyze results while testing is taking place? Often times, test data will not be what is expected by the user. This requires "on the spot" decisions of whether or not to continue testing or change to an alternate plan. If consultation with software or applications engineers not present at the test site is needed for this decision, a method for sharing the test results in "real time" is required.
- Does the facility require quarantine of DUTs and equipment that has been in the beam due to radioactivity? If so, for how long? What are the security measures and process to retrieve the DUTs and equipment?
- Is a user agreement with the facility required?
- What happens if equipment damaged in shipment? Does the facility have equipment to effect repairs (e.g., solder irons, etc) or should the user bring repair equipment?

For RTSER testing at remote (i.e., high altitude) locations, the following questions should be addressed during the site survey visit:

- What is the nature of power sources provided by the facility (i.e., Are there routine interruptions in supply? How well controlled and noise free is it? What is the total power capacity? etc.)?
- What are the environmental controls of the facility (i.e., HVAC system capacity and controls)?
- How will data be collected over the duration of the test, which is bound to take several months (i.e., Will there be personnel on site during the total duration of testing? Or will the user have access test controls and data collection remotely after initial setup?)
- In the event of unanticipated events (e.g., power supplies blowing up or HVAC system failure), what are the plans for human intervention (i.e., Are there personnel on site or close by? Or will the user have to schedule an emergency trip?)
- Is a user agreement with the facility required?

3.1 Test plan (cont'd)

- What happens if equipment damaged in shipment? Does the facility have equipment to effect repairs (e.g., solder irons, etc) or should the user bring repair equipment?
- Does the facility provide real time logging of high energy and thermal neutron flux/fluence? Or will the user need to make a calculation based on annex A?

Prior to the actual test campaign, exhaustive dry-run testing should be done with all the equipment at the user home facility. Considerations should also be made for provisioning spare equipment and DUTs wherever possible. This will minimize the impact of any hardware failures that might occur during shipment or at the remote test location (e.g., cables, power supplies, ESD damage of DUTs, etc). In addition, the ability to electronically link with the user's home location is critical to allow for patches in any software and test bugs that might be uncovered during testing. Having application/test engineers as part of the test team (either on site or available via telecom/internet connection) is highly recommended. Check with the facility about remote login requirements. Due to firewall restrictions, this might require running two separate networks during testing – one local for the DUT/ATE hardware and one remote for technical support at the user's home facility. Before travelling to the test site, it is strongly recommended that several dry runs be made with the hardware, software and DUTs to confirm trouble-free operation. The user should also consider the use of a "golden part" (i.e., one or more DUTs that has been previously tested and characterized to serve as a check for repeatability at the same site or from site to site). If this is the first test campaign, the user should consider creating a "golden part" and setting it aside for calibration of future campaigns. Since these "golden parts" can be exposed to high radiation doses from multiple campagins, radiation damage might occur. The user should perform electrical characterization on these parts and replace them with new "golden parts" when this occurs.

For all soft error testing it is important to understand the following:

1) Particle fluence at the DUT, either by estimation using annex A in the case of real time SER (RTSER) testing or measurement in the case accelerated SER testing using a particle beam, reactor or alpha particle source.
2) Number of circuit elements that are accessible to the user and subject to upset. The user should determine the basic schematic structure of the device (e.g., 4 kbit internal SRAM) to understand the internal elements at risk of soft errors. The user should understand how each applicable soft error type will be tested. In some cases, such as user visible bits, the SBU and MBU rates can be measured on a per bit bases. On the other hand, characterization of SEFIs may only be possible on a per device (or IC chip) basis if the source of the SEFI in unknown (i.e., details of which registers or sub-circuits caused the SEFI).
3) Number of upsets that occur in each circuit element or function. The user should think about how many of each type of upset event (e.g., memory SBU, SEFI, SEL, etc) should be measured.
4) The user should develop an initial estimate of the number of upsets to be measured in the allotted test interval. Prior published data on soft error rates can be used as a guide if the user has no prior experience. If no data are available, the user should decide on the lowest soft error limit of interest such that the observation of zero errors confirms this limit (See annex B – Real Time Counting Statistics).

3.2 Test equipment

3.2.1 ATE hardware

The automatic test equipment (ATE) hardware used for testing may be conventional electronic test gear or custom-built equipment. The ATE must be able to tolerate stray radiation (or be shielded or mounted remotely in a shielded area) and able to operate in potentially poor quality power conditions. The use of uninterruptible battery-backed power supplies is recommended in facilities that cannot provide highly reliable power.

The ATE hardware must be capable of exercising the DUT over the range of operating conditions such as power supply voltage, access cycle speed and temperature that are specified in the test plan. Proper operation of the ATE under all of these operating conditions must be rigorously confirmed prior to the beginning of testing with a radiation source. The use of cabling to connect the DUT and test equipment, power supply accuracy at the DUT, and the exposure of the ATE to scattered radiation during testing should all be considered. (Note – In general, power supplies are sensitive to radiation. Therefore, measures should be taken to minimize their exposure.)

3.2.2 ATE software

The ATE software creates the proper conditions for the test. It identifies and records errors as they are detected. Depending on the test, software can also be used to correct the errors before continuing. The user should make a determination of the fault coverage required. When designing the test system, the user should understand the portions of the die, signal path, and latching circuits of the device being tested in order to arrive at a quantitative result. The fraction of time the device is in an SEE susceptible mode and what fractions of the DUT's susceptible elements are not tested should be known. Complex devices do not always permit easy testing access.

The ATE software should be capable of:

1) Controlling device initialization and rudimentary functional checks.
2) Device operation in dynamic or static operation, as required by the test plan.
3) Resetting the DUT during beam irradiation or environmental real-time testing.
4) Error detection and logging, including the time that the error was detected. It is important during error detection that new errors are not omitted (i.e., the process of reading out errors does not interfere with the collection of new errors).

In addition to the characteristics listed above, the following features are also desirable:

1) Bit error mapping and data processing, storage and retrieval for display.
2) High-speed operation and a high duty factor (i.e., datasheet frequency and operating load specifications).
3) Real-time DUT data display capability providing a higher test throughput and allowing for more precise control of testing.
4) The ability to do preliminary data analysis while the test is in progress. This feature is desirable for modification / optimization of test procedures in light of the data being collected.
5) Reliable audit path for data collection to allow correlation of experimental notes and collected data from the ATE.
6) Recording the particle fluence, either automatically acquired from the test facility or manually entered.

3.3 Test conditions

Test conditions include the source of radiation, environmental conditions (voltage, temperature, frequency, etc), test patterns or applications and mode of operation (dynamic vs static). Considerations should be given to the actual application of the device in real operating environments. If the SER test cannot duplicate all of these conditions (e.g., if the component cannot be run at datasheet speeds during radiation testing), any techniques to extrapolate tested ~~SEU~~ soft error rates to application ~~SEU~~ soft error rates should be clearly explained in the final report.

3.3.1 Test pattern/applications

Based upon the product being tested, careful consideration should be given to test patterns/applications that cover the maximum functionality space of the device. For example, the basic data patterns for all memory circuits is a combination of logical checkerboard (alternating by address and bit) as well as solid 1 and 0s. If detailed layout information for the DUT is available, a physical checkerboard is also useful. A determination of the best test pattern s appropriate for the DUT and its use is left to the discretion of the user, but must be documented in the final report.

The use of physical data patterns, i.e., patterns that are related to the actual layout of the DUT, rather than logical addressing is recommended where possible. These patterns may provide additional insight into the ionizing radiation sensitivity of the DUT. Because layout information is generally proprietary only DUT manufacturers would generally be expected to be able to meet this recommendation.

Some devices, particularly dynamic RAMs (DRAMs) and logic elements often have a “preferred” soft error failure, either $0 \rightarrow 1$ or $1 \rightarrow 0$. The selected test pattern must consider this possibility in its design. For testing when there is no *a priori* knowledge of the device, a minimum of four test patterns should be used: all 0s, all 1s and checkerboard (and its inverse). (Note: If knowledge of the layout is available, these patterns should be physical.) If the relative failure rates are known, perhaps from previous test experience, the test pattern may be adjusted to improve statistics of the less likely transition. The use of an unbalanced test pattern (i.e., deviation from checkerboard, all 1s or all 0s) must be described fully in the final report and data analysis.

3.3.2 Environmental Conditions

The test plan defines the required supply voltage, temperature and operating frequency for the test. Since the soft error rate may be very sensitive to the supply voltage, temperature and frequency, it is critically important that these parameters be accurately measured and controlled. Some parts have internally regulated supply voltages that may interact with the measurement. These internally regulated supplies may automatically change their settings depending on operating mode, making the SER measurement dependent on the specific test method. If the test plan requires SER measurement from minimum to maximum voltage, the user should consider if internal voltage regulators are used and if they can be disabled without leaving the DUT unoperable or should be left in operation per the test plan. Considerations should be given to the junction temperature of the device vs monitoring temperature (eg thermocouple on or near the device package).

3.3.3 Static vs. dynamic testing

It is important to consider the interaction of the soft error test with the operating modes of the device. The following definitions help to clarify the use of the terms static and dynamic in the context of soft error test methods and device operating modes.

Static Device Operation – Many devices have a static (aka standby or idle) mode to reduce power consumption. This mode can be implemented in many different ways (e.g., reduced clock frequency, clock gating, lower Vdd or completely turning off parts of the device) depending on the IC design. These modes should be documented in the device datasheet. The soft error performance of a device can depend on the operating mode and the user should define what modes are of interest in the Test Plan (**3.1**).

Static Soft Error Testing – For static soft error testing, a device is first loaded with a test pattern or vectors and then put into a static or idle mode, or powered down completely in the case of non-volatile memory. The device is then radiated for a specified time. After radiation, the device is returned to normal operation so that upsets can be determined. Static soft error testing will expose errors in state elements (e.g., flops, latches, memory cells, etc.). If these elements are at reduced voltage or frequency during idle mode, then the soft error rates measured are for the reduced voltage or frequency used. These rates can be different than the rates measured when full power and frequency are applied. Self-heating effects (i.e., change in junction temperature due to voltage and frequency effects) can also have an impact. The limitation of static soft error testing is that the temporal information is not captured which prevents the user from separating temporal and physically adjacent single-event multiple-bit upsets.

Continuously-Read Soft Error Testing – For continuously-read soft error testing, the memory arrays are first loaded with a test pattern and then the arrays will be read in a loop for a specific loop count (e.g., 1 loop is a pass through the entire memory space), error count, or duration of time. For memory array, typically the read operation will be executed on a per address basis. Once the error is found, the address information should be reported along with the time stamp (i.e., time or loop count). To prevent the same error from being reported in the next iteration of the read loop, the correct data should be written back to the word with the error. The timing information of the errors can be used to help distinguished between temporal and physically adjacent single-event multiple-cell upsets. Errors that are found physically adjacent to each other but separated by more than 1 loop count cannot be from the single-event upset. The second error has to come from a different event, otherwise it would have been detected in the same loop as the first error (with the exception that the event happens right after one address is read and before the other address is read). However, care must be taken to ensure that the flux used in the test is not too high because if there are too many errors that need to be written back, a significantly delay in the completion of the read loop cycle could result in loss of the temporal data.

Dynamic Soft Error Testing – For dynamic soft error testing, the device is run in normal operating mode running user applications (or tests to simulate user applications) while it is being radiated. Typically, this involves running the device under typical datasheet conditions (i.e., nominal voltage, temperature and frequency). In addition, extended voltage, temperature and frequency conditions can be used to determine the soft error rates over a range of environmental IC operation window. This test mode exposes all of the elements of the device that are used in normal operation to soft error. It should be noted that many modern IC designs at advanced technology nodes use automated internal power saving features by shutting down various circuit blocks that are not in use for a particular test or operation. If these features are running during dynamic soft error testing, radiation strikes to the control circuits can cause these features to malfunction leading to possible SEFI events.

3.3.3 Static vs. dynamic testing (cont'd)

NOTE In order to characterize soft error events related to the device IO and power pins, the user should ensure that the DUT board design uses impedances consistent with the datasheet specification.

Depending on the objectives of the test program, static or dynamic operation of the DUT may be specified. For static tests the DUT is initialized to a known state (e.g., data pattern written into memory, and then the DUT is irradiated. Following the irradiation, the state of the DUT is read out and compared with the initialized value to determine the number of upset events.

In dynamic testing the DUT is also initialized prior to irradiation to a known state. Once irradiation begins, the DUT is continuously operated (e.g., continuous write-read operations) at a rate specified in the test plan, counting upset events as they are detected. Once the irradiation stops, sufficient time to read all of the DUT is allowed to assure that all upsets induced by the radiation have been tabulated. Generally, the DUT state is rewritten with a new complement pattern as it is being accessed, to correct upset events and to exercise more internal data states.

The pattern of accesses for dynamic testing has to be planned to minimize "dead-time" between a read of a location and a subsequent write to that location. Any upset that occurs between a read from a location and the next write will not be detected since it is overwritten. Failure to account for this dead time will result in an erroneously low estimate of SER. The final report must include details of the dead-time calculation.

Use of a "write array" followed by "read array" update is not recommended. Soft errors that occur between the last read of a location and its next write cannot be detected and result in excessive dead time. For the case where continuous updating of the array is used, this method would result in 50% of the test time being unused and the SER value being too low by a factor of 2. A better strategy would be to perform a write – soak – read followed by immediate write of new data (where soak is the delay time between write and read, the time the memory cell is susceptible to an upset that will be detected and not overwritten.) This minimizes the dead time to small period between read and re-write.

Dynamic testing of memory is often carried out through the device's normal access (i.e., row and column address circuits). Non-memory components may use test access modes, such as JTAG boundary scan, for access to internal logic.

One example of a dynamic test cycle uses 2 cycles per address. The first cycle reads the value stored at the address, comparing it with the expected value and noting any errors. The second cycle writes a value to the same address to correct any errors. The second access writes the complement of the expected value so that every bit in the DUT changes state with each complete pass through the memory. This cycle has a very short dead time of approximately 1 memory cycle for each complete scan through the DUT.

Both types of testing are illustrated in the flow diagram in Figure 3.1. For these flows, a logical "checkerboard" pattern of alternating 0 and 1 value is assumed, along with a complementary rewrite operation for the dynamic test.

When testing non-memory components, such as microprocessors, the choice of static or dynamic testing may have a very large effect on the measured results, particularly at clock rates over 200 MHz. The

3.3.3 Static vs. dynamic testing (cont'd)

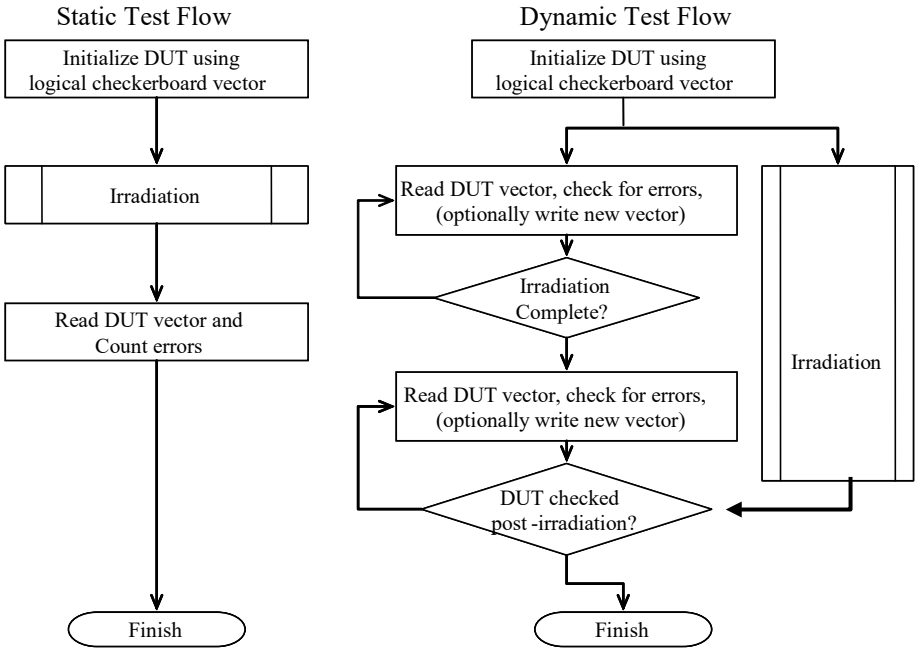

Figure 3.1 — Flow diagram comparing static and dynamic testing.

dynamic case will have a higher soft error rate due to the effects of errors in combinational logic being clocked into sequential logic elements and from race conditions created by particle strikes on the clock network.

3.4 Considerations for Soft Error Testing of Individual Circuit Elements

Modern IC components typically consist of several different types of circuit elements – latches, flops, memory cells, clock circuits, etc. How each of these building blocks respond to radiation can be very different. For example, higher voltages on a flip-flop or memory cell might decrease its SER (due to a higher stored charge) but increase the probability of SEL in a parasitic pnpn element. The purpose of this section is to outline the known soft error effects in these various circuit elements. The user should be familiar with the various circuits in the DUT of interest in order to formulate a valid Test Plan. If detailed circuit schematics of the DUT are not possible, familiarity with the various DUT functions from the datasheet should be used.

This section addresses soft error testing of the individual building block circuits used to design a modern IC product (FPGA, CPU, SoC, etc). Test chips can be designed with these elements in order to test SEU effects. Alternatively, the can user isolate and test these circuit elements individually on a complex IC product. 3.5 addresses soft error testing of the entire IC as a whole.

3.4 Considerations for Soft Error Testing of Individual Circuit Elements (cont'd)

3.4.1 Memory

Memory devices store digital data in memory cells, which can be addressed and read out. The logical address is the electronic representation and the physical address is the actual x-y coordinates of the cell. Typical memory cells store a 0 or 1 (e.g., DRAM, SRAM and single level NVM) but multi-level data storage is also possible (e.g., Multi-level cell NVM). Typically, memory cells are packed in close physical alignment and a single soft error event can lead to the upset of a single cell or multiple cells in close physical proximity. Upset rates can also depend on whether the bit flip is from a logical 0 --> 1 or 1-->0. The user should also be aware that there can be a difference between logical 0s and 1s vs voltage stored on a node or not. A memory cell is susceptible to an soft error event between the time data is written and when it is read back. If new data is overwritten before a read, then any soft errors will be erased and undetected.

3.4.2 Combinational Logic

In combinational logic, the output is a pure function of the present input only. An SET event can occur at any time on an input (or internal) node that changes the output state.

3.4.3 Sequential Logic

In sequential logic, the output depends not only on the present value of its input signals but on the sequence of past inputs. For synchronous sequential logic, the state of the circuit changes only at specific times in response to a clock signal. Therefore, soft errors will depend on a) any upsets in the input logic or signal lines, b) timing of the radiation strike and c) the clock frequency. For asynchronous sequential circuits, the state of the device can change at any time in response to changing inputs. In this case, the soft error event in the registers can occur at any point in time.

3.5 Considerations for Testing IC Products

Testing for non-memory components is a complex topic that cannot be completely described herein due to the wide variety of different ICs. This section addresses some specific issues to be considered for the fundamental soft error testing of various memory and non-memory components (e.g., random logic, microprocessors, and FPGAs, analog devices and power devices). In today's IC technology, many products have combined memory and logic functions. This section addresses considerations for testing the IC as a whole (e.g., normal operating functions). **3.4** addresses soft error testing of the individual elements (or building blocks) of the IC.

A carefully written test plan and report are essential for meaningful non-memory testing. It is particularly important to consider the number of storage elements that are exposed during irradiation and the observability of errors in those elements. Errors in sequential logic, control structures and even FPGA configuration logic is often not observed during operation because it is masked by the operational state of the device or choice of test vectors. A minor change in the test conditions may have a large effect on the rate of observed errors.

3.5 Considerations for Testing IC Products (cont'd)

3.5.1 Memory components

There are three basic functions of a memory component: write data, store data and read data. Any of these operations can be susceptible to soft errors. The memory cells (i.e., memory core) are common to each of these modes. Different periphery/logic circuits can be used for each of these operations. Therefore, for complete soft error testing of memory, each of these three functions should be exercised and a determination made of the soft error rate during each of these operations.

Example 1 - Determine the susceptibility in the storage mode
Data can be written into memory prior to irradiation (so soft errors won't occur in the write mode), the memory is then irradiated to induce soft errors and then data read out after radiation is turned off (so soft errors won't occur in the read mode). The soft error rate can be measured in normal operation (i.e., normal voltage supplied to the memory core) or in standby mode (i.e., core power is reduced but still maintains data). Care should be taken to insure that the only errors occurring in standby mode are due to radiation (i.e., the memory should be cycled through write-standby-read without radiation and display no errors).

Example 2 - Determine the susceptibility of read mode
Data can be written into memory prior to irradiation (so soft errors won't occur in the write mode), memory is then irradiated and read continuously. Soft errors in this mode can be due to cell upsets as well as read circuit upsets. Comparison of soft error data with Example 1 can give insight into how much and what types of errors are due to the memory cells vs the read circuits.

Example 3 - Determine the susceptibility of write mode
Data can be written and read continuously during irradiation. In this case, both read and write circuits are susceptible to soft errors as well as the memory cells. Comparison of data acquired in this mode with Examples 1 and 2 can give insight into the soft errors from the write circuits.

If the user is knowledgeable about cell asymmetries (i.e., if a 1 or 0 represents stored charge in a DRAM, or an SRAM cell is more sensitive to read or write disturb when transitioning from 1 → 0 or 0 → 1), this information can be helpful in explain if there are pattern dependent differences in error rates.

3.5.2 Random logic circuits

Testing procedures of the following types of logic circuits and devices are specified:

1) Sequential Logic (includes dynamic combinatorial logic)
2) Register Files
3) Static Combinatorial Logic

The SER testing procedure critically depends on the type of logic device under investigation. Testing of types 1 and 2 are somewhat similar to SRAM testing, since both types of cells are memory/storage cells with feedback devices at the state nodes. SER testing of type 3 is much more involved due to the transient nature of the propagating glitches and the dependency on the circuit's logic configuration and state at the time a transient reaches a sequential cell or output.

3.5.2 Random logic circuits (cont'd)

Sequential Logic: In this section, the procedure to measure the *nominal* SER of sequential logic (i.e., logic whose output depends not only on the present value of its input signals but on the sequence of past inputs) is described. (Note: The *nominal* SER refers to conditions where logic sequentials hold data statically, without clocks being exercised.) Clock upsets of nodes located in the sequential logic are not covered in this specification. Note that the actual SER of sequential logic in a product can be vastly different from nominal values and depends critically on the circuit context in which the sequential has been placed. The actual SER of sequential logic in a data path depends on the logic depth of the stage and on the clock frequency. The nominal SER of sequential logic can be tested using a shift register or array type architecture.

A sequential logic testing procedure typically involves the following steps:

1) The clock signal (or clock signals, if a race proof scheme is implemented) is running at a low speed (typically kHz to a few MHz range) and the data are shifted in.
2) The clock(s) is (are) stopped and the devices are irradiated.
3) Irradiation is stopped.
4) Clocks are turned on and data are shifted out and logged.

Due to the asymmetric nature of sequential nodes, critical charges and therefore failure rates of different sequential nodes are state dependent. At a minimum, data patterns must include a logical checkerboard pattern and its complement or both solid ones and solid zeros to cover all potential transitions and states. Patterns are written into the shift register before exposure and then irradiated for a given exposure time. After exposure data are shifted out and checked for any upsets. This procedure allows identification of the sequential logic cells that were upset during exposure.

For tests where the clock is running during irradiation, use of a test structure with a non-overlapping clocking scheme, where the main and secondary stages of a flip-flop are clocked separately, is recommended to avoid minimum-delay problems. If main/secondary flip-flops are used in a shift register topology together with a non-overlapping clock scheme, the state information of one stage (main or secondary) is lost because the shifting process overwrites the state of one of the stages after both clocks have been stopped. Testing is recommended at slow clock speeds, i.e., at clock speeds where the cycle time is orders of magnitude longer than the internal device delays.[1], [2]

The DUT can be designed to have significant soft error contributions from one node only by increasing the critical charge Qcrit of other nodes sufficiently. This allows for a separation of $1 \rightarrow 0$ and $0 \rightarrow 1$ transitions. Furthermore, by implementing various sequential flavors with different diffusion area sizes of the most critical node, the diffusion area scaling can be characterized [3].

The functionality of the sequential logic circuit must be tested prior to the radiation exposure for all patterns over the planned voltage range.

The nominal SER of sequential logic can also be assessed by exploiting scan chains implemented in products for testing purposes. The testing procedure in this case is very similar to the one above since scan chains are usually implemented in the form of shift registers.

3.5.2 Random logic circuits (cont'd)

Multiport Register Files: The SER of register files may be assessed using a memory array structure where all register file cells can be individually written and read. Testing guidelines are the same as for memory components. One important difference is, however, that for multiport devices the write and read logic also needs to be tested for its susceptibility to upsets.

Static Combinational Logic: The soft error rate of static combinatorial logic is defined here as the rate of latched glitches induced by upsets of combinational nodes. A glitch by itself is not considered a soft error and a static combinatorial gate by itself does not have a well-defined soft error rate in digital logic. Its SER contribution depends on the circuitry it feeds into. The glitch induced by radiation can be attenuated or even blocked by consecutive stages. The arrival time at the latching element determines if the glitch is latched and therefore whether the event is relevant and results in a SEU.

Static combinational SER has to be tested in its application environment. Static combinational SER can be tested and quantified using a shift register architecture as described in [4], [5] and [6]. This architecture comprises shift registers of various lengths and with different logic (i.e., shift register) depths to quantify the impact of clock speed and electrical masking on the failure rate. Because attenuation (electrical masking) depends on the gate delay relative to the pulse width, it is highly recommended that the static combinational test structures comprise paths with different logic depths and different logic-cell sizes (i.e., gate speeds). This technique quantifies the SET induced SEU rate that can be quantified per path or per gate and extrapolated to the circuit block or product level.

Another approach to estimate the contribution of ionizing particle strikes in combinational logic that relies on test-chips is circuitry that enables characterization of SET amplitude and width distributions for different static logic cells along circuit paths [7]. The pre-characterized distributions are then applied in a full product risk assessment which involves estimating the fraction of SETs that are latched in clocked receivers.

To maximize the signal due to upsets occurring in combinatorial nodes in a test circuit, the SER contribution of sequential elements needs to be minimized. This can be achieved by using a minimum number of hardened sequential elements.

Because the content of the receiving latch impacts the sensitivity to the minimum magnitude and width of the glitch to be latched, data patterns must include a logical checkerboard pattern and its complement as well as solid 1 and solid 0 patterns [8].

Recommended variable evaluations include:

1) Voltage: nominal +/- tolerance; Expanded range of test voltages is highly recommended.
2) Different cycle times; please note that the SER of static combinational logic increases linearly with clock speed.

3.5.3 Field programmable gate arrays

When testing FPGAs for single event effects, one should design the test strategy to detect:

1) SEU in the configuration memory
2) SEFI in the logic blocks
3) SEU and SEFI in the IO blocks
4) SEFI in the configuration circuitry
5) SET and SEU in flip-flops embedded in logic blocks
6) SEU in RAM blocks (or user memory)
7) SEL – either non-destructive (i.e., increased leakage) or destructive

FPGA supplier view vs user view of soft error testing – An FPGA supplier should characterize the soft error cross-section at the basic building block level. A user can use this information to do their own estimate of the total soft error cross-section of their design (not covered in this standard) or use the suppliers software tools (if available). The user might also choose to do actual soft error testing on an FPGA configured to their own application (or user configured circuit). The user derived soft error cross-section is design/application (or user configured circuit) dependent and does not apply to different design/applications on the same FPGA base die.

The final report should clearly show results for all failure mechanisms separately. On-line scrubbing (periodic reading and correction of configuration memory) detects soft errors within seconds to minutes of their occurrence (depending on scan time). Functional monitoring is capable of detecting errors in the application. With the combination of on-line scrubbing and functional monitoring it is possible to directly tie the FPGA's SEUs to the functional failure. Furthermore, on-line scrubbing will keep SEUs from accumulating, making it easier to do fault attribution.

For SEU in embedded logic blocks and RAM blocks, a similar approach to other stand-alone components may be used.

3.5.4 Microprocessors

The SER of microprocessors comprises failure contributions from the components described above. The microprocessor SER can be assessed either by properly adding up the contributions of those components tested individually, or by directly measuring the SER on the microprocessor itself [3].[9]. In the latter case the microprocessor needs to be tested in either a real system or on a high speed ATE. In both cases the failure rate of a microprocessor is application dependent.

Testing in a real system involves running diagnostic software on the system that logs detected upsets. Note that this constitutes only one potential contribution of the overall microprocessor SER. Changes in unobserved states, also known as silent data corruption, can be observed for only by transforming silent errors into detected errors. Another complication arises from the fact that a system might crash and no data might be available on what caused the crash. Great care needs to be taken to ensure that the system is stable and that other intermittent errors are not mistaken as radiation-induced soft errors. In the case of accelerated testing of microprocessors in systems, it is important that only the DUT be irradiated and other peripheral chips are not accidentally irradiated.

Running the microprocessor on a high speed ATE while exposing it to radiation has the advantage that more of the relevant errors can be detected and less ambiguity exists. In this case the SER is typically assessed for specific patterns that might yield SER values very different from actual systems deployed in the field.

4 Real-time (unaccelerated and high-altitude) soft error test procedures

4.1 Background

4.1.1 Introduction

The most direct way to measure SER in a device is simply to observe it under standard operating conditions under normal ambient background radiation. The inherent problem with this approach is that the effective failure rate is so low that a single device would take decades to generate a statistically significant number of soft errors. In order to circumvent this limitation, real-time (unaccelerated) SER (RTSER) testing utilizes a very large number of devices in parallel to reduce the required test time. The number of soft errors observed is linearly proportional to the number of DUTs multiplied by test time (ie device hours). Testing can also be done at elevated altitudes where the higher neutron flux will generate a higher error rate. The system can either be a set of custom designed boards populated with a large number of the devices to be tested or a large server or other complex system (or array of servers/systems) containing a high part count.

Since RTSER testing typically involves a large number of devices and relatively long test times (weeks or months), a good test plan is crucial. It is extremely helpful to have some accelerated SER data (alpha particle and neutron) to get an estimate of the average failure rate. This estimate can then be used with the chi-squared statistics in annex C.2 to optimize the sample size and test duration so that the measured real-time SER will be valid to the desired confidence interval.

The procedures for non-accelerated RTSER and accelerated testing are similar. For real-time testing, the neutron flux is generally assumed to be a nominal value, based on the location of the ATE (see annex A). Alternatively, a measurement of the actual flux during the test may be made. This is a difficult measurement and beyond the scope of this specification. The alpha particle flux from the DUT packaging materials is assumed to be representative of the actual packaging. Separating the alpha and neutron contributions is complicated, requiring accelerated beam testing or system tests conducted at multiple locations. If RTSER results are to be used for SER estimates at other locations, this separation of effects is required. The minimum test procedures are listed separately below.

4.1.2 Guideline

The test method described below defines the requirements and procedures for RTSER testing without a radiation source, i.e., only the natural ambient background radiation due to terrestrial cosmic rays and alpha particles from packaging and chip materials. Accelerated SER testing with alpha particles, high-energy neutrons/protons, and thermal neutrons are discussed in **5**, **6** and **7**, respectively.

4.1.3 Scope of test method

This test method can be used to test large arrays of SRAM or DRAM memory, and can be adapted for use with other types of components, such as microprocessors. The RTSER test algorithm and hardware must have allowances for separating actual radiation induced soft errors from errors induced by system noise. Since the RTSER test method does not discriminate between alpha particle and neutron induced soft errors, doing real-time tests on the same components in different environments, such as in a cave for shielding the terrestrial neutron flux, at high altitudes for enhancing terrestrial neutron flux, and thermal neutron shielding for shielding thermal neutrons (see **6.6**) allow the alpha particle SER contribution (which will be constant when in secular equilibrium) to be separated from the terrestrial high-energy and thermal neutron-induced SER [10].

4.1.4 Goal of test method

The primary goal of RTSER testing is to obtain a well-defined estimate of the total soft failure rate for products/components using a uniform test methodology.

4.2 Test facilities and equipment

4.2.1 Basic electrical test requirements

The basic RTSER test requirement is to monitor each DUT's output vector and continually verify that the measured output matches the expected output vector or by using built-in self-test (BIST) features. A vector could simply be a pattern of data stored within the memory array of a DUT, or a stream of data generated as an operation or sequence of operations performed by the DUT on an input vector. The latter would be relevant for logic devices such as microprocessors. If the vector from the DUT does not match the expected vector, then a soft error may have occurred. The system consists of the input stimulus generator and response recorder that is designed to accommodate the specified device. Testing requires some sequence of writing data to the DUT, reading the data back, comparing the output data to the written data, and tabulating the number of detected errors.

4.2.2 DUT board hardware

RTSER testing requires a DUT board capable of supporting a large number of DUTs. Several DUT boards may be used in a single system. The boards can be controlled by a computer driven system or on a board controller that monitors and communicates with the DUTs during the test interval.

4.2.3 Test hardware

The test cables should be short enough and designed with the proper shielding to allow sufficient test speeds without electrical noise problems. If this is not possible, then on-board controllers should be used to allow high-speed operation of the DUTs and low speed communication off-board. The ATE should be capable of being configured to do both static and dynamic testing.

The following features are also desirable:

1) the ability to adjust and monitor the temperature of the DUTs or at least the ambient in which the DUT boards are located;
2) the ability to monitor power supply current of individual DUTs to check for latchup (preferably the ability to individually remove power from latched-up DUTs should also be provided);
3) if knowledge of the thermal neutron contribution is of interest, the ability to shield the DUT enclosure from background thermal neutrons to determine their contribution to the SER (see **7**);
4) operation at the rated core cycle for the DUT. If this is not possible due to power consumption issues, the deviation should be noted in the final report.

4.2.4 Test software

The basic requirements for a RTSER DUT test system software are as follows:

1) Create test conditions for the DUT. A suite of test patterns (or benchmarks) should be selected that represents the intended operation of the DUT. In general, the test program for memories or arrays of latches should include patterns of ones, zeros and more complex variations, such as internal checkerboards, alternating rows and alternating columns to determine if the component has any preferred data states that are more robust or can be affected by nearest neighbors.

2) Identify and record any errors based on the selected test conditions. If an error does not go away when the component is rewritten or power cycled (powered down and then powered up), then it is a hard or intermittent fail. Hard fail events should be noted in the final report with an explanation of the source (e.g., a latent defect in the DUT, an early life fail, a power supply malfunction, etc.).

3) Provide adequate fault coverage and failure bit mapping (or analysis of output results). This is effective in distinguishing multiple independent failures from a cluster of nearest neighbor upsets from a single multi-cell upset caused by a single energetic particle (MCU). If a redundancy latch is hit and brings a defective row or column back into a repaired memory array, the signature of the error pattern should be distinguishable from a normal SCU or MCU. Likewise, if latchup occurs in a memory array, the signature of that event (typically inducing a large number of contiguous failing bits) should be uniquely distinguishable.

4) Initialization of control devices and rudimentary functional checks. Any upset of the control devices or power supplies should be distinguished from upsets of the DUT.

5) Select operation mode (dynamic or static operation) and provide resetting capability. For example, static testing of memory would be to write a test pattern once and store it for an extended period before reading the pattern back out. Dynamic testing of memory would involve writing once and then reading continuously or interleaving write and read operations at a specified operating frequency.

6) Provide error detection and logging. If the embedded ECC capabilities of the DUT are being enabled, the user must understand the details of the ECC operation (e.g., code, error registers, bit interleaving, etc.)

7) Data analysis and logging while the test is in process. This is required to help separate independent events due to multiple particle hits from single events that upset multiple cells. (Note: This is less of a concern for real-time SER than accelerated SER due to the lower flux levels, but should not be ignored.)

8) Ability to distinguish and report different soft error types (e.g., single memory cell upset, multiple cell upsets, latchup, functional interrupts from hits on the address or control registers, etc.). See **2** for definition of types of soft errors.

4.3 Testing procedures

4.3.1 Pretest preparations

4.3.1.1 Sample selection

Component variability for RTSER is generally small for components produced with the same masks and fabrication steps. The system user must be sure that components tested are equivalent to actual baseline production components, because manufacturers may make process/design changes affecting SER without changing the component's designation or advising users of the changes.

In general a minimum requirement to establish a product's RTSER is to run the test with roughly equal numbers of nominal devices from at least three different baseline lots. If a product is tested that has on-board error-correction codes/circuits (ECC), tests should to be run under two conditions, both with ECC enabled and with ECC disabled if possible. The presence of ECC and its on/off status during each data collection run must be included in the final report. (Note: In general, ECC is effective at masking single-bit cell upsets. But it will be ineffective with non-cell related events such as neutron-induced latchup or other single-event functional interrupts).

4.3.1.2 DUT preparation and orientation

The DUT package used for the RTSER test must be identical to the package used for production components. This is critical for the alpha component of RTSER. If a finned heat sink is required, this can have an impact on the neutron flux reaching the DUT. Since there is some angular dependence for high-energy neutrons (more high energy neutrons have normal incidence to the Earth's surface - see **A.5**), the DUTs should be mounted horizontally to expose them to the maximum flux where the tester does not dictate otherwise. Care must be taken in considering the path of atmospheric neutrons in the real-time SER setup and the effects of building shielding. For example, vertical stacking of DRAM DIMMs that are each oriented in a horizontal position would cause a neutron to traverse many DRAMs before reaching the final device (see [11] for discussion of neutron attenutation through DUT cards). The possibility of generating secondary particles as well as the attenuation of flux could lead to anomalous results. Therefore, the orientation of the DUTs in real-time SER testing should avoid this. If this is not possible, an attempt should be made to note any differences in SER FIT between the top and bottom devices. Ideally, where other constraints do not exist, the testing location should also be done on the top floor or roof to avoid building shielding effects. Finally, the orientation of the DUTs and stacking of DUTs should be noted in the final report. If heatsinks are used, then their geometry (e.g., thickness, fin height and number, etc.) and material should be described in the final report. If the user also intends to do accelerated beam testing (Sec 6), the orientation of the beam should be similar to the RTSER testing.

4.3.1.3 Load DUT

Place the desired population of DUTs on each DUT board and run the test program to verify proper operation of all the DUTs. Make necessary adjustments to system and DUTs to insure that the test program executes flawlessly on all DUTs in the test system.

4.3.1.4 Effective neutron flux at the test location

When performing real-time SER testing, it is necessary to make estimates based on the amount of building shielding and the terrestrial neutron flux (see annex A). Measurement of the actual neutron flux is beyond the scope of most experimental programs . The results should be normalized to the reference high energy neutron flux (see annex **A)** in the final report for purposes of standardization. An estimate of sensitivity to thermal neutrons should also be made using thermal neutron shielding for part of the experiment (see **7.6**).

If the testing is to be done at high altitude, several factors should be taken into consideration when designing the experiment.

1) The cosmic ray dosimetry method and how it is monitored. If the facility has a dosimeter, it should be used but is not manditory. (See annex **A** for the expected neutron flux at the test location).
2) The electrical power features and stability of the facility. The test setup often requires an independently stabilized uninterruptible power supply to run the test. Note that the overall power consumption for a large sample size can be significant. Make sure that the facility can provide the required power with good stability.
3) The lab should be protected against electrostatic discharge from lightning (i.e., presence of a Faraday cage, a lightning rod, etc.)
4) The environmental conditions that influence cosmic ray flux and how they are monitored (i.e., temperature, hygrometry, average pressure, average accumulation of snow, etc). An assessment of the impact of the variation of these environmental conditions (either important or insignificant) should be noted in the final report. If variation is determined to be insignificant, an average condition can be used in the final report. General guidance on the threshold for significant variation is a 50% impact on measured SER. Annex A details the impact of altitude and barometric pressure. As a quick rule of thumb:

   Example 1 — a 40mmHg drop in atmospheric pressure (which is a significant change in weather conditions), will lead to a 50% increase in neutron flux.

   Example 2 — based on typical values of snow density (~0.4-0.5 gm/cm^3), the reduction in neutron flux due to attenuation by snow on a roof is approximately 50% for 5 feet of snow.
5) It is convenient to have real-time monitoring of the experiment remotely through Ethernet access, as well as a remote reset function so that full-time staffing is not required.

4.3.1.5 DRAM and SRAM testing

At the minimum, data patterns must include a logical (external) checkerboard pattern and its complement, alternating by address and by bit. This will average out any asymmetry in SER behavior and represent actual application of the device. Read and write cycles should be selected so that all the elements of the DRAM or SRAM circuit (sense amps, storage capacitor or latches, decoders, multiplexers, etc.) are vulnerable to upset.

If the design supports a broad frequency range and different circuit elements will show different soft error rates as a function of frequency, care must be taken in selecting the core clock. A recommended solution is to run the RTSER test at a nominal frequency defined either by the tester capability or the product specification sheet to get a calibrated overall upset rate. Since the RTSER results can be frequency dependent, the nominal frequency used and how it was selected should be noted on the final RTSER report. Accelerated SER testing (see **5**, **6** and **7**) can then be used to determine the frequency dependent upset rate of the various circuit elements.

4.3.1.5 DRAM and SRAM testing (cont'd)

For those DRAM and SRAM designs that support a standby or reduced power mode (i.e., read and write operations are not allowed, but the device is expected to maintain its memory), a fraction of the real-time SER testing time should be dedicated to this mode of operation. The final report should include the estimate of SER from this mode vs. normal operating mode.

4.3.1.6 Other device testing

It might not be appropriate to use real-time SER testing procedures on all device types. Memory devices are good candidates because these devices are dominated by the core array and it is possible to capture and log all cell related upsets. Likewise, any FPGA or ASIC technologies using a high SRAM or DRAM content would be good candidates. On the other hand, not all upsets in logic devices will propagate to the output. This will depend on the static and dynamic design elements used. Therefore, an estimate of the expected fail rates should be made initially and the counting statistics discussed in annex B should be use to determine if a real-time SER test is appropriate for a device. Likewise, use of systems with large memory installations (like super-computers or server data-centers) might be appropriate for RTSER measurements. However, the user should be aware of confounding effects that happen at the system level (see **4.4**).

4.4 Differences in real-time soft error tests and actual end-user observed fail rates

While the error rates determined from real-time SER testing are representative of device performance under real-life radiation conditions (both alpha particle and atmospheric neutrons), the results are not necessarily directly applicable to end user system applications. In addition to the customer environmental conditions that can be accounted for using annex A (i.e., geomagnetic location, altitude, building construction, etc.), other factors that need to be taken into consideration in translating real-time SER FITs to actual end user error rates include (but are not limited to):

1) Geometry of end user system (e.g., Are components stacked? Are they above or below the system board? Are the system boards stacked? Are the system boards oriented parallel or perpendicular to the background radiation? etc.)
2) How are errors detected (e.g., by ECC or by comparing read data to write data)? Are all errors reported? For example, are hardware ECC errors reported to error registers? If multiple errors occur within a short period of time, will error registers be overwritten, loosing information about earlier errors?
3) How is determination made between a soft error event and signal integrity/noise, weak cells, hard fails?
4) What measures are taken to prevent multiple counting of a single event? For example, if hardware ECC corrects the error for the user but leaves the write-correct to a slower software operation, will the same event be counted multiple times (i.e., many hardware reads to same address before software corrects the data in memory)?
5) Can multiple errors from a single event be distinguished from single errors from multiple events?
6) What types of errors are masked by software error handling codes of the application?
7) What fraction of errors will be over-written before they are read? (Highly sensitive to application software.)
8) What fraction of errors will not be reported because they are not utilized by the application? This includes both unutilized memory as well as memory written to but never read.
9) Is the end-system using standard packaging or heat sinks (i.e., is the device packaging used in the system the same as the packaging used in the test configuration)?

5 Accelerated alpha-particle test procedures

5.1 Background

5.1.1 Introduction

Uranium and thorium impurities and their daughter products found in trace amounts in the various production and packaging materials as well as ^{210}Po contamination of lead and tin emit alpha particles. Alpha particles are strongly ionizing, so those that impinge on the active device create bursts of free electron-hole pairs in the silicon. This charge disruption can be collected at pn junctions (much like charge created by light), producing a current spike (noise pulse) in the circuit. These current spikes can be large enough to alter the data state on some circuits. This section deals with the method of determining a component's sensitivity to alpha particle radiation from accelerated experiments.

5.1.2 Scope

This section deals strictly with SER induced by alpha particles and the techniques of using intense alpha particle sources to accelerate the alpha SER and use the ratio of this source emissivity to the package emissivity in order to determine the device alpha SER. The alpha flux is independent of altitude, and is only a function of the type, location, and amount radioactive impurities present in the component or its package.

Alpha particle SER data cannot be used to predict high- or low-energy neutron cosmic-ray-induced failure rates. Conversely, neither can high-energy neutron nor low-energy neutron SER data be used to predict alpha-induced failure rates. An overall assessment of a device's soft error sensitivity is complete ONLY when the alpha AND high- and low-energy neutron induced failure rates have been accounted for.

5.1.3 Safety issues

All of the accelerated test procedures involve the use of ionizing radiation sources that are potentially hazardous. Proper safety and monitoring procedures are essential for tests utilizing these sources.

Test hardware and parts may become contaminated with radioactive material when recoil fragments or larger fragments of the radioisotope escape the alpha source encapsulation. Good ventilation should be provided as some unsealed alpha sources may emit radon as a decay product. When not in use, alpha sources should be stored away from personnel as most alpha sources also produce low-level gamma radiation. Alpha sources should be handled with care even though external alpha emission is not hazardous (alpha particles have insufficient energy to penetrate the dead layers of the skin). Alpha emitting contaminants are extremely hazardous if inhaled or swallowed as alpha particles damage living tissues inside the body. It is the responsibility of the user of this test method in consultation with radiation safety personnel to establish the appropriate safety and health practices and the applicability of and compliance with local, state and Federal/National regulatory limitations. Gloves should also be used in handling the source to prevent accidental contamination of other locations. The user should check if a license is required to operate a source used in this study and will need to go through a compliance process that is beyond the scope of this spec. (Each country or state will have its own regulations.)

5.1.4 Guideline

The test method described below defines the requirements and procedures for accelerated SER testing with alpha particle radiation. Generalized real-time (unaccelerated), or field testing has been dealt with in 4, while accelerated testing for SER induced by cosmic radiation is dealt with in 6 (high-energy) and 7 (low-energy).

5.1.5 Limits of test method

The accelerated test method in this section applies ONLY to alpha-particle-induced events. It does NOT apply to terrestrial-cosmic-radiation-induced events or events induced by the reaction of thermal neutrons with ^{10}B. This test method can be applied to the testing of memory, sequential logic, combinational logic, or components combining these circuit types.

5.1.6 Goal of test method

The end product of this accelerated testing is a well-defined estimate of the alpha-particle-induced failure rate for components. The soft failure rate can be characterized as a function of voltage, timing, and possibly other operating variables.

5.2 Alpha particle environment

See detailed description in annex D.

5.3 Packaging for alpha particle testing

Unlike accelerated high energy neutron and proton test methods where the package type is not critical, for accelerated alpha particle testing the DUT's surface must be directly exposed to an isotope source without any intervening solid material and with a minimal air gap.

Recommended DUT package types are the ceramic dual-in-line (CERDIP) or pin-grid array (CERPGA) package, as illustrated in Figure 5.1a and Figure 5.1b respectively. Certainly, other package types that offer access to the top surface of the chip can also be used but these types in particular are mechanically robust, particularly when used with zero-insertion force (ZIF) sockets allowing reliable loading and unloading over many cycles.

The die should be mounted and wirebonded within the well or cavity such that the surface of the die is as close as possible to the top surface of the package without anything, such as the bond wires, projecting above this plane. This configuration is required to minimize the alpha source-to-die spacing, while providing a convenient indexing surface for the isotope source. The metal lid for the package should be installed with tape to protect the DUT between tests.

If the product to be tested is already encapsulated in a plastic package, the material over the die must be etched back to fully expose the active area. If die coating is used in the product, the user should be aware of whether or not the die coating is removed during this package deprocessing. This information will be required in translating the accelerated alpha SER into real-time alpha SER. In this case it is best to have unpackaged, but coated, samples of the DUT provided by the manufacturer for alpha testing, rather than attempting to etch back the existing packaging material. Lead-over-chip (LOC) packages are not suitable since the lead frame shadows a large portion of the device. Product or test chips with solder bumps distributed over the face of the die (for flip-chip attachment) are also not suitable for the same reason.

5.3 Packaging for alpha particle testing (cont'd)

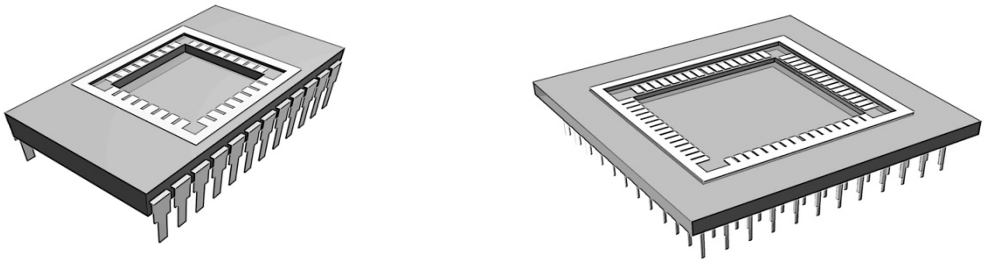

a) b)

Figure 5.1 — Recommended packages for alpha particle testing, a) ceramic dual-in-line package (CERDIP), and b) ceramic pin-grid array (CPGA).

Wafer-level testing can also be used to perform alpha-particle testing. The wafer-level test system must have a probecard configured to allow the alpha particle source to be placed accurately and in close proximity to the die without shorting the probe pins or the pins shadowing the source.

Many ICs use flip chip packaging (i.e., the die faces down in the package and its electrical connections are made through some form of metal bump or pillar). In this case, it is not easy to gain access to the surface of the die for alpha testing. Accelerated alpha SER testing can be accomplished by thinning the backside of the die and introducing the alpha source to the back of the device. Because alpha particles are strongly attenuated by silicon (see Fig D.3 of annex D), uniformity and measurement of the thickness of the remaining silicon is important. The user should first consider the source of alpha contamination from the flip chip package (typically from the pre-solder paste and metal bumps), estimate the energy and range of those alpha particles through the top layers (die coat, metal interconnects and dielectric layers). An alpha source and silicon thickness can then be selected that will mimic the energy deposition from the package materials. Due to the issues with respect to thinning the backside, it is recommended to do wafer level alpha SER testing instead.

5.4 Alpha particle sources

5.4.1 Alpha source selection

The alpha source should be selected considering the alpha emission from the impurites of the package type. The following factors should be considered:

1) Maximum Energy – 5.3MeV ^{241}Am vs 8.79MeV ^{232}Th (see annex D)
2) Energy Distribution – monoenergetic energies from thin foils vs broad spectrum from thick films (see annex D)
3) Source Emission Uniformity
4) Source Size (see **5.5.2**)
5) Source Activity – sufficient flux to create a statistically significant amount of soft errors. This requires that the user has some estimate of the range of the soft error rates to be expected, either from prior devices of similar design or a literature search of other alpha soft error work.

5.4.1 Alpha source selection (cont'd)

Sources that emit alpha particles with energy spectra similar to uranium and thorium impurities simulate the radiation environment of wirebonded components encapsulated in molding compound. Sources that emit alpha particles with similar energy spectra to ^{210}Po are used for simulating components in a flip-chip arrangement with solder bumps. Aside from the issue of 1) mono-energetic vs thick sources and 2) source uniformity, an ^{241}Am source might be advantageous over a ^{232}Th source because of its higher emission rate. A ^{232}Th source emission rate is fixed by its specific activity and easily calculated and measured assuming the daughter products are in secular equilibrium (steady state). Substitution of a source of a different energy spectrum should be noted in the final report.

Pure radioisotope foils or metallic substrate foils with the radioisotopes deposited or diffusion-bonded may be used. Solid sources that are physically thicker than the range of the highest energy alpha particle emitted are best since the alpha spectrum will be distributed as it would be in the real packaged device.

Since the range of alpha particles in metals is limited to < 40um at 10MeV, a solid source at least 0.04mm thick should ensure a distributed spectrum is emitted. Thin-film sources produce a mono-energetic spectrum (see Figure D.1) that is typically not representative of the distributed spectrum (see Figure D.2) that would occur in a real packaged device. This can lead to variation in resulting charge deposition profile in the device (see Figure D.3). These effects should be taken into account along with the availability of alpha sources before designing the experiment.

The energy spectrum should be measured and the emissivity calibrated on a regular basis (more frequently for sources with short half-lives) to ensure that the source is providing the expected spectrum and flux. The source area should ideally be larger than the device area to ensure that all angles of incidence are allowed.

An alternative is the use of an ion accelerator to provide a monoenergetic and uniaxial beam of alpha particles. The disadvantages of accelerators are the experimental complexity, beam time cost and the fact that many runs will be needed at different energies and angles to obtain the alpha SER. The advantage is that the localized and collimated beam allow identification of sensitive areas and angle dependencies that anisotropic, uncollimated radioisotope sources cannot provide.

5.4.2 Alpha particle source calibration

Alpha sources lose activity by sputtering induced by fragments ejected from the source. Annual calibration is recommended to ensure that the source flux is known, particularly for high activity sources whose intensity can change dramatically over a short period. The type, activity, physical configuration of the radioisotopic source, energy spectrum (if available), and date of last calibration must be included in the final report. Ion accelerator sources must be calibrated and the flux measured from time-to-time to ensure it is at the expected levels, which is usually part of ion source facility standard procedures.

5.4.3 Alpha particle source fluence

The total number of particles incident during a test must be sufficient to establish with a high statistical confidence that the entire sensitive volume on the DUT has been irradiated. A fluence and test time should be selected to meet the desired accuracy of the soft error rate (FIT with confidence level). See annex **B** for discussions on statistically based confidence levels.

5.4.4 Alpha particle source intensity and uniformity

The user should make sure that the measurement equipment can handle the error rate induced by the alpha source (linearity concern – see Sec 3 for discussion and make adjustments if required).

It is recommended that for large area (i.e., radius > 1 cm) alpha particle sources, the user should specify a +/- 10% uniformity or better for the activity across the active area of the source to their supplier. One of the ways a supplier or a user to can check the uniformity is to perform an activity distribution measurement. Examples of some techniques are:

1) For a source with a large radius (>2.5cm), one can use an SRAM test chip with a small active area or opening (i.e., smaller than 1cm x 1cm) to expose the device to different regions of the source simply by using small displacement of the source over the chip. The error counts from different parts of the source can then be used to determine the variation of activity across the source.
2) The source to DUT gap can be increased and if there is variation in the soft error rate (increase in some areas of the DUT and decrease in other areas of the DUT), this indicates radial variation of the source. With a uniform source, one would expect to see a monotonic decrease in the soft error rate due to attenuation of the alpha energy by air.
3) Another way to measure source uniformity is to scan the source across a small aperture and detector.

5.4.5 Loading the alpha source

After the component or wafer has been loaded and verified to be functioning as expected, a background test is run with no source as described in **3**. When this test is complete, the appropriate alpha source is centered over the DUT. The source-to-DUT spacing should be made as small as physically possible – **a spacing of less than 1mm is recommended**. The actual spacing must be recorded in the final report, especially important if a spacing of ≤ 1mm cannot be used. The active area of the alpha source should be larger than the device area and must also be recorded on the final report. Great care must be used to ensure that the surfaces don't touch, since any contact could short the device. The recommended configuration is shown in Figure 5.2 for a wire bonded device. The source should be handled with dedicated plastic tweezers and not metal tweezers to prevent damage at the source surface.

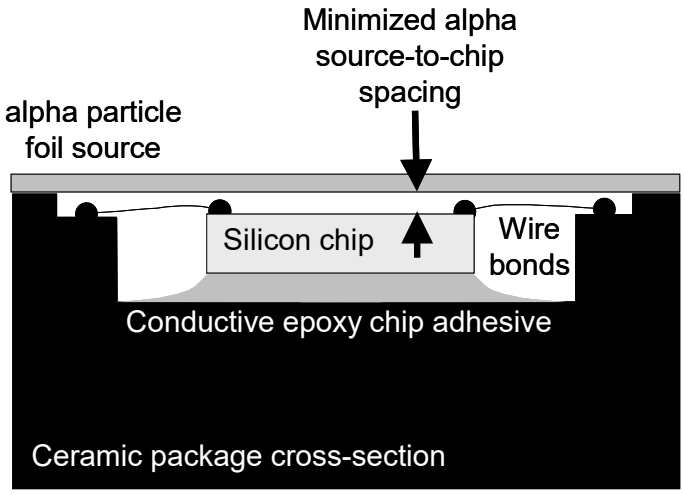

Figure 5.2 — Cross-section through ceramic package illustrating recommended alpha source size and placement – larger than the chip and as close to the chip as possible.

5.5 Test procedure and results

5.5.1 Basic alpha particle flux acceleration factor

The intensity of alpha particle sources is often reported in the International System of units (SI), the becquerel (Bq), representing a radioactivity of 1 disintegration/sec into 4 pi steradians (a spherical volume). To obtain a surface emission of alpha particles in $cm^{-2}h^{-1}$ (a hemispherical volume), the source can be placed in a detector capable of measuring the alpha particle flux. Since the high rate of alpha events from typical alpha sources can overwhelm the response of many standard detectors, care must be taken to ensure that the source activity is not underestimated.

A basic alpha particle source acceleration factor is simply the ratio of the number of alpha particles per unit time emitted by the source and those emitted by the packaging materials in contact with the die surface in the final component (the standard unit is cm^2-hr) as shown in Equation 5.1.

$$Acceleration\ Factor = \frac{Alpha\ Particle\ Source\ Flux}{Packaged\ Component\ Alpha\ Flux} \sim 10^5\ to\ 10^{14} \tag{5.1}$$

Depending on the emissivity of the alpha source selected, a large range of acceleration factors available. Ultimately the acceleration factor used should be determined by the desired test time and total dose and sensitivity considerations.

This simple acceleration factor cannot directly be used to extrapolate the alpha particle SER because of geometry and absorption effects that must be accounted for (See Equation 5.2).

NOTE 1 The alpha emissivity of the package materials can be specified and controlled in the manufacturing process (controlled alpha material) or determined by a statistical sampling (uncontrolled alpha material). For uncontrolled material, there is no guarantee that the alpha emissivity will not spike out of control at a later date. The method of determining the emissivity of materials used in manufacturing must be noted in the final report. If the user is concerned with alpha SEU rates for their product, ultra-low alpha or controlled alpha material should be specified.

NOTE 2 Accurate measurement of low alpha emissivity materials (~1 to 10 α/cm2-khr) is difficult and can lead to variation of up to 1.7x from site to site [12], [13].

5.5.2 Geometry factor and shielding

If the accelerated alpha SER test is performed in a vacuum with a source that is very much larger than the component being tested, with a known and calibrated source flux and with a small DUT-to-alpha source spacing (< 1 mm), the need for an accurate geometry calculation is minimized, since the acceleration factor will be close to the ratio defined in Equation 5.1.

In most test situations however, a more elaborate model is needed to accurately determine the flux incident on the component. In general, **not accounting for, or miscalculating geometry and shielding factors leads to significant errors in the extrapolated alpha SER of the actual component**. Using a simple analytic model for a circular DUT and alpha source centered about a central axis [14], the effect of source size and source spacing on the alpha flux incident on the DUT area were calculated (Figure 5.3). The dotted line represents the point source approximation. When both the source and device are the same size (solid squares) with a spacing of 1mm, the incident flux is reduced by more than 30%! For a larger source area (solid triangles) at the 1mm spacing the reduction in flux is nearly 10%. Clearly, minimizing the source-device spacing and using a source that is larger than the device being tested ensures that errors are minimized.

5.5.2 Geometry factor and shielding (cont'd)

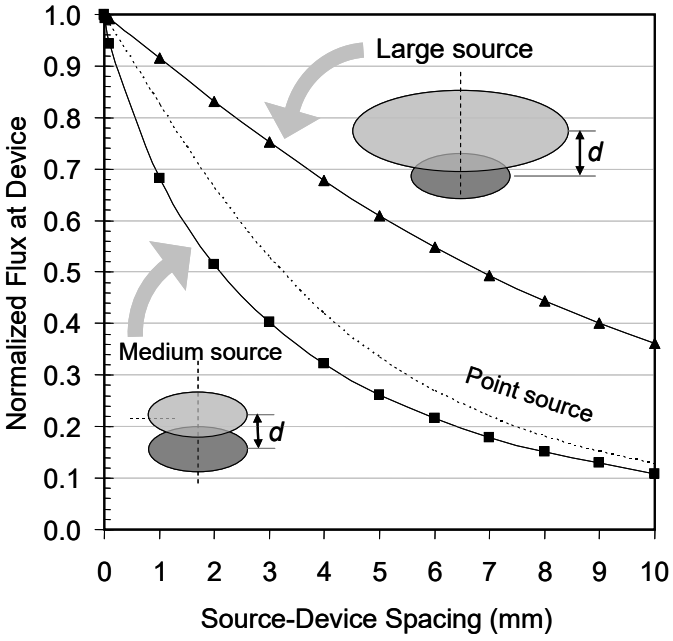

Figure 5.3 — Normalized alpha flux, averaged over the entire device area, incident on a device as a function of the source-device spacing and the source size.

The calculation shown here is given only as an example. For rectangular component areas these curves fall-off even more rapidly with increased spacing. Actual device and source geometries can be calculated more accurately with computer modeling accounting for typical test situations such as rectangular die and non-axial alignments. The final alpha flux incident on the active device area must be recorded in the final report.

NOTE If a thin-film source with mono-energetic spectra is used, see annex D, the air gap will introduce some energy dispersion effects along with a reduction of the flux. This effect might actually maximize the measured SER by fine-tuning the alpha particle energy to stopping range in the device (Bragg Peak). While this technique can be used to characterize the sensitive volume of the device, the intent of this specification is to allow extrapolation of accelerated alpha SER to real use conditions. In most cases, the package is either in intimate contact, for plastic mold compound or underfill, or very close proximity, for ceramic packages.

A further complication results if a test chip is being used to extrapolate the SER of a different component. The extrapolation will only be accurate for a component that has the same number, type, and thicknesses of metal, dielectric, passivation, and polyimide layers. Often test chips have fewer metal layers, while production components have significantly more layers, providing a higher level of alpha particle shielding. Not accounting for, or miscalculating the loss of alpha flux from shielding during testing and in the actual production component can lead to significant errors in the final extrapolated SER.

To properly account for shielding it is strongly recommended that simulations to determine the differences in shielding due to differences in the number of different layers, or controlled accelerated SER experiments with components utilizing different numbers of metal layers be performed.

5.5.3 Extrapolating the failure rate to use conditions

To determine the actual field product failure rate from soft errors requires extrapolating the accelerated test results to use conditions. The product SER under normal use conditions can be obtained by multiplying the observed SER (rate of soft errors) during the accelerated testing by the ratio of the alpha particle flux reaching the DUT active device area under normal use conditions and the alpha flux reaching the DUT active device areas during the accelerated test according to Equation 5.2.

$$Unaccelerated\ Alpha\ Particle\ SER = \frac{(\dot{\Phi}_{pkg}) \cdot (F_{geopkg}) \cdot (F_{shieldpkg})}{(\dot{\Phi}_{dut}) \cdot (F_{geodut}) \cdot (F_{shielddut})} \cdot ASER \quad (5.2)$$

where ASER is the soft error rate obtained from the DUT during accelerated testing (number of errors for a given number of alpha particle events), and in the numerator of the ratio, $\dot{\Phi}_{pkg}$ is the alpha particle flux reaching the actual production component ($cm^{-2}h^{-1}$), F_{geopkg} is the geometry factor associated with the production component (usually this is 1 unless there is some distance between the chip surface and the final packaging materials see Figure 5.3), and $F_{shieldpkg}$ is the amount of shielding, respectively, in the final production package (this accounts for energy lost by alpha particles traversing metal layers and polyimide layers). In the denominator, $\dot{\Phi}_{dut}$ is the alpha particle flux reaching the DUT during the experiment (normalized to $cm^{-2}h^{-1}$), F_{geodut} is the geometry factor during the experiment (defined by the source-to-die spacing and source and die size, offset, etc.), and $F_{shielddut}$ is the amount of absorption loss (due to polyimide and metal layers), respectively, in the DUT under the accelerated experimental conditions. As mentioned earlier, since the accelerated source uses an alpha particle source with a flux that is significantly higher than the nominal package environment, this ratio will always be much less than 1 and consequently the unaccelerated SER will be significantly lower than the SER observed during accelerated testing. This equation and method are not part of the actual requirement, however, all alpha particle SER data must include a description of the assumptions made for geometry factor and shielding along with all experimental parameters (e.g., source size, DUT active area, source-to-DUT spacing, etc.) that would enable an outside observer to verify that the assumptions used were valid.

NOTE 1 This equation makes the simplifying assumption that all the sources of alpha particles are coming soley from the packaging material and not the wafer or wafer fab material. Actual geometry and absorbtion effects can be quite complex [15]. If the user chooses to take these into account and do a more thorough analysis than Equation 5.1 and 5.2, the details should be stated in the final report.

NOTE 2 Equation 5.2 applies to each individual type of soft error event (e.g., SCU, MCU, SEL, SEFI, etc.). The count of different types of soft error events should be kept separate in calculating the accelerated soft error rate (ASER) and the final report should provide the information used to calculate each type of unaccelerated alpha particle SER.

If the same metal-dielectric stack is used both for the test component and the final product, then $F_{shieldpkg} = F_{shielddut}$ thus simplifying the extrapolation. If the alpha source used for the accelerated testing is placed in direct contact with the active layers and is sufficiently large to mitigate edge effects, assuming that packaging materials were in direct contact with the final product die, then $F_{geopkg} = F_{geodut}$. In reality, due to practical and safety concerns, the alpha source will generally not be placed in direct contact with the die so the geometry factor will probably need to be calculated.

Finally, it is not uncommon to use dedicated test structures instead of the final product during accelerated testing. This is particularly true in cases where a technology's alpha-particle SER sensitivity is being determined prior to actual qualified production. It is recommended that alpha testing of at least a few actual production components be done following test chip data to ensure that the test chip used is representative of the SER sensitivity in actual products.

5.6 Interferences

5.6.1 Total dose

Some parts may suffer total dose damage. This damage may show up as hard failures or as parametric degradation. Parametric degradation may affect the soft error rate and is also an indication that the device is approaching the level where significant damage is occurring. Dose damage may also manifest as timing sensitivity where the DUT may fail at its rated speed but operate adequately at lower speeds

If total dose is a problem, it may be necessary to reduce the targeted number of failures or distribute testing over more DUTs. Total dose effects are evaluated by subjecting a DUT to the same test conditions for the first and last tests of a series. If the results are the same, within experimental error, then total dose is not affecting the results.

5.6.2 Package shadowing

Packaging materials between the top surface of the die and the alpha particle source may attenuate the alpha flux and energy leading to errors in the calculated error rate. This includes die coats, encapsulants, package lids, and surface contamination such as fingerprints.

Another concern is the use of polymer (polyimide, etc.) layers as mechanical stress relief and for shielding alpha particles. If these layers are used in the final product, the test chip used for alpha particle characterization should have these layer as well. If the test chip does not, then layer absorption simulation methods must be used to determine the effect of these layers in the final product, since depending on the thickness and density of the layers, they may make the final SER better or worse than what is extrapolated from the test chip without the layers.

NOTE While it might be straightforward to calculate the attenuation of alpha particles of different energies by a die coat of a given thickness using programs like SRIM [16], it is much more difficult to assess the impact on soft error rate by moving the peak energy deposition closer to (or farther away from) the active region of the device (see Figure D-3). For this reason, actual measurements with the die coating in place are preferred over simulation techniques.

If the product die is in a flip-chip package, access to the die surface is an issue. Furthermore, even in die form, overlying solder bumps or other materials that mask portions of the active areas from radiation access prevent testing of devices in this configuration. Backside etching to expose the active silicon region may be considered. In this case, the device must be etched to within a few microns of the active silicon region to expose it to an external alpha source. Note that self-heating properties may change with thinner silicon. If this method is used, some testing to demonstrate its equivalence to conventional front side irradiation is required to justify results.

6 Accelerated high-energy neutron test procedures

6.1 Background

6.1.1 Introduction

When cosmic rays enter Earth's atmosphere, they collide with atomic nuclei in air and create cascades of particles of every kind, some of which reach the ground. Among these terrestrial cosmic rays are particles which interact strongly with nuclei: primarily neutrons, plus some protons and a few pions. These particles interact with Si and other nuclei in the electronic device and package via strong nuclear interactions. These processes produce a variety of secondary particles - protons, neutrons, alpha particles and heavy recoil nuclei. Some of these secondary particles are strongly ionizing, so those that impinge on the active device create bursts of free electron-hole pairs in or near the active region. This charge disruption can be collected at pn junctions (much like charge created by light), producing a current spike (noise pulse) in the circuit. These current spikes can be large enough to alter the data state and other single event effects. This section deals with the method of determining component sensitivity to high-energy neutron events from accelerated experiments.

6.1.2 Scope

This section deals strictly with soft errors induced by high-energy neutron events. The high energy neutron flux is dependent on altitude, latitude, longitude, barometric pressure and solar activity (see Annex **A**).

High-energy neutron soft error data cannot be used to predict alpha particle or low-energy neutron (i.e., thermal neutron) cosmic-ray induced failure rates. Conversely, neither can alpha particle nor thermal neutron soft error data be used to predict high-energy neutron-induced failure rates. An overall assessment of a device's soft error sensitivity is complete ONLY when the alpha, high-energy neutron AND thermal neutron induced failure rates have been accounted for.

6.1.3 Guideline

The test method described below defines the requirements and procedures for accelerated soft error testing with high energy proton and/or neutron radiation. Real-time SER testing is dealt with in **4**, while accelerated testing for soft errors induced by alpha particles is dealt with in **5** and soft errors induced by thermal neutrons is dealt with in **7**.

6.1.4 Limits of test method

The accelerated test method in this chapter applies ONLY to terrestrial-cosmic-ray-induced events, which are dominated by high energy (E> 10 MeV) atmospheric neutrons. It does NOT apply to alpha-particle events or events induced by the reaction of thermal neutrons with ^{10}B. This test method can be applied to the testing of memory, sequential and combinational logic, or components combining these circuit types.

6.1.5 Goal of test method

The end product of this accelerated testing is a well-defined estimate of the high-energy neutron induced error rate for components using a uniform methodology. The soft failure rate can be characterized as a function of voltage, timing, and possibly other operating variables. For standardization purposes, the reference level for the high energy terrestrial neutron flux above 10 MeV is 3.596×10^{-3} cm^{-2} s^{-1} or 12.946 cm^{-2} h^{-1} (see annex **A**).

6.2 Test facilities

To simulate how the atmospheric neutrons induce single event effects in microelectronic components at a highly accelerated rate, high energy particle beams may be used. Three different types of facilities are discussed in this chapter which provide such high energy particle beams: 1) spallation neutron source, 2) quasi-monoenergetic neutron source and 3) monoenergetic proton and neutron sources. Neutron and proton facilities available for soft error testing are discussed in annex **E**.

Spallation neutron sources provide neutrons over a wide range of energies, with the shape of the spectrum being similar to that of the terrestrial neutron environment. Annex A contains the details of the terrestrial neutron spectrum and 6.6 compare the spectra from the spallation neutron sources to that of the terrestrial neutron spectrum.

There is limited access to spallation neutron sources. Therefore monoenergetic neutron and proton sources have been shown to be effective for measuring the soft error response of products and circuits at several energies, which can be used to obtain the soft error rate from the full spectrum of the terrestrial neutron flux. The details for utilizing the monoenergetic soft error data from protons and neutrons is discussed in **6.5.**

In addition, there is a related source, a quasi-monoenergetic neutron source that may be utilized to measure monoenergetic SEU responses at high energies. This source is discussed more fully in **6.5**.

6.3 Angular Dependence Considerations

The angular dependence of terrestrial neutrons is complex. Neutrons above 10MeV have a predominantly vertical angle of incidence (perpendicular to the ground) because they are primarily from spallation in the upper atmosphere. Neutrons in the 1 – 10MeV range are more isotropic due to secondary scattering and energy loss taking place in the local environment (see annex **A** for more detail). Device orientation in actual applications can be horizontal or vertical. Due to these complications, it is recommended to perform tests with the beam at normal incidence as a minimum requirement. It is up to the user to determine if additional angles of incidence are needed.

6.4 Beam parameters

6.4.1 Beam check

Most facilities provide beam calibration and have published results on energy spectrum, flux, beam uniformity, etc. The user should consult with the beam facility manager on these details.

NOTE A technique to monitor the fluence of the beam in real time should be used to allow for accurate estimation of the integrated particle dose. If this is not possible, then periodic sampling of the beam fluence should be used between DUT exposures.

6.4.2 Beam fluence

In determining the beam fluence required (beam flux x test time), the user should have an initial idea of 1) the accuracy of the soft error rates to be established and 2) prior knowledge or published literature of the range of soft error rates expected.

EXAMPLE 1 – The user wishes to establish an upper bound to the SEL rate with a 90% confidence level. For a beam flux that is 10^7 more intense than the terrestrial neutron flux ($\dot{\Phi}_{ref}$ = 12.95 n/cm^{2}hr, see annex A), a 1hr test time is a fluence of 1.295 10^8 n/cm^2. If 0 SEL events are observed, then the upper bound of the SEL rate is (see annex B and C for statistical discussion and the inverse chi square function, X_{inv}):

$$SEL\ FIT = \frac{1}{2}\,\mathrm{X}_{inv}(probability, degrees\ of\ freedom)\ \frac{\dot{\Phi}_{ref}}{\Phi_{beam}\cdot test\ time}\ 10^9$$
$$= \frac{1}{2}\,\mathrm{X}_{inv}\big(90\%, 2(0+1)\big)\ \frac{12.95}{1.295\cdot 10^8}\ 10^9 = 230\ FIT$$

That is, if no SEL events are observed, the user has only established to a 90% confidence level that the SEL rate is ≤ 230 FIT. If determination of a lower FIT is desired, the user must increase the fluence. If a 10x increase in fluence is used (by either increasing the beam flux or extending the exposure time) and there are still 0 SEL events observed, then

$$SEL\ FIT = \frac{1}{2}\,\mathrm{X}_{inv}(90\%, 2)\ \frac{12.95}{1.295\cdot 10^9}\ 10^9 = 23\ FIT$$

This example shows how using more fluence, especially in cases with a null cross section, will decrease the FIT estimate.

EXAMPLE 2 – If the user wishes to determine to a high degree of accuracy that the single cell upset rate (SCU) is within a certain range, then many SCU events will have to be observed. For example, if 1 SCU events is observed for a fluence of 1.295 10^7 n/cm^2, then the upper and lower bounds are

$$SCU\ FIT\ (90\%\ upper\ bound) = \frac{1}{2}\,\mathrm{X}_{inv}(90\%, 4)\ \frac{12.95}{1.295\cdot 10^7}\ 10^9 = 3890 FIT$$

$$SCU\ FIT\ (10\%\ lower\ bound) = \frac{1}{2}\,\mathrm{X}_{inv}(10\%, 4)\ \frac{12.95}{1.295\cdot 10^7}\ 10^9 = 532\ FIT$$

That is, there is a 10% probability that the SCU rate is **above** 3890 FIT and a 10% probability it is **below** 532 FIT. If this is too wide an interval, the user can increase the fluence by 100x to observe 100 SCU events and obtain

$$SCU\ FIT\ (90\%\ upper\ bound) = \frac{1}{2}\,\mathrm{X}_{inv}(90\%, 202)\ \frac{12.95}{1.295\cdot 10^9}\ 10^9 = 1141\ FIT$$

$$SCU\ FIT\ (10\%\ lower\ bound) = \frac{1}{2}\,\mathrm{X}_{inv}(10\%, 202)\ \frac{12.95}{1.295\cdot 10^9}\ 10^9 = 884\ FIT$$

which is more than a 10x decrease in the uncertainty of the FIT (see Figure C.1).

6.5 Fundamental quantities: soft error cross-section and soft error rate

There are two complementary quantities to characterize the soft error sensitivity of a chip/circuit: (1) the soft error cross section, and (2) the soft error rate, also known as soft error rate (SER), or soft fail rate.

The soft error cross section is an *intrinsic parameter* of a chip/circuit that specifies its *response to a particle species* (e.g., neutron, proton, pion, heavy ion, etc.). It is measured using a beam of particles produced at an accelerator. The soft error cross-section depends on the particle type and particle energy. In general it is also a function of the operating conditions of the irradiated chip (e.g., applied voltage, temperature, etc.). The units commonly used for soft error cross section are cm^2/bit, cm^2/Mb or cm^2/device.

The soft error rate is a measure of a chip or circuit *response to a particular type of radiation environment*. Its value varies from one location to another, depending on the radiation environment that is present. For example, due to the variations of the terrestrial neutron flux (altitude and geomagnetic effects), the neutron-induced soft error rate of a chip is larger at high altitudes than at sea level. Also the soft error rate is lower at locations close to the geomagnetic equator, compared with locations close to the geomagnetic pole. The computation of terrestrial neutron flux is essential for the evaluation of fail rates, and it is discussed in annex A.

For terrestrial applications, based on the knowledge of soft error cross section (as a function of particle energy) and the particle energy spectrum at a given location, the soft error rate at any given location can be computed. It is important to note that from the soft error rate measurements alone one cannot extract any information on the energy dependence of soft error cross section. In general the equation that relates soft error rate with soft error cross section cannot be inverted to solve for the soft error cross section from a given soft error rate (see Equation 6.14 formulated in **6.5.4.1**).

Proton-induced and neutron-induced soft error cross sections are often used interchangeably as the basic parameters to characterize soft error sensitivity. Protons and neutrons interact with semiconductor materials via nuclear reactions. Over a wide energy range, e.g., MeV to GeV, these reactions produce charged, ionizing fragments like alpha particles, recoil nuclei and other secondary particles; these secondary particles induce upsets in circuits. In general the nuclear interactions of protons and neutrons with most semiconductor materials (especially light elements like Si and O) are very similar for incident particle energies above 50 MeV [17]. Therefore, ≥50MeV protons can be used in place of equivalent energy neutrons.

6.5.1 Soft error cross-section dependence on type of facility

The list of neutron an proton facilities available is found in annex **E**. Here we summarize the basic measurements made in these facilities during soft error testing.

6.5.2 Measured quantities using particle beams

6.5.2.1 Monoenergetic proton beam: proton-induced soft error cross-sections at E_p

Proton-induced soft error cross sections are measured using a monoenergetic proton beam. They can be defined in two ways (per device or per bit):

$$\sigma_{p\text{-}dev,i}(E_p) = N_{p,i} / (\Phi_{proton}) \quad (6.1)$$

and

$$\sigma_{p\text{-}bit,i}(E_p) = N_{p,i} / (\Phi_{proton} \times N_{bit}) \quad (6.2)$$

In Equations 6.1 and 6.2, E_p is the proton energy; $N_{p,i}$ is the number of soft error events of type i (e.g., i=1 could represent a single cell upset, i=2 could represent a multi-cell upset, i=3 could represent a single event latchup, etc.) measured in the irradiated sample during each test; Φ_{proton} is the fluence of the protons to which the device was exposed in units of protons/cm^2; N_{bit} is the number of bits in the sample under test; $\sigma_{p\text{-}dev}(E_p)$ is in units of cm^2/device and $\sigma_{p\text{-}bit}(E_p)$ is in units of cm^2/bit. Equation 6.1 is general for all devices (logic and memory). Equation 6.2 is more applicable to memory arrays.

Example 1 – A device displays a single event latch-up (SEL) every 10 minutes with a 100MeV proton flux of 10^7 protons per cm^2 per second. The SEL cross-section of the device is 1 event/(10^7 protons per cm^2 per second x 600 seconds) = 1.67 10^{-10} cm^2 at 100 MeV.

Example 2 – A 256Mb SRAM displays a single cell upset every 1 second and a multi-cell upset every 10 seconds with a 50 MeV proton flux of 10^7 protons per cm^2 per second. The single cell cross-section is 1 event/(10^7 x 256 10^6) = 3.91 10^{-16} cm^2/bit and the multi-cell cross section is 3.91e^{-17} cm2/bit at 50 MeV.

NOTE 1 Proton range in thick packaging or materials in front of the DUT – When testing with mono-energetic proton beams, the energy and range of the protons needs to be considered. The energy of the proton can be degraded as it passes through the material in front of the active area and no longer satisfy the neutron equivalency criteria (i.e., >50MeV). A nuclear program such as SRIM/TRIM, GEANT, FLUKA, etc should be used to ensure the proton energy is in the correct range and can be used to translate to a neutron cross-section (see **6.6.3**).

NOTE 2 Use of beam degraders to obtain lower proton energies – Use of beam degraders to lower the peak proton energy creates an added uncertainty by introducing contributions from the high energy tail. The user should assess whether or not this can be significant and should note this in the final report.

6.5.2.2 Monoenergetic neutron beam: neutron-induced soft error cross-sections at E_n

Neutron-induced soft error cross sections can be measured using a monoenergetic neutron beam. Monoenergetic neutron beams are to be distinguished from quasi-monoenergetic neutron beams discussed in 6.6.2.3. There are three main types of truly monoenergetic neutron beams > 1 MeV in which almost all of the neutrons are within ±1 MeV of the peak energy. All are produced by accelerating a charged particle into a tritium (T) or deuterium (D) target. D-T reactions produce neutrons of 14 MeV, and this is the most common type of neutron generator. D-D reactions produce neutrons of 3-5 MeV, depending on the energy of the deuteron, and p-T reactions produce neutrons with energies depending on the energy of the proton. For more detail on neutron production, the user can refer to annex **E**. Similar to the proton case, monoeneergetic neutron soft error cross sections can be defined in two ways:

$$\sigma_{n\text{-}dev,i}(E_n) = N_{n,i} / (\Phi_{neutron}) \quad (6.3)$$

and

$$\sigma_{n\text{-}bit,i}(E_n) = N_{n,i} / (\Phi_{neutron} \times N_{bit}) \quad (6.4)$$

In Equations 6.3 and 6.4, E_n is the neutron energy, $\Phi_{neutron}$ is the fluence of neutrons to which a device is exposed, in units of neutrons/cm^2; $\sigma_{n\text{-}dev,i}(E_n)$ is in units of cm^2/device and $\sigma_{n\text{-}bit,i}(E_n)$ is in units of cm^2/bit and all other parameters are as in 6.6.2.1.

6.5.2.3 Quasi-monoenergetic neutron beam: neutron-induced soft error cross-sections at E_n

Above 20MeV, monoenergetic neutron sources are not possible due to multi-body breakup effects of ^{7}Li(p,n) and ^{9}Be(p,n) sources (i.e., particles other than neutrons). Neutron-induced soft error cross sections above 20MeV can also be measured using a quasi-monoenergetic neutron beam [18]. This beam differs from a truly monoenergetic neutron beam in that a significant fraction of the neutrons are at energies less than the peak energy. Figure 6.1 shows an example of the spectrum obtained from a ^{7}Li(p, n) source for various incident proton energies. As a minimum, at least four different peak energies should be used, similar to the mono-energetic proton and neutron measurements. A summary of these facilities can be found in annex **E**.

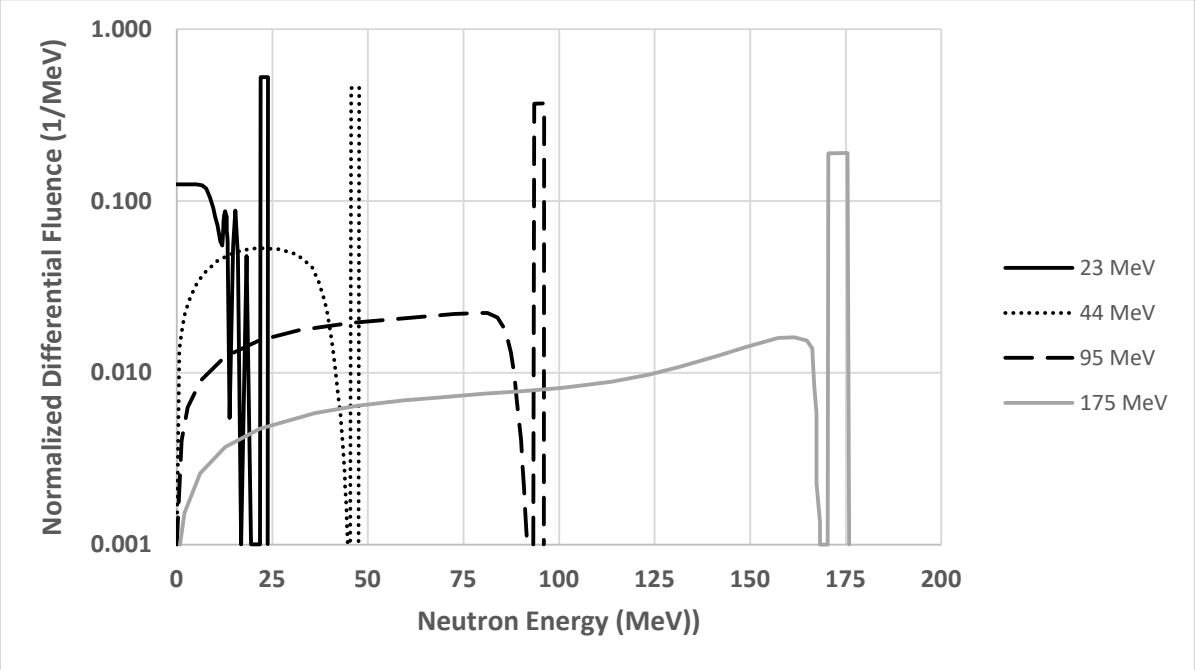

Figure 6.1 — Normalized quasi-monoenergetic neutron differential fluence from ^{7}Li(p,n) source for various proton energies from [19], such that the integral of each spectrum across all neutron energies is 1.

The neutrons from this beam comprise a two-part distribution, the neutrons at the peak energy, ~1-2 MeV below the proton energy incident on the target, and the neutrons within the so-called low energy tail, from E_{peak} -2 MeV down to ~0 MeV. Thus, the tail may contain neutrons spread out over more than 100 MeV. The challenge in using this type of source is to separate out the soft error contribution of the neutrons in the low energy tail from those at the energy peak. The contribution of the tail neutrons must be calculated in order to derive the monoenergetic neutron cross-sections in Equations 6.3 and 6.4. There are two techniques available to unfold the contribution of the tail neutrons and derive the cross section at the peak neutron energy (E_n):

6.5.2.3.1 Iterative Unfolding Algorithm

The iterative unfolding technique uses an algorithm of estimating the tail contribution to the measured cross-section and subtracting it from the total cross-section [20]. A first estimate is made of the neutron cross-section at several peak energies E_j

$$\sigma_{est1}(E_j) = \frac{N_j}{\Phi_j} \tag{6.5}$$

where the subscript j represent the peak energy (e.g., if the energies in Figure 6.1 are used, 23MeV, 44MeV, 95MeV and 175MeV), N_j is the number of soft errors and Φ_j is the peak fluence. This first estimate ignores the contribution of the tail to the soft error count, but can be used to generate a first fit of the energy dependent cross-section (see Equation 6.13)

$$\sigma_1(E) = \sigma_{L1}\left(1 - e^{-\left[\frac{E-E_{01}}{W_1}\right]^{S_1}}\right) \tag{6.6}$$

The various terms are defined in Eq 6.13 and the subscript 1 represents the first attempt to fit the overall cross-section. A second estimate of the peak energy cross-section, $\sigma_{est2}(E_j)$, can now be made including the tail contribution

$$N_j = \sigma_{est2}(E_j)\Phi_j + \int_0^{E_j}\sigma_1(E)\frac{d\Phi_{tail}}{dE}\,dE = \sigma_{est2}(E_j)\Phi_j + \overline{(\Phi_{tail}\sigma_{tail})_1} \tag{6.7}$$

where the second term represents a first estimate of the tail contribution. Solving for $\sigma_{est2}(E_j)$

$$\sigma_{est2}(E_j) = \frac{N_j - \overline{(\Phi_{tail}\sigma_{tail})_1}}{\Phi_j} = C_{tail,j1}\frac{N_j}{\Phi_j} \tag{6.8}$$

$C_{tail,j1}$ represents a first estimate of the tail correction factor for each peak energy j. A new energy dependent cross-section can now be generated similar to Equation 6.6:

$$\sigma_2(E) = \sigma_{L2}\left(1 - e^{-\left[\frac{E-E_{02}}{W_2}\right]^{S_2}}\right) \tag{6.9}$$

and a new estimate of the tail correction factor, $C_{tail,j2}$, can be made by repeating the process in Equation 6.7 and 6.8. This process is repeated until the series $C_{tail,jn}$ converges to the desired accuracy (e.g., for an accuracy of 10%, $C_{tail,j(n+1)}$ should be within +/-10% of $C_{tail,jn}$).

6.5.2.3.2 Multiple Angle Neutron Irradiation

This method relies on the property that the quasi-monoenergetic neutron spectrum is a function of the angle between the protons and the neutrons coming off the target [30]. It requires knowledge of the differential neutron fluence vs. angle. By measuring the total upset rate at two angles (e.g., 0° and x°) from the incident proton beam, the cross section from the monoenergetic neutron peak energy of E_{peak} can be extracted from the combined peak and tail distribution:

$$\sigma_{n,i}(E_{peak}) = \frac{\Phi_{0°}(E_{peak})N_{x°} - \bar{\Phi}_{x°}N_{0°}}{\Phi_{0°}(E_{peak})\bar{\Phi}_{x°}} \quad (6.10)$$

where $\Phi_{0°}(E_{peak})$ and $\bar{\Phi}_{x°}$ are the fluence of the peak at 0°and the integrated tail fluence at x°,$N_{0°}$ and $N_{x°}$ are the number of soft error events at angle 0° and x°. (Note - 0° and x°refer to the angle between the neutrons coming off the source with respect to the incident protons and not the angle of neutrons with respect to the DUT). The cross section can be interpreted per bit or per device similar to Equation 6.3 and 6.4 depending on whether $N_{0°}$ and $N_{x°}$ refer to soft error count per bit or per device. Equation. 6.10 assumes there is no peak distribution at x° and that the energy dependence of the tail distribution changes only in magnitude and not shape with angle. These assumptions should be verified with the facility manager.

NOTE E_{peak} is the neutron peak energy, which will be slightly less than the incident proton energy.

6.5.2.4 Spallation neutron beam: averaged neutron soft error cross-section over neutron spectrum

A spallation neutron source (see annex E for facilities) allows one to measure the soft error rate and derive an energy *averaged* soft eerror cross section. Because the neutrons produced from a spallation source cover a wide energy spectrum, the user cannot extract a soft error cross section at a specific energy from such measurements, but rather obtains the contribution of soft error events from neutrons of all energies within the spectrum. The major reason that a spallation neutron source is widely used is that the shape of the energy spectrum from this beam is similar to the spectrum of the terrestrial neutrons on the ground and in the atmosphere [21]. Figure 6.2 shows a compar ison of the neutron spectra from various facilities with the scaled neutron spectrum at ground level from annex A.

The flux of neutrons at the DUT can be different than the flux at the facility's neutron monitor detector. The user should cnsult with the facility manager to determine this ratio. For example, the ICE-II spectrum in Figure 6.1 is at the location of the LANL fission detector, which was at a point 19.97 meters down the flight path from the tungsten target. DUTs are located further down the flight path, so that the neutron flux will be reduced by the following ratio $r^2/(r+d)^2$, where r is the distance to the detector (19.97 m in this case) and d is the distance between the detector and the DUT. At TRIUMF the spectrum in Figure 6.1 also applies at the location of the DUT so no correction needs to be made.

6.5.2.4 Spallation neutron beam: averaged neutron soft error cross-section over neutron spectrum (cont'd)

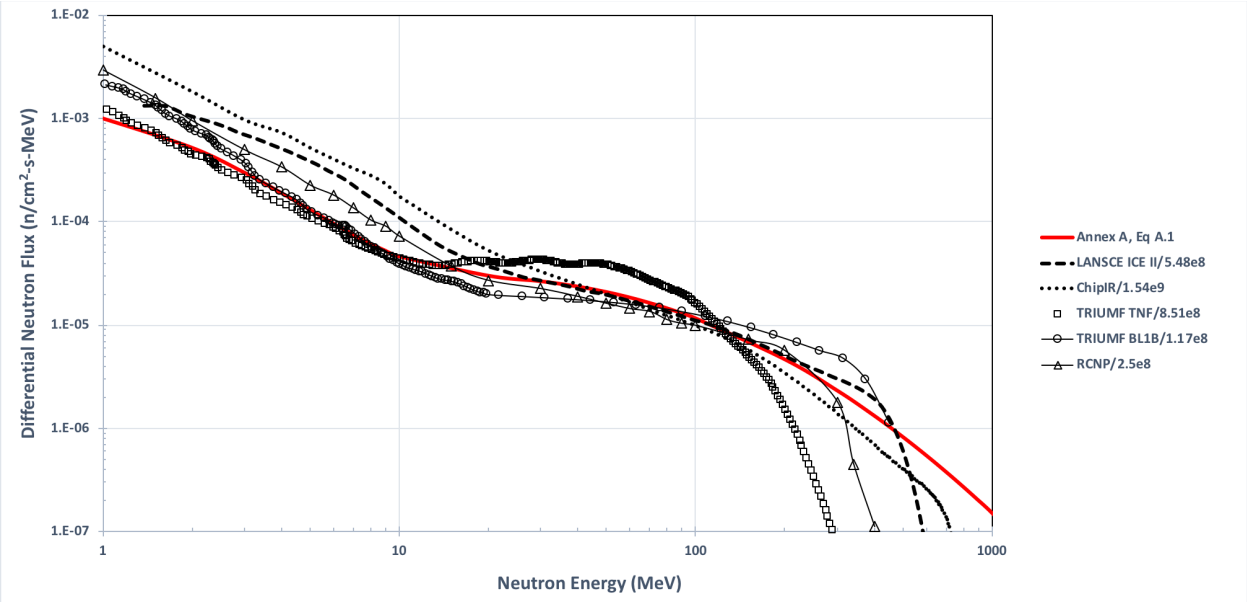

Figure 6.2 — Comparison of several neutron beam spectra normalized to the terrestrial neutron spectrum (see annex A). The scaling factor of each facility is shown in the legend (e.g., 5.48×10^{8} for LANSCE ICE II means the differential flux has been divided by 5.48×10^{8}). The scaling (or acceleration) factor is the ratio of the flux of the facility to the ground level reference flux integrated above 10 MeV.

If a spallation neutron source is used that contains thermal neutrons, then the thermal neutrons can contribute to the overall soft error and skew the data (see **7**). The user should consult the facility manager to determine the thermal neutron content and techniques to screen them out.

With measurements using spallation neutrons, one can derive an energy *averaged* neutron soft error cross which can be defined in two ways:

$$\overline{\sigma_{dev,\iota}} = {}^{N_i}/_{\Phi_{beam}} \tag{6.11}$$

and

$$\overline{\sigma_{bit,\iota}} = {}^{N_i}/_{(\Phi_{beam} \times N_{bit})} \tag{6.12}$$

In Equations 6.11 and 6.12, the energy averaged cross sections depend on the entire spallation neutron spectrum; Φ_{beam} is the integrated fluence of neutrons over the spectrum from E>10 MeV, in units of cm^{-2}; $\overline{\sigma_{dev,\iota}}$ is the spallation soft error cross section of event type i (e.g., single cell, multi-cell, SEL, etc) in units of cm^2/device and $\overline{\sigma_{bit,\iota}}$ is in units of cm^2/bit and all other parameters are as in 6.6.2.2. It is important to emphasize that the energy *averaged* neutron soft error cross sections defined in this section *not be confused* with the energy dependent proton and neutron soft error cross sections discussed in **6.6.2.1**, **6.6.2.2** and **6.6.2.3**.

Example 1 – A device displays a single event latch-up (SEL) every 60 minutes with a broad energy neutron flux of 10^6 neutrons per cm^2 per second. The SEL cross-section of the device is 1 event/(10^6 neutrons per cm^2 per second x 3600 seconds) = 2.78 10^{-10} cm^2.

Example 2 – A 256Mb SRAM displays a single cell upset every 360 seconds with a broad energy neutron flux of 10^6 neutrons per cm^2 per second. The single cell cross-section is 1 event/(10^6 x 256 10^6) = 1.09 10^{-17} cm^2/bit.

6.5.2.5 Complementing broad beam neutron soft error data:

Test campaigns using the few available broad spectrum spallation sources (Sec 6.6.2.4) can be time-consuming and subject to scheduling difficulties. A complementary technique is to use alternative ionizing radiation sources that reproduce the neutron LET distribution such as a high energy proton beam to establish a correlation factor (CF) at the introduction of a technology node/standard cell (or circuit building block) level. Once the CF has been established, IC product built on that technology node/design can be tested at the alternative source and the results translated to an equivalent broad spectrum neutron SER. The potential alternative sources include (but are not limited to) high energy protons (where energies above ~50MeV have identical cross sections to neutrons [126]), mono-energetic and quasi-monoenergetic neutron beams.

NOTE 1 Correlation needs to be demonstrated for all key building blocks and/or devices for conditions that include soft error relevant operating conditions (such as voltage, temperature, frequency, etc).

NOTE 2 Irradiation sources that do not have a significant nuclear cross section, such as heavy ions or pulsed lasers, will not be sensitive to changes in material makeup in regions close to the active region; Examples include ^{10}B content and high-Z elements that are known to change LET distributions relative to ^{28}Si for high energy protons and neutrons.

Figure 6.3 shows the CF over a wide range of 22nm device types - SRAM devices, sequential elements, unhardened and hardened flip-flops and latches, and static combinatorial logic. The figure shows that the CF dependence on device type is within measurement uncertainties. Consistency in CF across several technology generations and voltages is demonstrated in reference [22].

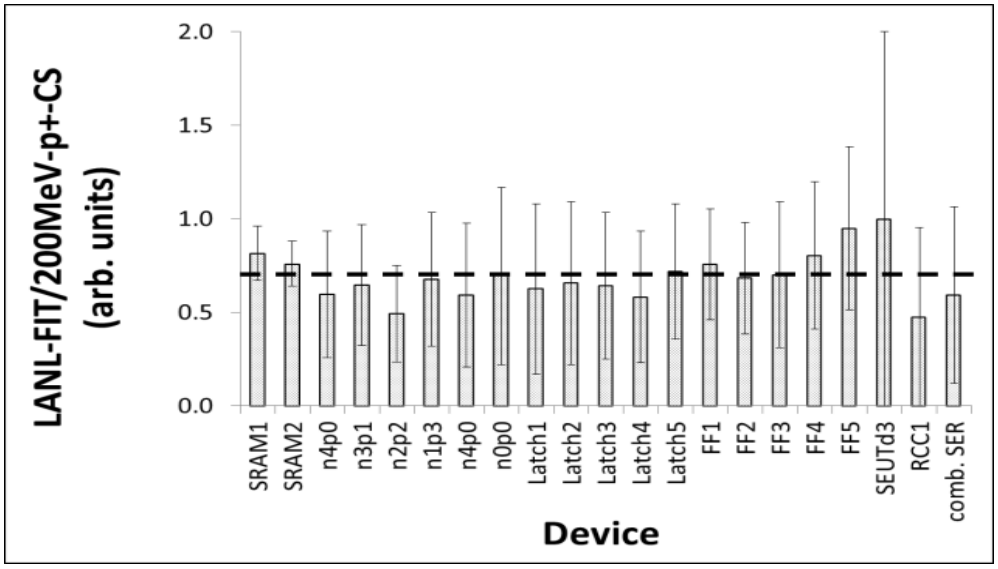

Figure 6.3 — Correlation factors (CF) and the corresponding 90% confidence intervals for various measured devices. CF corresponds to LANSCE neutron FIT (per JESD89A) divided by 198MeV proton cross sections collected at IUCF. Dotted line denotes the weighted average CF. Adapted from [23].

The validity and CF value of the correlation is soft error mechanism dependent (SBU, MCU, SEL, etc) and has to be established for each technology and each mechanism. Further, the CF value is a function of the alternate ionizing radiation source used and needs to be validated and calibrated for each facility and beam energy. Once a CF for one technology has been established, the alternate radiation beam sources can be leveraged to test more devices and to expand the test condition parameter envelope at a reasonable cost.

6.5.3 Energy variation of soft error cross section

Figure 6.4 shows an example of the variation of the soft error cross section per bit and per device with neutron or proton energy. It contains two of the recommended types of measured soft error cross sections discussed in **6.6.2**, using monoenergetic protons and monoenergetic neutrons. These were measured in two different SRAMs [24], [29]. For the SRAM from [24], the cross section for single cell upset (SCU) is in units of cm^2/bit. For the SRAM from [29], the cross section for single event latch-up (SEL) is in units of cm^2/device. Above a threshold energy, the soft error cross section curve rises rapidly with increasing energy and tends to reach a plateau.

It is often convenient to fit the soft error cross-section data points by a smooth curve. The preferred method is the four-parameter Weibull equation [26], which has the form of:

$$\sigma_{Weib,i}(E) = \sigma_{L_i}\left(1 - e^{-\left[\frac{E-E_{0i}}{W_i}\right]^{S_i}}\right) \tag{6.13}$$

where σ_{Li} is the limiting or asymptotic proton or neutron cross-section (Note – above 50MeV, the proton and neutron cross-sections are the same); E_{0i} is the cutoff energy below which soft error cross section is zero; W_i is the "width" parameter; S_i is the shape factor and the subscript i represents the particular soft error event of interest (e.g., SCU, SEL, etc.).

Another alternative is to use a piece-wise linear fit between the data points, an approach which has occasionally been used. However, the Weibull fit is the preferred method for obtaining the smoothed function fit, since it provides a "best" fit in a least squares sense to all of the soft error cross section data, and allows for averaging "dips" at one or more energies. An effective way to implement the Weibull fit is to use the SOLVER routine within the EXCEL spreadsheet application since this allows the user to obtain a set of the four parameters that minimizes a function such as the square of the difference between the smooth curve and the actual data.

A minimum of four data points, at four different energies should be used to obtain the Weibull fit. Suggested energies are: a) in the range of 1 to 14 MeV (monoenergetic neutron), b) 50-60 MeV (proton), c) 90-100 MeV (proton) and d) > 200 MeV (proton). However, more data points are always helpful, each based on a large enough number of upsets to be statistically valid, in order to improve the internal consistency of the data, as well as of the fit to the data. Using a low energy (E < 10 MeV) monoenergetic neutron beam would allow a value of E_0 < 10 MeV to be accurately obtained. Note that for SCUs in [24], most of the cross section variation is between 1 to 10 MeV and saturation occurs below 50MeV. For SEL in [25], saturation was not experimentally observed and was modeled to occur well above 1 GeV(add simulation wording).

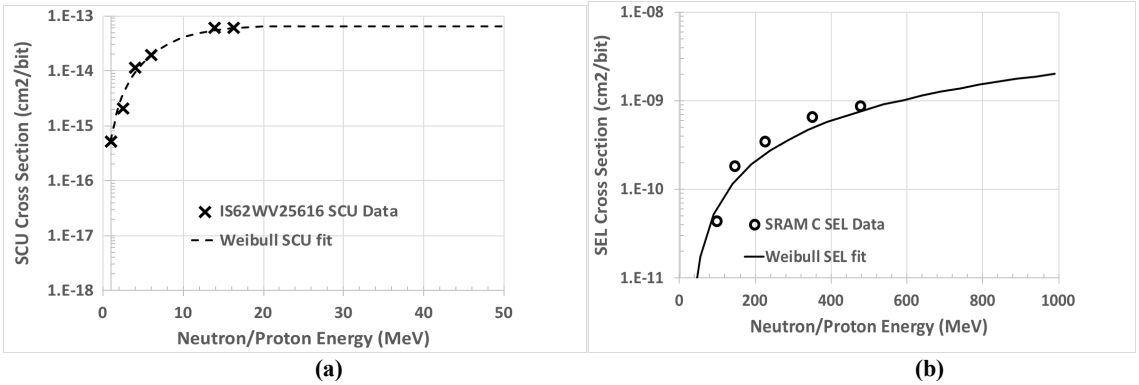

(a) (b)

Figure 6.4 — Measured SCU cross section from [24] and SEL cross section from [25] for monoenergetic neutrons (<20 MeV) and protons (>50MeV).

Weibull fit to data is shown in the dashed line in (a) and the Weibull fit to simulation the solid line in (b).

6.5.4 Analysis Methods Available

6.5.4.1 Computation of Fail Rate from Mono-energetic Proton- or Neutron-Induced Soft Error Cross Section and Quasi-monoenergetic Neutron-Induced Soft Error Cross Section

The soft error rate can be computed from the soft error cross-section and particle spectrum as follows:

$$SER_i = \int_{E_{min}}^{E_{max}} \left(d\dot{\Phi}(E)/dE\right)\sigma_{Weib,i}(E)dE \tag{6.14}$$

In Equation 6.14, $d\dot{\Phi}(E)/dE$ is the differential flux of the particle, given in units of particle number $cm^{-2}MeV^{-1}s^{-1}$; $\sigma_{Weib,I}(E)$ is the soft error cross section of event type i *using the Weibull approximation*, given in units of $cm^2 \times device^{-1}$ or $cm^2 \times bit^{-1}$; E_{min} and E_{max} are the lower and upper limits of the energy spectrum over which $\sigma(E)$ is defined. For the Weibull approximation in Equation 6.13, $E_{min} = E_{0,i}$. For E_{max}, the terrestrial cosmic ray spectrum becomes insignificant above 10 GeV. Note that $\sigma_{Weib,i}(E)$ in Equation 6.14 is a generic term: if $\sigma_{p/n\text{-}dev}$ (defined in Equations 6.1 and 6.3) is used, the soft error rate will be in units of $fails \times device^{-1}s^{-1}$; if $\sigma_{p/n\text{-}bit}$ (defined in Equations 6.2 and 6.4) is used, the soft error rate will be in units of $(fails \times bit^{-1}s^{-1})$. For most commercial IC devices, terrestrial neutrons are the most important source of soft errors. Recent measurements of the terrestrial neutron flux and an effective parameterization of the differential flux $d\dot{\Phi}(E)/dE$ is given in annex **A**, which should be used to calculate the fail rate. The $\sigma_{Weib,i}(E)$ term in Equation 6.8 should be the Weibull fit to the soft error cross section data taken at various neutron and/or proton energies.

Since the neutron flux is given in annex A as either values in 36 different energy bins (1-1000 MeV) or in analytical form, and the Weibull fit to the SE cross section is in analytical form, the integration in Equation 6.14 can be calculated very easily in spreadsheet format (using averaged values across the energy bins or Simpson's rule).

Equation 6.14 can be approximated by using a linear-log algorithm:

$$SER_i = \sum_{j=1}^{j=N+1} (F_{j-1} - F_j)(E_{j+1} - E_j)/ln(F_{j+1}/F_j) \tag{6.15}$$

In Equation 6.15, $Fj = d\dot{\Phi}(E_j)/dE \times \sigma_{p/n,i}(E_j)$, E_j is the *j-th* energy point*; j=1* corresponds to the lowest energy point E_{min}, and $j=N$ corresponds to the highest energy point E_{max}.

6.5.4.2 Computation of fail rate from spallation soft error cross section

From the spallation (averaged) soft error cross section discussed in **6.6.2.4**, the soft error rate per device for event type i calculated as follows:

$$SER_{dev,i} = \dot{\Phi}_{ref} \times \overline{\sigma_{dev,i}} = N_i \frac{\dot{\Phi}_{ref}}{\Phi_{beam}} \tag{6.16}$$

The soft error rate per bit for event type i is calculated as follows:

$$SER_{bit,i} = \dot{\Phi}_{ref} \times \overline{\sigma_{bit,i}} = \frac{N_i}{N_{bit}} \frac{\dot{\Phi}_{ref}}{\Phi_{beam}} \tag{6.17}$$

Example 1 – Using the SEL example from **6.5.2.4**, $\dot{\Phi}_{ref}$= 3.596 10^{-3} n/cm^2s or 12.95 n/cm^2hr (see annex A.2) and assuming the broad spectrum neutron source is well matched to the terrestrials high-energy neutron spectrum, the device SEL rate is 2.78 10^{-10} cm^2 x 3.596 10^{-3} neutrons per cm^2-sec = 9.99 10^{-13} per sec or 36 FIT.

Example 2 – Using the 256Mb SRAM example from **6.5.2.4**, the single cell upset rate is 1.09 10^{-17} cm^2 per bit x 3.596 10^{-3} neutrons per cm^2-sec = 3.90 10^{-20} per bit-sec or 1.4 10^{-6} FIT/bit.

6.5.4.2 Computation of fail rate from spallation soft error cross section (cont'd)

Here, the nominal integral neutron flux on the ground above 10 MeV $(\dot{\Phi}_{ref})$ is obtained by integrating the differential flux $d\dot{\Phi}/dE$ in E (see annex **A.2**). This upset rate can be adjusted for specific locations and conditions using the scaling factors given in annex A. The flux > 10 MeV is used because the neutron flux in the range of 1-10 MeV, constitutes ~ 35% of the entire neutron spectrum > 1 MeV ($\dot{\Phi}_{ref}$), but these lower energy neutrons contribute only a few percent of all of the soft error events over the entire spectrum [27].

NOTE The ratio of terrestrial flux ($\dot{\Phi}_{ref}$) and beam fluence (Φ_{beam}) is impacted by selection of E_{min} for the lower integral limit. Emin = 1MeV accounts for a non-zero cross-section below 10MeV (Figure 6.4a) but introduces a larger error in Φ_{beam}due to the mis-match in the various spallation sources and the terrestrial spectrum (Figure 6.2). Therefore, using 10MeV as the lower limit of the flux/fluence energy integral leads to more accurate results in Equation 6.16 and 6.17.

6.6 Interferences - Scattering, secondary ion effects and thermal neutrons at the DUT

Particle scattering can be a problem in any beam experiment, particularly when dense high Z materials are placed in the beam in close proximity to the DUT. Thermal neutrons are more easily scattered due to their low energy and thus any shielding that is done must enclose the device. It should also be noted that the higher the Z of the shield or scattering material, the larger the likelihood that high-energy protons will be emitted as a reaction product (this is mainly a concern in neutron beams containing high energy neutrons). These higher energy protons can penetrate the DUT and cause additional soft errors. Spurious results might be obtained if a high Z metal shield were to be used to enclose a DUT if a large fraction of the observed SER was related to the resulting secondary protons. If this is thought to be a problem, using boron as a shielding material (e.g., borated polyethylene or borax bricks) instead of Cd or Gd should reduce this effect considerably.

The scattering effects can also be seen if large metallic heat sinks are used in the DUT. Any type of scattering material in the neutron beam during the experiments needs to be described in detail in the final report. If a large metallic heat sink is part of the DUT in the neutron beam, the user should consider repeating the neutron testing at several different beam incidence angles. If the user wants to minimize scattering effects, the test assembly should be oriented with the heatsink behind the DUT.

If the high energy beam contains a significant amount of thermal neutrons (consult the facility manager), then steps should be taken to eliminate these thermal neutrons from the DUT during high energy testing. A variety of materials containing high concentrations of isotopes with high thermal neutron cross-sections can be used as a thermal neutron shield. The user should use enough shielding to ensure that the thermal neutron effects are minimal.

Three materials that have been commonly used for shielding thermal neutrons are boron (B), cadmium (Cd) and gadolinium (Gd). The very dramatic increase in the thermal neutron cross-section for these three materials is shown in Figure 6.5. The neutron cross section is commonly expressed in units of barns (10^{-24} cm²). The ^{10}B cross-section is seen to decrease with energy at an almost constant slope, its cross section varying as 1/v or as $1/E^{½}$ where v and E are neutron velocity and energy, respectively. In contrast, the cross sections for both ^{113}Cd and ^{157}Gd are seen to have a very sharp increase for low energies, E < 0.4 eV. As the energy decreases from 0.4 eV to 0.1 eV, the cross section for these two metals increases by about two orders of magnitude, thus these metals are very effective in shielding out low energy neutrons with E < 0.4 eV, while allowing higher energy neutrons and gamma photons to pass through.

6.6 Interferences - Scattering, secondary ion effects and thermal neutrons at the DUT (cont'd)

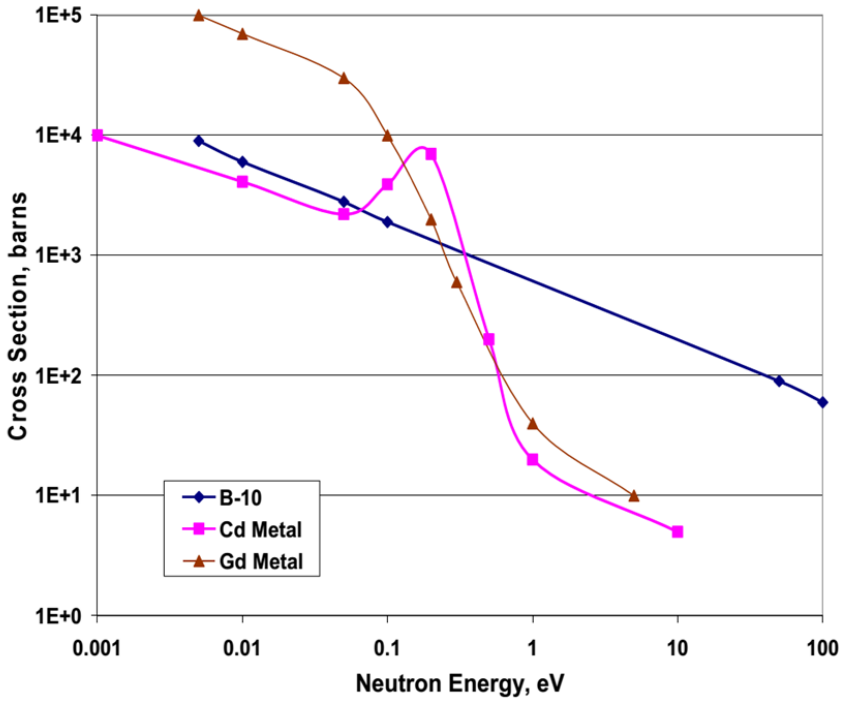

Figure 6.5 — Variation of the low energy neutron cross section with energy for ^{10}B and natural abundance Cd and Gd.

Cd and Gd may be used to shield DUTs in a neutron beam comprised of both thermal and higher energy neutrons with the advantage that higher energy neutrons (En > 0.4 eV) pass unaffected [28]. Because the thermal neutron cross sections are so high, only a minimal thickness is required, <1mm, to virtually shield out all neutrons with E < 0.4 eV as shown in Table 6.1.

Table 6.1 — Neutron attenuation as a function of thickness for various materials

Shield Thickness, mm	Boron (^{10}B)	Cadmium (^{113}Cd)	Gadolinium (^{157}Gd)
.01	9.1E-1	8.9E-1	3E-1
.1	3.7E-1	3.1E-1	5.8E-6
1	4.7E-5	8.8E-6	4.3E-53

Another standard approach to shielding thermal neutrons has been to use products that contain large quantities of boron, such as boric acid and borated polymer sheets (sold commercially) but several millimeters of these materials will be needed since the shield is not composed entirely of boron.

Whatever the material, it must be conformal or at least placed in such a way that the entire device is surrounded by shielding material. This is necessary to preclude any stray scattered thermal neutrons from reaching the device and causing errors during the shielded test. In some facilities it may be possible to place the shielding material in the beam upstream from the DUT such that the number of scattered thermal neutrons is reduced – but the efficiency of such a shield should be confirmed with neutron detectors prior to running any component tests.

7 Accelerated thermal neutron test procedures

7.1 Background

7.1.1 Introduction

Thermal neutrons are a result of the high energy terrestrial neutrons coming into thermal equilibrium with the environment (~25 meV, see Figure A.4.1). The interaction of most concern for single event effects is the absorption of thermal neutrons by ^{10}B. The ^{10}B nucleus has a very high capture cross section for thermal neutrons. Boron has two isotopes, ^{10}B (approximately 20% in natural abundance) and ^{11}B (approximately 80% in natural abundance). Like most other nuclides when ^{11}B captures a neutron it emits a photon which cannot cause a single event upset. In stark contrast, ^{10}B not only has a very high neutron capture cross-section but upon capturing a neutron the ^{10}B nucleus has a high probability of fissioning into two highly ionizing particles each of which can cause a single event effect [29], [30]. The nuclear reactions are [31]:

$$n + {}^{10}B \rightarrow {}^{7}Li\ (0.84\ MeV) + {}^{4}He\ (1.47\ MeV) + gamma\ (0.48\ MeV) \qquad 94\% \qquad (7.1a)$$

$$n + {}^{10}B \rightarrow {}^{7}Li\ (1.02\ MeV) + {}^{4}He\ (1.78\ MeV) \qquad 6\% \qquad (7.1b)$$

The relative probability (i.e., branching ratio) of these reactions are shown after the capture process.

The resultant alpha and lithium particles from the ^{10}B neutron reaction are both strongly ionizing, so if either impinges on the active device it creates bursts of free electron-hole pairs in the silicon. The range of a 1.47MeV alpha particle is ~5um (see Figure D.3), so all sources of ^{10}B within the active region are potential sources for thermal neutron upset. ^{10}B can be present in large quantities in the device in the form of polysilicon doping, substrate doping or boro-phospho-silicate glass (BPSG) and other boron sources (e.g., B_2H_6) [32]. Using high concentrations of boron in its natural isotopic abundance in any of these layers is the primary concern [33] for this reaction because it contains high amounts of boron (for example BPSG typically contains 4 - 9% boron by weight) and covers a large portion of the chip area. It should be noted that in more recent technologies, very highly doped substrates, polysilicon layers and implants are being used that could place high concentrations of ^{10}B in proximity to the active devices. Even if the device does not use BPSG, this is not sufficient grounds to rule out the need to do thermal neutron soft error testing. If there is uncertainty about either the presence of ^{10}B in the device or the contribution of ^{10}B to the soft error cross section when it is present, thermal neutron testing is recommended to make a determination of the single event error cross-section. The results of the thermal neutron testing or assessment of why thermal neutron testing was not ~~conducted~~ needed must be included in the final report. Unlike many of the high-energy neutron reactions discussed in 6 that have reaction thresholds of > 5 MeV, the ^{10}B neutron capture reaction actually increases as the neutron energy is reduced (see Figure 6.5). This reaction is dominated by neutron energies below 0.4 eV.

7.1.2 Scope

This chapter deals with the method to determine the relative sensitivity of a component to soft errors from thermal neutrons from accelerated experiments. soft error from reactions by low energy neutrons, i.e., thermal and epithermal neutrons (i.e., energies less than 25 meV), with ^{10}B depends on altitude, latitude, solar activity, the local shielding environment, and most importantly, to the amount of ^{10}B present in the IC.

7.1.3 Limits of test method

The accelerated test method in this section applies ONLY to events caused by low energy (E ~ 25 meV) neutron reactions with ^{10}B. It does NOT apply to high-energy neutron-induced events nor does it encompass errors due to alpha particles. This test method can be applied to the testing of memory, sequential logic, combinational logic, or components combining these types of circuits.

7.1.4 Goal of test method

The goal of this test method is to determine the thermal neutron cross section or soft error rate of the component or circuit under study. Thermal neutrons can manifest themselves as several different types of soft errors.

7.2 The terrestrial thermal neutron environment

For a description of the thermal neutron spectrum, see annex A.4.

7.3 Packaging for thermal neutron testing

The DUT package has little effect on thermal neutron testing and on the test results since neutrons are uncharged and interact only by nuclear reaction with matter (unless the package contains materials with high thermal neutron cross sections, e.g., B, Cd or Gd). For example, components encapsulated in plastic, lead-over-chip (LOC), and most chip-scale packages are suitable for thermal neutron testing. This is not a complete list of packages suitable for thermal neutron testing. The only limitations related to packages are those with large metal heatsinks that might modify the thermal neutron beam.

7.4 Thermal neutron sources

7.4.1 Thermal neutron source selection

Testing for chip soft errors due to thermal neutrons can be done using various sources (see annex **E**). Thermal neutrons are available from both nuclear reactors and particle accelerators. Particle accelerator facilities use nuclear reactions such as energetic protons on Li targets to produce neutrons. These neutrons are then moderated (lowered in energy) by passing the neutrons through low-Z materials like polyethylene; a few such facilities are indicated in annex E. Neutron generators, such as 14 MeV D-T or 2.2 MeV D-D may also be used to produce thermal neutrons, again by using a moderating material to slow down the higher energy neutrons. Calibration is a critical issue for thermal neutron testing because the soft errors cross-section varies significantly with small changes in neutron energy – thus the measurement is very sensitive to the energy distribution of the low energy neutrons. Thermal neutrons are also available at nuclear reactors, where the flux calibration may already exist, but the associated gamma ray field in the reactor volume and its effect on the DUT must be accounted for (see **7.7.6**). Figure 7.1 shows a comparison of three thermal neutron facilities with the low energy (<100 keV) terrestrial neutron background (see Fig A.4 in annex **A**).

NOTE Cold neutron sources (i.e., enhanced spectrum below 25 meV) should be avoided because the $E^{-1/2}$ cross-section dependence will lead to an soft error rate that is higher than that due to thermal neutrons.

7.4.1 Thermal neutron source selection (cont'd)

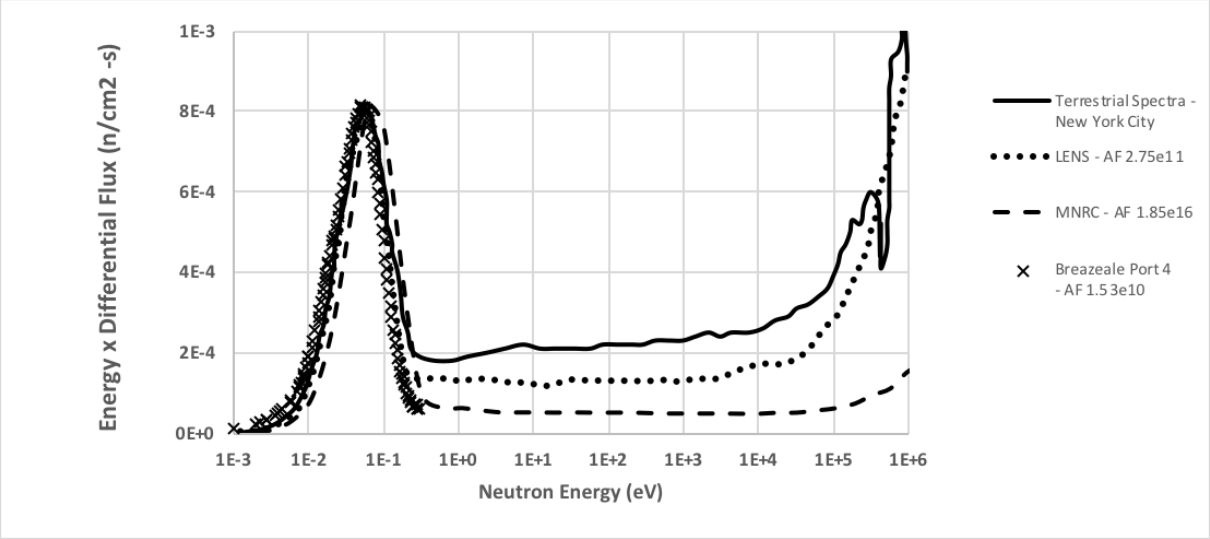

Figure 7.1 — Comparison of terrestrial neutron energy times differential flux (see annex A.2) with three thermal neutron facilities (see Table E.2.1). The facilities have been normalized to the thermal neutron peak at Yorktown Heights (see Figure A.4.1) by dividing by the acceleration factor (AF) shown in the legend.

Since low-energy neutrons are easily scattered, the concept of a well-defined beam is not necessarily applicable as there may be significant dispersion such that a neutron field exists within a large volume of the test area. This has ramification for shielding personnel, equipment, and DUTs. Thus the term "beam" is used loosely in this chapter and can in fact refer to a neutron field with little directional dependence. The user should consult with the facility manager about the angular dependence of the thermal neutrons.

High energy spallation facilities can provide a source of thermal neutrons by use of moderators, such as polyethylene. However, the resulting spectra might still contain a high percentage of neutrons above 1MeV, confounding the results of soft error measurements. The user should consult with the facility manager on the ratio of thermal neutron flux (<200 meV) to high energy neutron flux (>1 MeV) before attempting this technique.

7.4.2 Source calibration

Most facilities provide beam calibration. In most cases users will rely on calibration and beam uniformity at the facility. In cases where facility calibration is not well established, then it will be necessary to measure the flux, energy, and spatial uniformity (area) of the beam following standard procedures such as ASTM E262-03 (Standard Method for Determining Thermal Neutron Reaction and Fluence Rates by Radioactivation Techniques). This is generally done with activation foils, such as with ^{197}Au or ^{23}Na, but the details vary with facility and are beyond the scope of this document.

7.4.3 Thermal neutron source fluence

The total number of neutrons incident on the DUT must be sufficient to establish with a high statistical confidence that the entire sensitive volume has been irradiated uniformly. See annex **B** for discussion on statistically based confidence levels. Soft error experiments using thermal neutrons are similar to those using particle accelerators (discussed in **6**). The beam almost always activates any chips or socketsplaced in the beam (activate means to make temporarily radioactive), so the facility manager should be consulted in terms of quarantine period.

7.5 Test procedure and results

7.5.1 General test specification

The test method utilizes a beam of neutrons or neutron field from a reactor with most neutrons being at thermal energies or below. The flux of thermal neutrons should be well defined and validated with activation foils and/or a calibrated neutron detector. The purpose of this test method is to determine the thermal neutron soft error cross section. Two approaches are recommended here for determining the impact of thermal neutron soft error.

7.5.1.1 Thermal Neutron Source - The first approach involves doing dedicated soft error testing at a facility that provides a calibrated thermal neutron beam and minimal high-energy neutrons, like a nuclear reactor (see annex E for facilities). After the background runs are completed the DUT is irradiated with the thermal neutron beam and the number of soft errors are recorded.

7.5.1.2 High Energy Neutron Source - The second approach assumes that both the thermal and high-energy neutron soft error testing will be done at a single high-energy neutron spallation source. This requires that the spallation source contain a well-quantified thermal neutron component whose flux level is similar to that of the high-energy neutron component, like TRIUMF. In spallation facilities that do not have an appreciable thermal neutron flux, the use of a moderator could adequately increase the thermal neutron component, but it would have to be calibrated; see annex **E** for other facilities.

7.5.2 Computation of fail rate from thermal neutron soft error cross section

For low energy neutron sources, such as nuclear reactors, a significant fraction of the fluence is centered around the thermal neutron energy. D-T/D-D generators and high energy spallation sources can also be used for thermal neutron soft error measurements if they appropriately moderated (i.e., there are sufficient number of high energy neutrons slowed down to thermal energies) or already have a significant thermal neutron flux. However, higher energy neutrons (>1 MeV) can possibly contribute to the measured cross section (see discussion of E_0 in **6.6.3**). Therefore, a thermal neutron shield should be used to help differentiate the thermal and high energy contributions. The thermal neutron acceleration factor A_{th} is

$$A_{th} = \frac{\dot{\Phi}_{th,beam}}{\dot{\Phi}_{th,ref}} = \frac{\dot{\Phi}_{beam\ wo\ shield} - \dot{\Phi}_{beam\ w\ shield}}{\dot{\Phi}_{th,ref}} \tag{7.2}$$

where $\dot{\Phi}_{\mathrm{th,beam}}$ is the accelerator thermal neutron flux and $\dot{\Phi}_{th,ref}$ is the reference thermal neutron flux (6.5 n/cm^2-hr or 1.8×10^{-3} n/cm^2-s, see annex A.4). $\dot{\Phi}_{beam\ wo\ shield}$ is the total accelerator flux without a thermal neutron shield and $\dot{\Phi}_{beam\ w\ shield}$ is the total flux with the thermal neutron shield. The thermal neutron cross section for an soft error event of type i is

$$\sigma_{th,i} = \sigma_{total,i} - \sigma_{HE,i} = \frac{N_{wo\ shield,i}}{\Phi_{beam\ wo\ shield}} - \frac{N_{w\ shield,i}}{\Phi_{beam\ w\ shield}} \tag{7.3}$$

where $\sigma_{total,i}$ is the total (high energy plus thermal neutron) cross section, $\sigma_{HE,i}$ is the cross section from high energy neutrons only, $N_{wo\ shield,i}$ is the number of soft error events of type i (e.g., single cell upset, multi-cell upset, single event latchup, etc.) measured without the shield and $N_{w\ shield,i}$ is the number of events with the shield. If high energy neutrons do not contribute to the total cross-section, then the second term in Eq 7.3 will become small. If there is a significantly large flux of high energy neutrons in comparison thermal neutrons (e.g., incompletely moderated spallation source), the difference between two large numbers ($N_{wo\ shield,i}$ and $N_{w\ shield,i}$ in Equation 7.3) can become very small, leading to a large statistical uncertainty in the thermal neutron cross-section. (See annex H for error determination.)

7.5.2 Computation of fail rate from thermal neutron soft error cross section (cont'd)

The thermal neutron soft error rate for event type i is

$$SER_{th,i} = \sigma_{th,i}\, \phi_{th,ref} = \sigma_{th,i}\, \frac{\phi_{th,beam}}{A_{th}} \quad (7.4)$$

at the reference level thermal neutron flux similar to the high energy neutron cross section in **6**. The thermal neutron soft error rate can be expressed per device or per bit similar to Equation 6.16 and 6.17.

Example – A 256Mb SRAM displays 10,000 single cell upsets in one minute of unshielded beam exposure of 9 10^7 n/cm^2-sec for a total cross-section of 1.85 10^{-6} cm^2. Using a thermal neutron shield, the respective numbers are 5,000 upsets in one minute with a high energy flux of 7 10^7 n/cm^2-sec for a high energy cross-section of 1.19 10^{-6} cm^2, resulting in a thermal neutron cross-section of 6.61e^{-7} cm^2. Using the reference thermal neutron flux of 1.8 10^{-3} n/cm^2-s, the single cell soft error rate is 1.19 10^{-9} per second (4,290 FIT) or 4.65 10^{-18} per second per bit (1.67 10^{-5} FIT/bit).

7.6 Gamma flux from nuclear reactor neutron beams

If performing neutron experiments at a nuclear reactor facility, the effect of the large gamma photon flux mixed with the neutron flux must be determined. While many advanced components do not have a high sensitivity to gamma irradiation, a test should be performed using a neutron shield that ensures that no thermal neutrons are getting to the DUT even when it is in the beam. In this case only gamma photons and whatever high energy neutrons are not shielded will be reaching the DUT. The user should consult the facility manager on the flux of the shielded high energy neutrons. The DUT should be exposed for the longest planned duration. If the gamma photons and unshielded high energy neutrons do not contribute to the soft errors, it is expected that no errors will be observed. If errors are observed in the shielded case then the component is sensitive to either the gamma flux or unshielded high energy neutrons and this must be included in the final report.

It is important to note that for long exposures or in intense neutron beams that contain gamma photons, total dose effects may also manifest themselves. . These permanent damage or change in device characteristics can interfere with soft error characterization. The user should take this into consideration (See Sec 1.1 Related Documents for standards that address these effects.)

Annex A - Determination of terrestrial neutron flux (normative)

A.1 Introduction

This annex provides the cosmic-ray-induced neutron differential flux above 1 MeV for a reference location and conditions and also provides formulas and tables that allow the reference spectrum to be scaled to other locations and conditions. This annex describes the use of a Web-page calculator that is available to simplify determination of the flux scaling factor. The presence of cosmic-ray secondary protons, the neutron spectrum below 1 MeV, especially thermal-energy neutrons, the directional distribution of the neutrons, and the effects of shielding by buildings are also discussed.

The intensity of cosmic-ray-induced neutrons (and other secondary cosmic radiation, including protons) in the atmosphere varies with altitude, location in the geomagnetic field, and solar magnetic activity. Atmospheric shielding at a given altitude is determined by the mass thickness per unit area of the air above, called areal density or atmospheric depth. The geomagnetic field deflects low-momentum primary cosmic particles back into space, lowering the neutron flux produced in the atmosphere. The minimum momentum per unit charge (magnetic rigidity) that an incident (often, vertically incident) particle can have and still reach a given location above the Earth is called the geomagnetic cut-off rigidity (cutoff) for that point. The varying magnetic field carried outward from the Sun by the solar wind plasma that permeates the solar system also reduces the cosmic-ray intensity at Earth. This solar modulation has been measured for decades by a number of neutron monitors on the ground at various locations. The cosmic-ray-induced terrestrial neutron flux is highest when sunspots and other solar activity are at a minimum (quiet sun), and lowest when the sun is most active. The effects on the terrestrial neutron flux of atmospheric depth, geomagnetic cutoff, and solar activity are not independent. For example, the change in flux with cutoff depends on solar activity and to some extent on atmospheric depth.

The most important parameter determining the terrestrial neutron flux is atmospheric depth, which is proportional to barometric pressure and changes with altitude. The neutron flux is roughly 10 times higher at an altitude of 3,000 m (9,843 ft) than it is at sea level. The global variation with cutoff is about a factor of 2 from equator to pole at sea level, and 3 at the highest inhabited altitudes. Solar modulation is smaller still, about a 25% decrease from maximum to minimum recorded monthly-averaged rates at polar locations near sea level and ~7% at the equator, and 30% to 12% for polar and equatorial sites at high elevations.

Fortunately, the *shape* of the outdoor ground-level neutron spectrum above a few MeV does not change very much with altitude, cutoff, or solar modulation. This makes it possible to describe the neutron differential flux at one location under reference conditions and then scale the reference spectrum to obtain the neutron differential flux anywhere on Earth at any time.

A.2 Reference neutron spectrum

The location and conditions for the reference cosmic-ray-induced terrestrial neutron differential flux have been chosen to be New York City outdoors at sea level at a particular time of average solar activity. Values of the neutron flux in units of neutrons/(cm^2 MeV s) at 46 energies above 1 MeV are given in Table A.2-A. The reference spectrum was determined primarily by measurements, and is taken from Gordon et al. [34], where those interested can find details of the measurements and the scaling functions described below in A.3.

A.2 Reference neutron spectrum (cont'd)

Table A.2-A — Cosmic ray induced neutron differential flux for reference conditions (sea level, New York City, mid-level solar activity, outdoors)

Neutron Energy (MeV)	Differential Flux ($cm^{-2}\ s^{-1}\ MeV^{-1}$)	Neutron Energy (MeV)	Differential Flux ($cm^{-2}\ s^{-1}\ MeV^{-1}$)	Neutron Energy (MeV)	Differential Flux ($cm^{-2}\ s^{-1}\ MeV^{-1}$)
1.054	6.83×10^{-4}	5.220	1.53×10^{-4}	130.7	9.64×10^{-6}
1.165	8.19×10^{-4}	5.769	1.25×10^{-4}	224.6	4.30×10^{-6}
1.287	7.61×10^{-4}	6.376	1.16×10^{-4}	386.3	1.33×10^{-6}
1.423	7.02×10^{-4}	7.047	8.90×10^{-5}	664.2	3.99×10^{-7}
1.572	6.00×10^{-4}	7.788	7.16×10^{-5}	1.142×10^{3}	1.02×10^{-7}
1.738	5.72×10^{-4}	8.607	6.73×10^{-5}	1.964×10^{3}	2.24×10^{-8}
1.920	5.06×10^{-4}	9.512	5.53×10^{-5}	3.376×10^{3}	3.36×10^{-9}
2.122	5.02×10^{-4}	10.51	4.58×10^{-5}	5.805×10^{3}	4.71×10^{-10}
2.346	5.44×10^{-4}	11.62	4.09×10^{-5}	9.982×10^{3}	9.87×10^{-11}
2.592	4.30×10^{-4}	12.84	3.80×10^{-5}	1.716×10^{4}	3.83×10^{-11}
2.865	3.34×10^{-4}	14.19	3.44×10^{-5}	2.951×10^{4}	8.60×10^{-12}
3.166	2.65×10^{-4}	16.16	3.02×10^{-5}	5.074×10^{4}	2.17×10^{-12}
3.499	1.86×10^{-4}	18.52	3.22×10^{-5}	8.725×10^{4}	6.97×10^{-13}
3.867	1.64×10^{-4}	25.70	2.59×10^{-5}	1.500×10^{5}	1.88×10^{-13}
4.274	1.73×10^{-4}	44.19	2.09×10^{-5}		
4.724	1.88×10^{-4}	75.98	1.53×10^{-5}		

To provide values at energies between those given in Table A.2-A, an analytic expression has been fit to the reference spectrum:

$$\frac{d\dot{\Phi}_0(E)}{dE} = 1.006\times10^{-6}\exp\left[-0.35\left(\ln(E)\right)^2 + 2.1451\ln(E)\right] + 1.011\times10^{-3}\exp\left[-0.4106\left(\ln(E)\right)^2 - 0.667\ln(E)\right], \quad \text{(A.1)}$$

where E is neutron energy and $d\dot{\Phi}_0(E)/dE$ is the reference neutron differential flux.

The total flux of the measured reference spectrum above 10 MeV is 3.596×10^{-3} $cm^{-2}\ s^{-1}$ (12.946 $cm^{-2}\ h^{-1}$). **This is the value of the *reference flux* above 10 MeV for this JESD89B standard.** The total flux of the analytic fit above 10 MeV is 3.585×10^{-3} $cm^{-2}\ s^{-1}$ — within 0.3% of the measurement. The estimated uncertainty in the measured value of the neutron flux above 10 MeV is over 10%, [35] but for the purposes of this standard, the reference flux is considered to have no uncertainty.

Figure A.2.1 is a graph of the reference spectrum, the differential flux of cosmic-ray-induced neutrons as a function of neutron energy. The points are the values in Table A.2-A. The solid curve is the analytic fit.

A.2 Reference neutron spectrum (cont'd)

Figure A.2.2 presents the same information as Figure A.2.1, but using a different representation of the neutron spectrum, plotting energy times differential flux as a function of energy. This representation is standard in the field of radiation protection, but it is not yet routine in the literature on soft errors or cosmic-ray physics. It is conceptually simpler to plot the differential flux, $d\dot{\Phi}/dE$, but for neutrons, that typically requires a log–log plot covering many orders of magnitude on both axes, making details difficult to see. The large range of neutron $d\dot{\Phi}/dE$ stems from its characteristic $1/E$ dependence when neutrons slow down in a scattering medium. $E\left(d\dot{\Phi}/dE\right)$ is relatively flat and can be plotted on a linear scale. $E\left(d\dot{\Phi}/dE\right)$ is mathematically identical to $d\dot{\Phi}/d(\ln(E))$. In a plot of $E\left(d\dot{\Phi}/dE\right)$ against $\log(E)$, equal areas under the spectrum in different energy regions represent equal integral fluxes.

In Figure A.2.2, the histogram is the measurement-based reference spectrum, and, as in Figure A.2.1, the solid curve is the analytic fit to the reference spectrum.. Note that Figure A.2.2 begins at 0.1 MeV.

The reference spectrum applies only to locations on the ground. It is not accurate for airplanes or any situation far from the ground.

High-energy secondary protons are also present in the cosmic-ray-induced particle showers that produce neutrons, and such protons can also cause single-event effects in electronics. The reference neutron spectrum does not include protons. Calculations indicate that the terrestrial cosmic-ray proton flux is roughly 5% to 15% of the neutron flux above 10 MeV, depending on altitude and cutoff, with the higher fraction of protons at high altitude and high cutoff.

A.2 Reference neutron spectrum (cont'd)

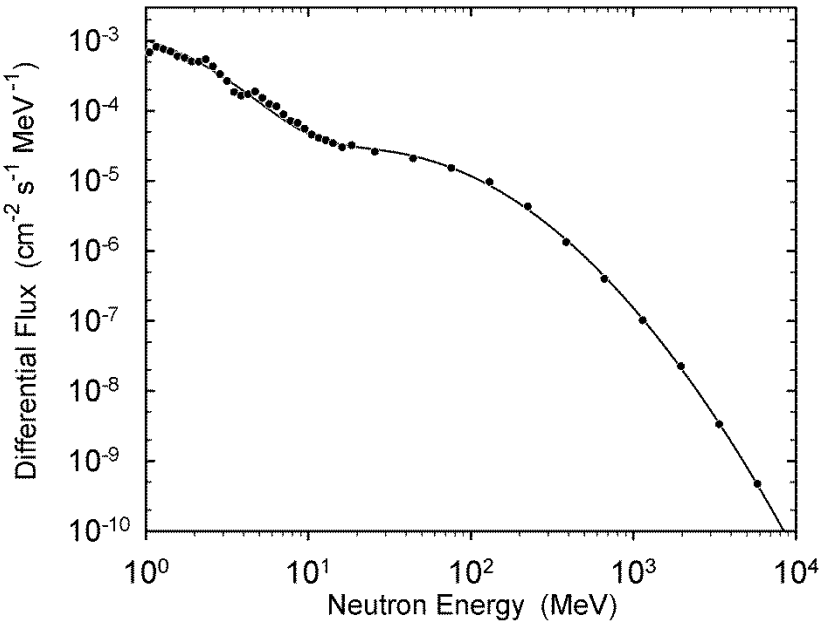

Figure A.2.1 — The differential flux of cosmic-ray-induced neutrons as a function of neutron energy under reference conditions (sea level, cutoff = 2.08 GV, mid-level solar activity, outdoors). The data points are the reference spectrum, the solid curve is the analytic fit to the reference spectrum.

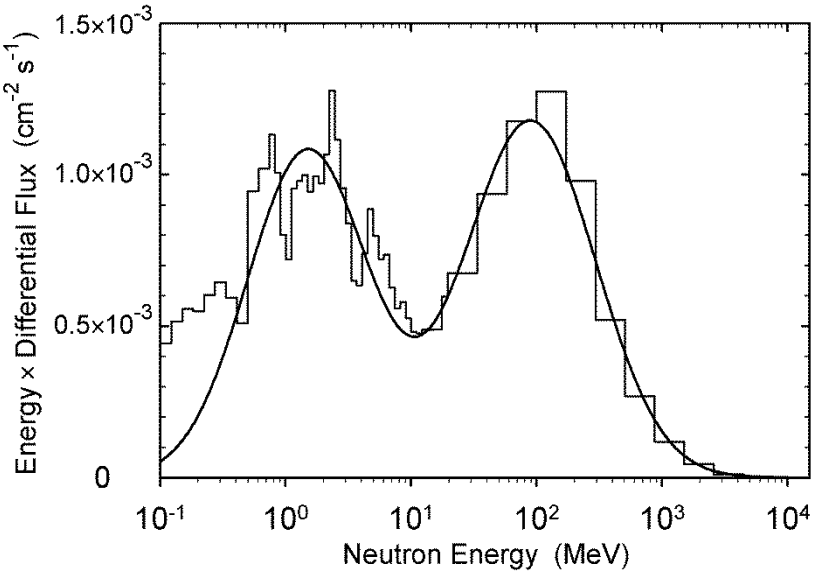

Figure A.2.2 — Reference spectrum of cosmic-ray-induced neutrons plotted as energy times differential flux as a function of neutron energy. The histogram is the reference spectrum, and the solid curve is the analytic fit to the reference spectrum.

A.3 Scaling the reference neutron spectrum to other locations/conditions

To account for the effects of altitude, cutoff, and solar modulation, the neutron spectrum outdoors at any location can be expressed as follows:

$$\frac{d\dot{\Phi}(E)}{dE} = \frac{d\dot{\Phi}_0(E)}{dE} \cdot F_{\mathrm{A}}(d) \cdot F_{\mathrm{B}}(R_{\mathrm{c}}, I, d), \tag{A.2}$$

where $d\dot{\Phi}_0(E)/dE$ is the reference spectrum, d is the atmospheric depth, R_c is the vertical geomagnetic cutoff rigidity, I is the relative count rate of a neutron monitor measuring solar modulation, $F_{\mathrm{A}}(d)$ is a function describing the principal dependence on altitude (i.e., on atmospheric depth) and $F_{\mathrm{B}}(R_{\mathrm{c}}, I, d)$ is a function describing the dependence on geomagnetic location and solar modulation which also has a dependence on depth. Atmospheric depth is given by $d = p/g$, where p is the barometric pressure and g is the acceleration of gravity. Vertical cutoff depends primarily on the horizontal component of the Earth's magnetic field. It is near zero at the poles and has a maximum of 13 to 17 GV at the equator. (GV is a unit of rigidity; GeV is a unit of energy.) Consequently, the cosmic-ray induced neutron flux is higher at the poles and lower at the equator. Values of R_c for cosmic rays reaching the atmosphere have been calculated several times for a grid of locations covering the globe. Values of F_{B} given in this standard have been calculated using values of R_c provided by the U.S. Federal Aviation Administration Civil Aerospace Medical Institute, Protection And Survival Research Laboratory. The cutoff values were calculated by D. F. Smart and M. A. Shea from the International Geomagnetic Reference Field for 2010 [36]. Figure A.3.1 shows contours of the values of R_c plotted on a world map.

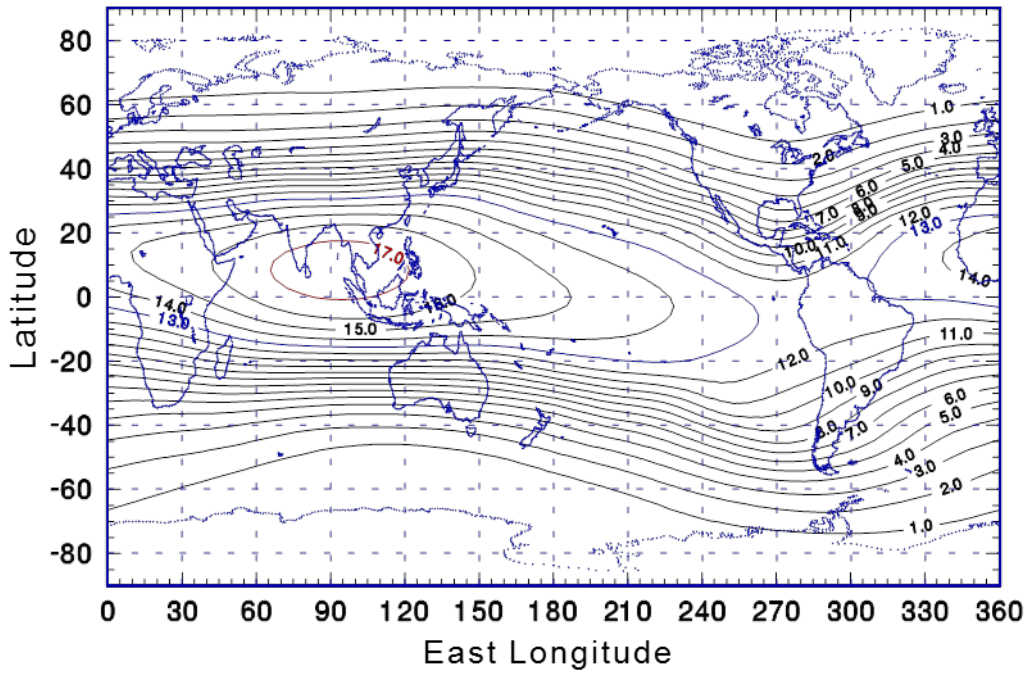

Figure A.3.1 — Contours of vertical geomagnetic cutoff rigidity plotted on a world map.

A.3 Scaling the reference neutron spectrum to other locations/conditions (cont'd)

The neutron differential flux at any location is the product of the reference spectrum and the scaling factor $F_A \cdot F_B$. Formulas for F_A and F_B, a table of F_B at sample values of cutoff rigidity, and a table of $F_A \cdot F_B$ for several cities and other locations are given below. A Web-page calculator has been developed to calculate the scaling factor $F_A \cdot F_B$ for an arbitrary location on Earth given the latitude, longitude, and barometric pressure or elevation at the location. In Equation A.2, the main altitude dependence is exponential attenuation:

$$F_A(d) = \exp[(1033.2 - d)/131.3], \tag{A.3}$$

where 1033.2 g/cm^2 is the mean atmospheric depth at sea level, and 131.3 g/cm^2 is the effective mass attenuation length in the atmosphere for neutrons above 10 MeV. Barometric pressure is often given in millibar (hectoPascal, hPa) or in mmHg. Standard sea level pressure is 1013.25 millibar or hPa, which is equal to 760 mmHg. Using barometric pressure p in hPa, atmospheric depth d in g/cm^2 is given by

$$d(\mathrm{g/cm^2}) = p(\mathrm{hPa})/0.980665, \tag{A.4}$$

where 0.980665 is the average acceleration of gravity at sea level, 9.80665 m/s^2, divided by 10. Atmospheric depth is best determined from actual barometer readings, but when the barometric pressure is not available, its average value at a given elevation, z, in meters can be determined using

$$p(\mathrm{hPa}) = ((44331.514 - z)/11880.516)^{5.255877}. \tag{A.5}$$

Although F_A describes the main dependence of the neutron flux on atmospheric depth (altitude), for best accuracy it should not be used alone, even when the cutoff is held constant (for example, comparing the flux at the bottom and top of the same mountain) because F_B also contains some depth dependence. Without the depth dependence of F_B, the attenuation length in air would be about 135 g/cm^2.

The expression for F_B comes from theoretical calculations [37], [38] that were done only for the extreme conditions of solar modulation: quiet sun, when the terrestrial cosmic ray flux is at its peak, and active sun, when the terrestrial cosmic ray flux is at its minimum. For these two conditions,

$$F_{B,\mathrm{quiet}}(R_c, h) = 1.098\left[1 - \exp\left(-\alpha_1 / R_c^{k_1}\right)\right] \tag{A.6}$$

and

$$F_{B,\mathrm{active}}(R_c, h) = 1.098\left[1 - \exp\left(-\alpha_2 / R_c^{k_2}\right)\right] \times \left[1 - \exp\left(-\alpha_1 / 50^{k_1}\right)\right] / \left[1 - \exp\left(-\alpha_2 / 50^{k_2}\right)\right], \tag{A.7}$$

where the parameters α and k are given by

$$\alpha_1 = \exp[1.84 + 0.094h - 0.09\exp(-11h)], \tag{A.8}$$

$$k_1 = 1.4 - 0.56h + 0.24\exp(-8.8h), \tag{A.9}$$

$$\alpha_2 = \exp[1.93 + 0.15h - 0.18\exp(-10h)], \tag{A.10}$$

and

$$k_2 = 1.32 - 0.49h + 0.18\exp(-9.5h). \tag{A.11}$$

Unlike Equations A.2 – A.5, Equations A.6 – A.11 use barometric pressure, h, in bar (1 bar = 10^5 Pa) instead of depth or pressure in millibar: $h = p/1000$.

A.3 Scaling the reference neutron spectrum to other locations/conditions (cont'd)

Since the terrestrial neutron flux changes by less than 30% between these extremes (less than 20% for most locations), in many cases, especially at low altitudes and latitudes, it is practical to set F_B equal to the average of the results from Equations A.5 and A.6 and ignore solar modulation. This should not be done for determinations of the neutron flux at high-altitude facilities used for accelerated testing with natural radiation. In such cases, where an especially accurate knowledge of the neutron flux is desired, readings from a neutron monitor during the test period should be used to determine the state of solar activity, and an interpolation made between the values from Equations A.5 and A.6.

For example, if monthly average neutron monitor readings are 20% of the way from their typical minimum values at active sun to their typical maximum values at quiet sun, interpolate 20% of the way from $F_{B,\,active}$ to $F_{B,\,quiet}$. ("Typical minimum values" means exclude the very low values seen in some months of 1989 – 1991, and "typical maximum values" means exclude the very high values from late 2008 through early 2010.) The neutron monitor must be one with available data over several solar activity cycles so the neutron monitor count rate during the test period can be compared to its rate during typical extremes of solar activity. Data and graphs for many neutron monitors are available from the Neutron Monitor Database at http://www.nmdb.eu/nest/search.php. Neutron monitor stations with consistent long-term data include Kerguelen (KERG), McMurdo (MCMU), Newark (NEWK), Oulu, (OULU), and Thule (THUL).

Table A.3-A gives values of $F_{B,\,active}$, $F_{B,\,quiet}$, and their mean at sea level for integer values of geomagnetic vertical cutoff rigidity from 0 (magnetic poles) to 17 GV (the maximum value, found in southeastern Asia). Multiplying the reference neutron spectrum by these values gives the terrestrial cosmic-ray neutron differential flux at sea level locations with the indicated cutoff rigidity. At the time the reference spectrum was determined, the cutoff rigidity at New York City was 2.08 GV. (It has since increased because the geomagnetic field has changed over the years [36]) Since 2.08 GV is the reference cutoff, the value in Table A.3-A at 2 GV for average solar modulation is very close to 1. The values in Table A.3-A (and Table A.3-B) are given to 3 significant figures so that trends may be understood more easily, but the overall uncertainty of the values for F_B is as large as 10%, especially for low latitudes (high cutoffs), where the relative flux factor has not been verified by measurements.

Table A.3-A — Relative neutron flux at sea level vs. geomagnetic vertical cutoff rigidity

Cutoff Rigidity (GV)	Relative Neutron Flux			Cutoff Rigidity (GV)	Relative Neutron Flux		
	Active Sun Minimum	Quiet Sun Peak	Average		Active Sun Minimum	Quiet Sun Peak	Average
0	0.939	1.098	1.019	9	0.686	0.737	0.712
1	0.938	1.097	1.018	10	0.657	0.702	0.679
2	0.929	1.076	1.002	11	0.630	0.670	0.650
3	0.902	1.030	0.966	12	0.606	0.640	0.623
4	0.866	0.975	0.920	13	0.583	0.614	0.598
5	0.827	0.919	0.873	14	0.562	0.589	0.576
6	0.789	0.867	0.828	15	0.542	0.567	0.555
7	0.752	0.819	0.786	16	0.524	0.547	0.535
8	0.718	0.776	0.747	17	0.508	0.528	0.518

A.3 Scaling the reference neutron spectrum to other locations/conditions (cont'd)

Table A.3-B gives a brief list of cities and some high-elevation research locations with the latitude, longitude, and elevation (altitude) of each, and the corresponding geomagnetic vertical cutoff rigidity, typical atmospheric depth, and $F_A \cdot F_B$ for active sun, quiet sun, and average solar modulation. To determine the long-term average cosmic-ray induced neutron differential flux for one of the listed locations, multiply the reference spectrum by the number in the last column of the table for the location of interest. The elevations given in Table A.3-B may not be correct for a particular point in the city or high-altitude research site, but they are the elevations assumed for the flux factor calculations.

For some locations, the cutoff rigidity values in the table and the corresponding flux factors are slightly different from the values in Table A.3-B of JESD89A because the Earth's magnetic field, and therefore the geomagnetic cutoff rigidity, has changed [36]. The flux factors in JESD89A were determined using a cutoff map calculated from the International Geomagnetic Reference Field for 1995. Flux factors given in JESD89B are determined using cutoffs calculated from the International Geomagnetic Reference Field for 2010 [36]. The difference between the previous and new flux factors is less than 1% for many locations. The largest change for any location on land at a habitable elevation is 4%, which occurs near Buenos Aires, Argentina. From 1995 to 2010, the cutoff at New York City changed from 2.08 GV to 2.32 GV, and the neutron flux decreased by almost 1%, so the flux factor for New York City at sea level in Table A.3-B is 0.99. The calculated flux factors for locations at high cutoffs have an uncertainty of about 10%.

A.3 Scaling the reference neutron spectrum to other locations/conditions (cont'd)

Table A.3-B — Cosmic-ray neutron flux at selected places relative to reference flux

City or location	Latitude (°)	Longit. (° E)	Elevat. (m)	Atm. Depth (g/cm^2)	Cutoff Rigidity (GV)	Relative Neutron Flux		
						Active Sun Low	Quiet Sun Peak	**Avg.**
Cities								
Bangkok, Thailand	13.4 N	100.3	20	1031	17.4	0.51	0.53	0.52
Beijing, China	39.9 N	116.4	55	1027	9.0	0.72	0.77	0.75
Berlin, Germany	52.5 N	13.4	40	1028	2.8	0.94	1.08	1.01
Bogotá, Columbia	4.6 N	285.9	2586	753	12.3	3.71	4.01	3.86
Chicago, IL, USA	41.9 N	272.4	180	1011	1.8	1.09	1.27	1.18
Denver, CO, USA	39.7 N	255.0	1609	851	2.8	3.43	4.08	3.76
Hong Kong, China	22.3 N	114.2	30	1030	15.9	0.54	0.56	0.55
Houston, TX, USA	29.8 N	264.6	15	1031	4.6	0.85	0.95	0.90
Johannesburg, S. Africa	26.2 S	28.0	1770	834	7.2	2.93	3.27	3.10
La Paz, Bolivia	16.5 S	291.9	4070	623	11.8	8.78	9.63	9.21
London, UK	51.5 N	359.9	10	1032	3.0	0.91	1.04	0.98
Los Angeles, CA, USA	34.0 N	241.7	100	1021	5.1	0.90	1.00	0.95
Mexico City, Mexico	19.4 N	260.9	2240	787	7.8	3.88	4.32	4.10
Moscow, Russia	55.8 N	37.6	150	1015	2.1	1.06	1.23	1.14
New Delhi, India	28.6 N	77.2	220	1007	14.1	0.66	0.70	0.68
New York, NY, USA	40.78 N	286.0	0	1033	2.32	0.92	1.06	0.99
Paris, France	48.9 N	2.3	50	1027	3.8	0.91	1.03	0.97
Seattle, WA, USA	47.6 N	237.7	50	1027	2.0	0.97	1.13	1.05
Seoul, South Korea	37.6 N	127.0	50	1027	10.5	0.67	0.71	0.69
Sidney, Australia	33.9 S	151.2	30	1030	4.5	0.87	0.97	0.92
Singapore City, Singapore	1.3 N	103.9	15	1031	17.2	0.51	0.53	0.52
Stockholm, Sweden	59.3 N	18.1	30	1030	1.4	0.96	1.12	1.04
Taipei, Taiwan	25.0 N	121.5	10	1032	15.2	0.54	0.57	0.55
Toronto, Canada	43.7 N	280.6	120	1019	1.7	1.04	1.21	1.13
Tokyo, Japan	35.7 N	139.8	20	1031	11.2	0.64	0.67	0.66
High Altitude Locations								
IAO, Hanle, Ladakh, India	32.8 N	79.0	4500	589	11.9	10.91	11.99	11.45
Jungfraujoch, Switzerland	46.5 N	8.0	3580	664	4.6	11.57	13.70	12.64
Leadville, CO, USA	39.25N	253.7	3100	706	3.0	9.74	11.86	10.80
Los Alamos Natl. Lab., USA	35.9 N	253.7	2250	786	3.8	5.16	6.07	5.62
Mauna Kea (summit), HI, USA	19.8 N	204.5	4207	612	12.7	8.92	9.73	9.32
Mt. Fuji, Japan	35.4 N	138.7	3776	647	11.4	7.75	8.50	8.12
Plateau de Bure, France	44.6 N	5.9	2550	757	5.2	5.75	6.64	6.19
South Pole Station	90.0 S	-	2820*	695*	0.0	11.41	14.47	12.94
White Mtn. Res. Sta., USA	37.4 N	241.6	3810	644	4.3	13.64	16.30	14.97

*The atmospheric pressure at the south pole is significantly lower than given by the standard atmospheric profile—the mean barometric pressure is 681.2 hPa, equivalent to 3226 m elevation.

A.3 Scaling the reference neutron spectrum to other locations/conditions (cont'd)

A Web-page calculator has been developed to calculate the scaling factor $F_A \cdot F_B$ for an arbitrary location on Earth given the latitude, longitude, and barometric pressure or elevation at the location. The URL of the website containing the calculator is http://www.seutest.com. Below is a procedure to determine the neutron flux for an arbitrary city or location at a given time using the Web-page flux-factor calculator followed by two examples. It is assumed that the user has Internet access and is familiar with Web browser software.

1. Obtain the latitude and longitude of the city or location and an average or typical barometric pressure for the time of interest. If the barometric pressure cannot be determined, the elevation of the location may be used instead.
2. Type http://www.seutest.com into the address window of your Web browser. Click/select "Flux calculation". Read the instructions on the Web page for the use of the calculator. They may differ from the instructions given here.
3. Enter the latitude and longitude in the boxes provided. Choose North or South for latitude and East or West for longitude. Latitude and longitude should be in decimal degrees, and 0.1 degree accuracy is more than sufficient.
4. Enter a value for *one* of the following: barometric pressure, elevation (altitude), or atmospheric depth. Caution: use the station (actual) barometric pressure, not the pressure corrected to sea level. The pressure may be entered in millibar (hPa), mmHg, or inches Hg. Be sure to select the unit you use. If you do not know the barometric pressure, enter the elevation of the location in the box for elevation and select the unit (meters or feet).
5. Under "Solar Modulation", generally choose the default value, 50%. For high-altitude locations where the most accurate value is desired for a particular time period, obtain count rate data or graphs from one or more neutron monitors for that time period and for several solar cycles. (A solar cycle with both polarities of the solar magnetic field is ~22 years.) Compare the average rate for the time of interest with the historical maximum and minimum monthly average rates and interpolate between the quiet and active sun values of F_B accordingly. Data and graphs for many neutron monitors are available from the Neutron Monitor Database at http://www.nmdb.eu/nest/search.php. Neutron monitor stations with consistent long-term data include Kerguelen (KERG), McMurdo (MCMU), Newark (NEWK), Oulu, (OULU), and Thule (THUL).
6. Click/select "Submit" to start the calculation. The calculator will return a value for the flux scaling factor, for the two pressure-related quantities that were not entered, F_A and F_B from Equations E.3 and E.6 – E.11, and the geomagnetic cutoff used in the calculation.
7. Read the flux scaling factor. Also, check that the values returned by the calculator for the two pressure-related quantities that were not entered seem reasonable. To assure that correct values of the latitude and longitude were entered, including N-S and E-W, check that the value returned for the geomagnetic rigidity cutoff is reasonable by comparing it with Figure A.3.1 or the cutoff contour map displayed when you click on the "Rigidity cutoff" link next to the value displayed.
8. Multiply the reference differential flux from Table A.2-A or Equation A.1 by the flux scaling factor to obtain the differential flux at the location.

Example 1: City location — Albuquerque, New Mexico, USA.
Latitude = 35° 40' N ≅ 35.7° N; Longitude = 106° 39' W = 106.65° W.
Barometric pressure hard to find; use elevation. Elevation = 4945 feet = 1507 m.

A.3 Scaling the reference neutron spectrum to other locations/conditions (cont'd)

Type http://www.seutest.com/ into Web browser address window. Click/select "Flux calculation". In the "Latitude" box, enter 35.7 and select "North"; in the "Longitude" box, enter 106.65 and select "West". In the "Elevation" box, enter 1507 and choose "meters". Leave the "Station pressure" and "Depth" boxes blank. In the box labeled "Solar modulation" leave the default value, 50%.

Click/select "Submit" to start the calculation. Calculator returns a flux scaling factor of 3.23. It also returns a value of 633.7 mmHg for pressure and 861.5 g/cm^2 for depth. The returned values of F_A = 3.70 and F_B = 0.87 are appropriate for a location at a high elevation and a cutoff above that of New York City. The returned value of rigidity cutoff, 3.92, is consistent with the contours on the map similar to Figure A.3.1 displayed when you click the "Rigidity cutoff" link..

Example 2: High-altitude research location — Mt. Washington, NH, USA, June 2003.
Latitude = 44.27° N; Longitude = 71.30° W.
Mean station barometric pressure during test = 607.7 mmHg (Elevation = 1905 m).
Solar modulation for June 2003: about 20% of the way from typical minimum monthly average rate to maximum monthly average rate.

Type http://www.seutest.com/ into Web browser address window. Click/select "Flux calculation". In the "Latitude" box, enter 44.27 and select "North"; in the "Longitude" box, enter 71.3 and select "West". In the "Station pressure" box, enter 607.7 and select mmHg. Leave the "Elevation" and "Depth" boxes blank. In the box labeled "Solar modulation" enter 20.

Click/select "Submit" to start the calculation. Calculator returns a flux scaling factor of 4.46. It also returns a value of 1847 m for elevation and 826.2 g/cm^2 for depth. Since the calculated elevation is slightly below the actual elevation, the entered pressure value was above average, but reasonable. The returned value of F_A = 4.84 is appropriate for a location at a high elevation. The returned value of F_B = 0.92 seems low for a location with a cutoff below that of New York, but that is because of the solar modulation (and high altitude). The returned value of rigidity cutoff, 1.80, is consistent with the contours on the map similar to Figure A.3.1 displayed when you click the "Rigidity cutoff" link.

A.4 The neutron spectrum below 1 MeV, including thermal-energy neutrons

While the shape of the cosmic-ray-induced terrestrial neutron spectrum above a few MeV is approximately constant, that is not the case at lower energies, where the shape of the spectrum depends on how local materials scatter neutrons. Figure A.4.1 shows full energy range cosmic-ray neutron spectra measured outdoors (one was in a thin-roofed building) at five locations.[34] Each spectrum has been scaled to sea level and the reference cutoff of 2.08 GV using the Equations in A.3 and plotted as energy times differential flux as a function of neutron energy. Above a few MeV, the spectra lie practically on top of one another, justifying the use of one reference spectrum. At lower energies, these spectra vary by up to 66%, lowest to highest, and the relative flux at thermal energies (<0.4 eV) does not correlate well with the relative flux at higher energies. For these spectra scaled to reference conditions, the thermal neutron flux ranged from 1.84×10^{-3} cm^{-2} s^{-1} (6.6 cm^{-2} h^{-1}) to 2.8×10^{-3} cm^{-2} s^{-1} (10 cm^{-2} h^{-1}) and averaged 2.27×10^{-3} cm^{-2} s^{-1} (8.2 cm^{-2} h^{-1}).

A.4 The neutron spectrum below 1 MeV, including thermal-energy neutrons (cont'd)

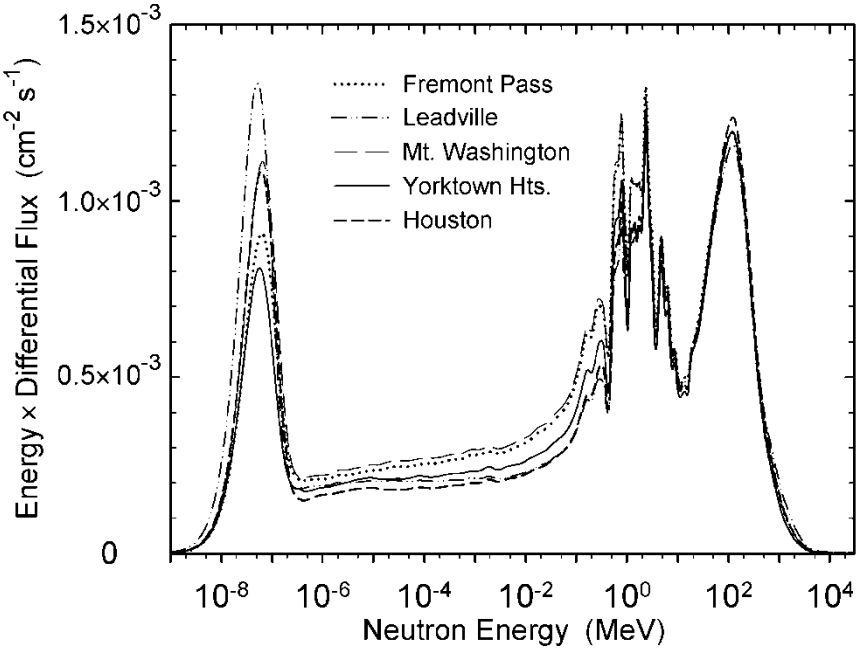

Figure A.4.1 — Spectra of cosmic-ray-induced neutrons measured at five locations. Each spectrum has been scaled to sea level and the cutoff of New York City and plotted as energy times differential flux as a function of neutron energy.

Other measurements [39] have found somewhat lower values of the thermal neutron flux. Figure A.4.2 shows a bar chart of the results of measurements of the thermal neutron flux made in 2003 at 52 sites near sea level within 160 km of Annapolis, MD (39.0°N, 76.5°W) on the top floor inside low buildings and outdoors.

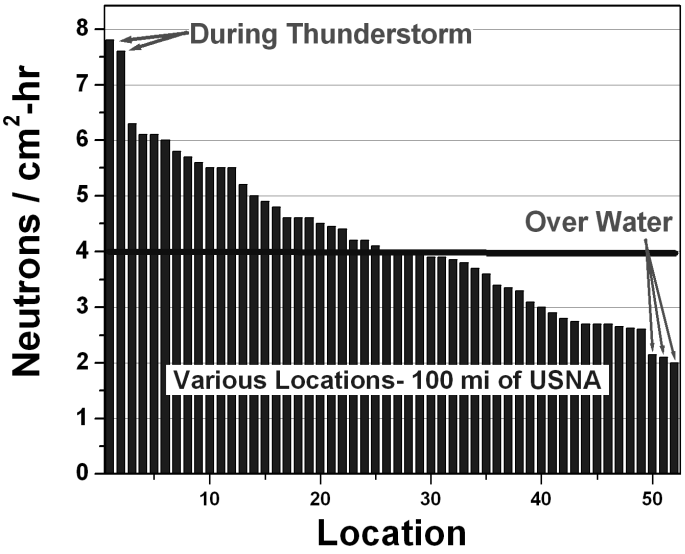

Figure A.4.2 — Thermal neutron flux measured at 52 sites near sea level within 160 km (100 miles) of the U.S Naval Academy in Annapolis, MD (39.0° N, 76.5° W) [19]. The fluxes shown have not been adjusted to the reference conditions.

A.4 The neutron spectrum below 1 MeV, including thermal-energy neutrons (cont'd)

On land and not during thunderstorms, the measured thermal neutron flux ranged from about 2.6 to 6.3 cm^{-2} h^{-1}, averaging 4 cm^{-2} h^{-1}. Assuming an average elevation of 10 m and an average roof shielding of 5 g/cm^2, scaling the results of these measurements to the reference geomagnetic cutoff rigidity at sea level with no shielding and average solar modulation multiplies them by 1.087, giving thermal neutron fluxes ranging from 2.8 to 6.8 cm^{-2} h^{-1} with an average of 4.35 cm^{-2} h^{-1}. This set of measurements does not agree with the measurements shown in Figure A.4.1, but the two sets do overlap at 6.6 to 6.8 cm^{-2} h^{-1}.

The *reference value* for the flux of cosmic-ray-induced terrestrial neutrons at thermal energies (<0.4 eV) is 1.8×10^{-3} cm^{-2} s^{-1} (6.5 cm^{-2} h^{-1}). This value is the average of the means of the two sets of measurements described above [34], [39] after scaling to the reference conditions. Some of the individual measurements differ from the reference value by as much as a factor of 2.3, and this is indicative of the variations that may be encountered in different surroundings. In general, the flux of thermal neutrons may be estimated within about a factor of 2.3 by using the reference value together with the methods described in A.3 to scale the reference thermal flux.

A.5 Angular distribution

The angular distribution of high-energy cosmic-ray-induced neutrons is not isotropic. As the energy increases, the neutrons tend to be directed more and more downward. Figure A.5.1 shows the calculated normalized differential angular distribution, $d\dot{\Phi}/d\Omega$, of the neutron flux, $\dot{\Phi}$, for various energy regions of the neutron spectrum. The differential flux per steradian of solid angle Ω is plotted against $\cos\theta$, where θ is the angle from vertically downward, (zero degrees is down) and $\Omega = 2\pi \cos\theta$. The flux at each vertical angle is integrated over the azimuthal angle, averaging the azimuthal dependence, which has an east-west asymmetry for the higher energies, especially at high cutoff rigidities. Each curve is normalized to a total flux of 1 cm^{-2} s^{-1} sr^{-1}. The figure shows that the higher-energy neutrons are mostly downward, while neutrons with energies from epithermal to 1 or 2 MeV are nearly isotropic. Thermal-energy neutrons are mostly upward, with roughly 1.75 times as much thermal flux going upward as going downward. The calculation was done for the reference conditions (near New York City, sea level, average solar modulation) using MCNP6 to transport cosmic-ray particles through the atmosphere following the methods in McKinney et al.[40] and McMath et al.[41] The flux of thermal neutrons depends strongly on the material of the ground, which for this calculation was a 15-cm thick concrete slab on top of typical soil.

Figure A.5.2 shows results from the same calculation in a different way, plotting the neutron energy spectrum for different angles from vertically downward. The spectra are plotted as energy times differential flux per steradian as a function of energy (see A.2). At downward angles, there are a lot of high-energy neutrons—for angles within 18° of vertically downward, 64% of the neutrons have energies above 10 MeV. As the angle changes from downward to sideways to upward, the flux at high energy decreases dramatically and the flux at thermal energy increases.

A.5 Angular distribution (cont'd)

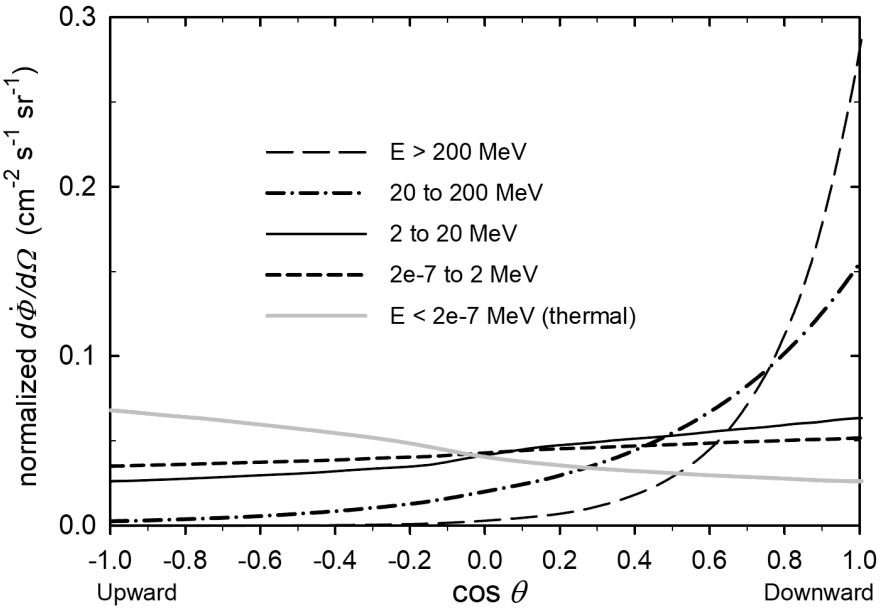

Figure A.5.1 — Calculated normalized differential angular distribution, $d\dot{\Phi}/d\Omega$, of the neutron flux, $\dot{\Phi}$, for five different energy regions of the neutron spectrum at the reference conditions. The angle θ is measured from vertically downward.

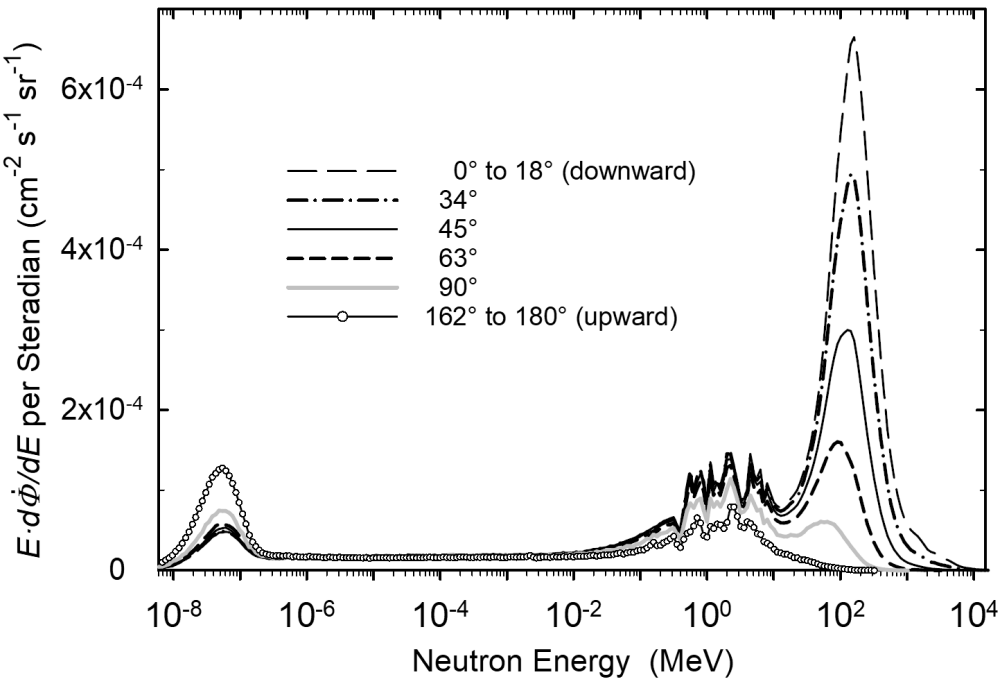

Figure A.5.2 — Calculated neutron spectra at different angles from vertically downward for the reference conditions. The spectra are plotted as energy times differential flux per steradian as a function of energy.

A.6 Effects of shielding by buildings and other material

The procedures in A.3 give the nominal neutron flux to which a deice or circuit is exposed at a location without shielding, that is, outdoors with no enclosure. Most applications are indoors, and the materials of the building attenuate the actual flux that impinges on the electronics.

The attenuation by moderate layers of low-atomic-number materials such as wood is roughly similar to that by an equal mass thickness (areal density) of air, so the shape of the spectrum above 10 MeV is not significantly changed, and the attenuation may be treated as similar to increasing the atmospheric depth.

For concrete, in a large building it was found that two 15-cm (6-inch) slabs (plus associated roofing, ceiling, and flooring material, ductwork, etc. in an industrial building) reduced the high-energy portion (E > 10 MeV) of the neutron spectrum by a factor of 2.3, while the total neutron flux was reduced by a factor of only 1.6. As they penetrate the concrete, low-energy neutrons are scattered, thermalized, and absorbed, but the high-energy neutrons are attenuated by interactions which cause the nuclei in the shielding to emit neutrons with energies in the MeV range, regenerating the low-energy portion of the neutron spectrum.

For the portion of the spectrum above 10 MeV, the attenuation by horizontal concrete layers above the point of interest may be estimated using exponential attenuation with an attenuation length of 1.2 feet or 0.37 m:

$$\dot{\Phi} = \dot{\Phi}_0 \exp(-x / 0.37) \tag{A.12}$$

where $\dot{\Phi}$ and $\dot{\Phi}_0$ are the attenuated and initial flux and x is concrete thickness in meters. Assuming a density of 2.3 g cm^{-3}, the mass attenuation length of concrete floor slabs is roughly 85 g cm^{-2}. The lower energy portion of the neutron spectrum does not decrease as fast; the attenuation length for the total flux is about 0.65 m or 150 g cm^{-2}. The cosmic ray secondary protons are presumably attenuated more than the neutrons.

If there are thick concrete walls as well as floors and roofs and an accurate differential neutron flux is desired, a high-energy radiation transport code, such as MCNP6 [42], FLUKA [43], Geant4 [44], or PHITS [45], should be used to model radiation transport through the building.

Large amounts of steel (such as aboard ships) or other materials with high atomic number (e.g., lead shields) can significantly distort the neutron spectrum. Each incident high-energy neutron can liberate several neutrons with energies ~1 MeV, sometimes creating an increase of a factor of 2 or more in that region of the spectrum. However, steel shielding above the point of interest attenuates the portion of the spectrum with E > 10 MeV. Steel (or iron) also absorbs thermal neutrons, and a room or enclosure with steel walls will have a significantly reduced thermal neutron flux.

Annex B – Counting statistics (normative)

B.1 Confidence Interval

In accelerated SER testing, the total number of particles incident on the DUT must be sufficient to establish with a high statistical confidence that all sensitive volume has been irradiated uniformly. After certain particle fluence, each memory element either passes or fails. The probability of failure for each memory element is calculated as

$$P_E = \frac{F}{N} \tag{B.1}$$

where P_E is an estimation of probability of failure, N is the total number of memory elements, F is the total failures. (Note: F must be >0. If F = 0, see annex C for statiscal analysis.) If it is desirable that, with (1-α) confidence level, the estimated probability of failure P_E is within a plus and minus ε% bounds of the true probability of failure P, the following condition needs to be satisfied according to the definition of the confidence interval:

$$\Phi^{-1}(\frac{\alpha}{2}) \bullet \frac{1}{\sqrt{F}} \bullet \sqrt{\frac{N-F}{N-1}} \le \varepsilon\% \tag{B.2}$$

where $\Phi^{-1}(\alpha/2)$ is the inverse cumulative standard normal distribution function, F is the total observed errors and N is the total number of memory elements.

B.2 Estimating probability for results with low numbers of observed events

In this example, the DUT is an SRAM of 512 K bit, i.e., N=512*1024=524288. After a certain time of radiation exposure, we observed 100 errors, i.e., F=100. Therefore, the estimated error probability p_E is F/N=0.00019, with 95% confidence level, the precision of the estimated probability of failure will be:

$$\Phi^{-1}(\frac{\alpha}{2}) \cdot \frac{1}{\sqrt{F}} \cdot \sqrt{\frac{N-F}{N-1}} \approx 1.96 \cdot \frac{1}{10} = 19.6\% \tag{B.3}$$

In other words, with 95% confidence level, we can say that estimated probability of failure per bit is within the bounds of minus and plus 19.6% of the true probability of failure. According to Equation B.3, it seems that precision increases with increasing F. In reality, when F approaches N, the effect of the same bit getting hit more than once can no longer be ignored, thus one must be careful to avoid accumulating too many errors or else the soft error rate will be underestimated.

Annex C – Real-Time Testing Statistics (normative)

C.1 Statistics for Real-Time Testing

In the typical real-time test, N devices are placed on test under normal (unaccelerated) operating conditions and the number, location, and time of each soft failure is recorded. Since soft errors are not permanent (eliminated when new data is written) this test can be thought of as a life-test with replacement (in which a failing device is replaced with a new device immediately upon failure detection).

Let us assume the soft failures are random in time and that the probability of an error at any time is constant. Secondly we assume that the number of errors is small relative to the number of units in the test – for soft failures in components this is a good assumption (ignoring big solar events or large changes in barometric pressure that would alter the neutron flux – in any case, these types of events will be averaged out during the test). Thus we apply the exponential or **Poisson distribution** assuming the form:

$$f(t) = N\lambda e^{-N\lambda t} \tag{C.1}$$

Where λ is the mean error rate and N is the number of units on test. Given a real-time experiment, we first want to understand the SER maximum likelihood estimate which is simply the number of errors divided by the time and the number of units on test, according to:

$$component\ SER_{avg} = \frac{r}{NT_r}(10^9)\ \text{FIT} \tag{C.2}$$

Where r is the number of errors observed at T_r. For the purposes of this test we have multiplied the standard formula by 10^9 to convert errors/hour to FIT. The second issue we need to understand is, do we have enough errors to confidently proclaim that the component has an SER below or above certain intervals. The longer a test is run and the more errors accumulated, the greater our confidence in the average failure rate. Since real-time testing can take months, it is crucial to understand when enough errors (enough test time) have been logged to make an acceptable estimation of the component SER. Because Poisson distributed variables have a probability distribution function that is a gamma function, we can use a special case of the gamma function, the chi-squared (χ^2) distribution to answer questions about variance in the mean. Using the χ^2 distribution, the two-sided upper and lower 100 (1-α) percent confidence intervals with k=2(r+1) degrees of freedom for the SER can be expressed as:

$$LowerLimit\frac{\chi^2_{1-(\alpha/2);k}}{2NT_r}(10^9), UpperLimit\frac{\chi^2_{(\alpha/2);k}}{2NT_r}(10^9)\ \text{FIT} \tag{C.3}$$

For example, selecting a 90% confidence interval (α=0.1), the average SER of the entire population of devices has a 90% probability of being between the lower and upper limits in C.3. There is a 1-(α/2)=95% probability the average SER is greater than the lower limit and there is only a (α/2)=5% probability that the average SER is greater than the upper limit. As in the previous equation we have multiplied the standard formula by 10^9 to convert errors/hour to FIT.

C.2 Determining Upper and Lower Confidence Intervals

A common aspect of this type of testing is to calculate confidence limits as a function of the number of errors observed so that the experimenter can judge when to terminate the experiment. In other words, when is the SER known to be below a certain failure rate with a certain confidence. Probably the most straightforward way to understand this is to use an actual example of an experiment. The experiment was a real-time test on 3500 identical components. Since this was a soft error rate test and patterns were rewritten after reading, we consider this a test with replacement. The test was continued until nine failures were observed and was terminated on the ninth fail after 1982 hours. The soft failures occurred at 150, 450, 811, 950, 1197, 1327, 1512, 1768, and 2045 hours. The experimental data and the maximum likelihood estimate for the SER are tabulated in Table C.1.

Table C.1

T_r (hr)	Number of Devices	Errors (r)	Component SER FIT,avg
150	3500	1	1905
450	3500	2	1270
811	3500	3	1057
950	3500	4	1203
1197	3500	5	1193
1327	3500	6	1292
1512	3500	7	1323
1768	3500	8	1293
2045	3500	9	1257

Equation C.2 was used to generate the SER maximum likelihood estimate SER column labeled here simply as SER. Applying Equation C.3 we can calculate both the upper and lower confidence bands for this data set. In Table C.2 the chi-squared table is generated for the upper and lower confidence intervals for 90%, 80%, and 60%. Note that k is the degrees-of-freedom (number of errors). In Table C.3 we show the data and in Figure C.1 the plot for SER confidence intervals for 90%, 80%, and 60% based on χ^2 values from Table C.2 and using Equation C.3.

C.2 Determining Upper and Lower Confidence Intervals (cont'd)

Table C.2 — χ^2 values for upper/lower 90, 80, and 60% confidence intervals

		χ^2					
Confidence Interval (1-α)		90%		80%		60%	
Lower, Upper Limits 1-(α/2),α/2		95%	5%	90%	10%	80%	20%
Errors (r)	Degrees of Freedom 2(r+1)						
0	2	0.103	5.991	0.211	4.605	0.446	3.219
1	4	0.711	9.488	1.064	7.779	1.649	5.989
2	6	1.635	12.592	2.204	10.645	3.070	8.558
3	8	2.733	15.507	3.490	13.362	4.594	11.030
4	10	3.940	18.307	4.865	15.987	6.179	13.442
5	12	5.226	21.026	6.304	18.549	7.807	15.812
6	14	6.571	23.685	7.790	21.064	9.467	18.151
7	16	7.962	26.296	9.312	23.542	11.152	20.465
8	18	9.390	28.869	10.865	25.989	12.857	22.760
9	20	10.851	31.410	12.443	28.412	14.578	25.038

Table C.3 — Component SER 90, 80, 60% confidence intervals

			Lower and Upper confidence limits for component SER					
Confidence Interval (1-α)			90%		80%		60%	
Lower, Upper Limits 1-(α/2),α/2			95%	5%	90%	10%	80%	20%
Time (hr)	Errors (r)	Degrees of Freedom 2(r+1)						
149	0	2	98	5744	202	4415	428	3086
150	1	4	677	9036	1013	7409	1570	5703
450	2	6	519	3997	700	3379	975	2717
811	3	8	481	2732	615	2354	809	1943
950	4	10	593	2753	732	2404	929	2021
1197	5	12	624	2509	752	2214	932	1887
1327	6	14	707	2550	839	2268	1019	1954
1512	7	16	752	2485	880	2224	1054	1934
1768	8	18	759	2333	878	2100	1039	1839
2045	9	20	758	2194	869	1985	1018	1749

C.2 Determining Upper and Lower Confidence Intervals (cont'd)

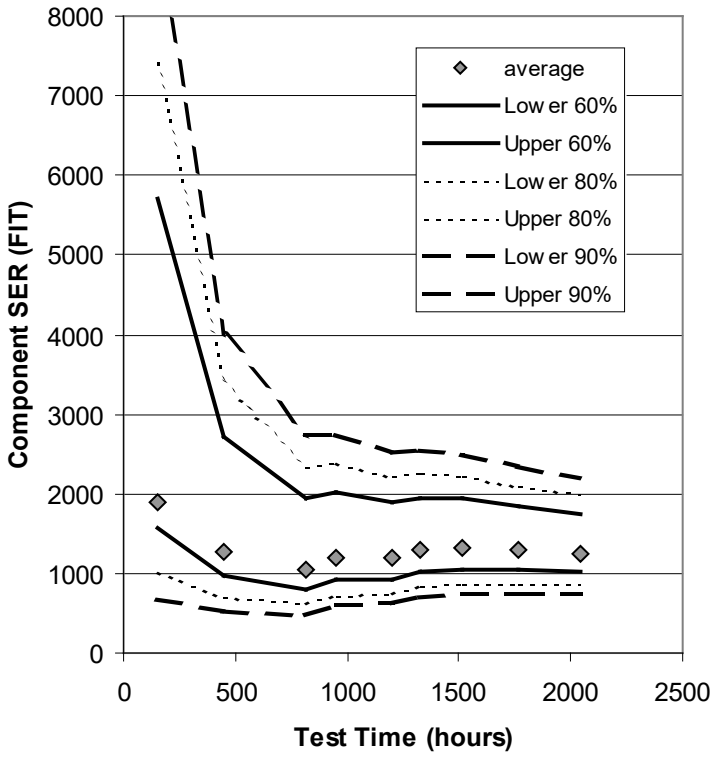

Figure C.1 — Plot showing the max. likelihood SER (average) and the upper and lower confidence intervals at 90, 80, and 60% levels.

Obviously using higher confidence levels means longer test times. If one wanted to be sure that the component tested had an SER < 2000 FIT, at 60% confidence the 3500 units would have to stay on test for about 800 hours while at 80% confidence the same components would need to be tested out to nearly 2000 hours. Conversely, the huge confidence interval shows the risk of using short field tests with no or few errors to test some assumption about average failure rate.

Annex D – The alpha particle environment (informative)

A significant source of ionizing radiation in components is from alpha particles from the naturally occurring radioactive impurities in materials. Alpha particles can be emitted when the nucleus of an unstable isotope decays to a lower energy state. The alpha particle is composed of two neutrons and two protons emitted with specific kinetic energy typically from 4 to 9 MeV.

The activity of a particular isotope is directly proportional to its natural abundance and inversely related to its half-life (the time required for a population of atoms to decay to one-half their original number). ^{238}U, ^{235}U and ^{232}Th (and their associated daughter products) have the highest activities of the naturally occurring radioactive species and are the dominant source of alpha particles in materials. 73.1% of the observed alpha flux would be from ^{238}U decay, 23.5% from ^{232}Th, and 3.4% from ^{235}U respectively if these isotopes were present in equal amounts.

If the half-life of the daughters is less than the half-life of the parent (usually the case for natural isotopes), then their alpha emissivity must also be considered since they can also contribute to the soft error calculation. A population of ^{238}U atoms in equilibrium emits eight different alpha particles at discrete energies ranging from 4.15-7.69 MeV, a population of ^{232}Th will emit six alpha particles from 3.96-8.79 MeV, and an equilibrium population of ^{235}U will emit seven alpha particles from 4.15-7.45 MeV. The spectrum emitted from the natural occurring U and Th populations in a thin film are shown in Figure D.1. Figure D.2 is the emission spectra from at thick film ^{232}Th source showing spectral broadening due to alpha particle energy loss through the film.

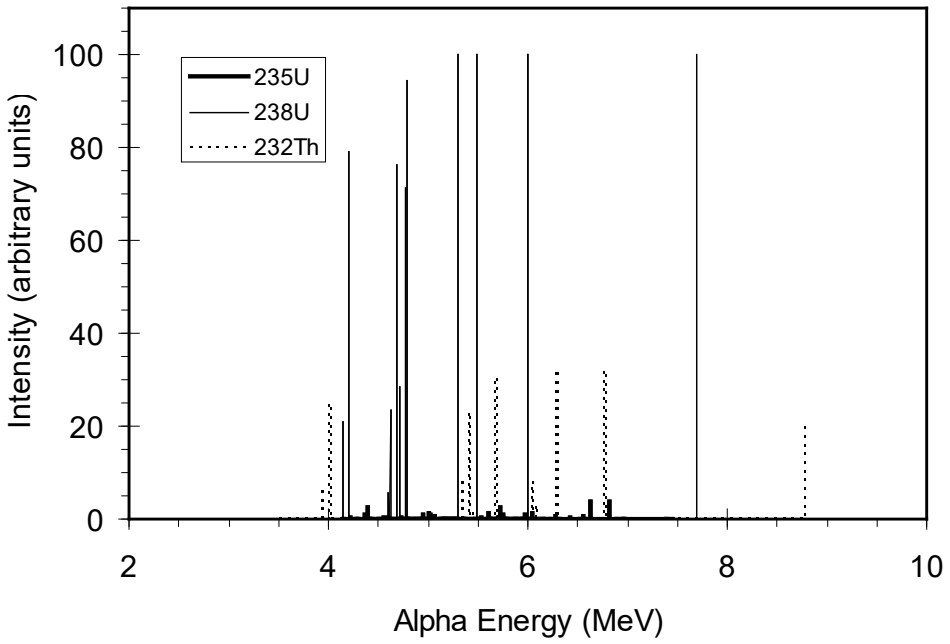

Figure D.1 — Emission Spectra from thin-film ^{238}U, ^{232}Th, and ^{235}U, the predominant natural alpha emitters. Emission is based on activity and natural abundance.

Annex D – The alpha particle environment (informative) (cont'd)

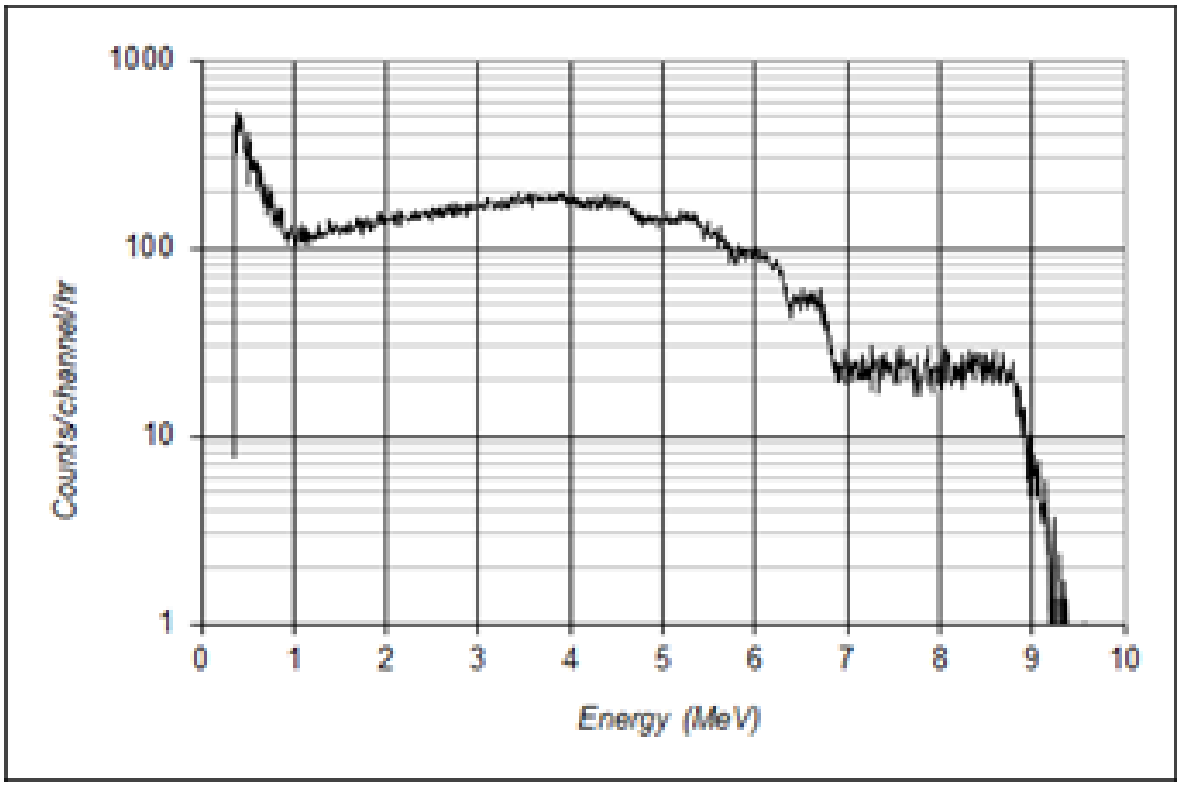

Figure D.2 — Emission Spectrum from thick-film of ^{232}Th. Since alpha particles can be emitted at any depth from the surface, discrete emission lines are broadened into a continuous spectrum of alpha energies.

^{241}Am is also commonly used as a alpha particle source. The alpha energy spectra is different than Th/U sources. If ^{241}Am is used, the user should consult with the supplier on the energy spectrum and flux of the source. It is up to the user to determine if there is an energy mismatch between package contamination and alpha source and assess the impact.
Secular equilibrium is only valid if the material has not undergone any chemical separation or purification. Since virtually all semiconductor materials are highly purified, in general, the alpha emitting impurities will not be in secular equilibrium since various isotope concentrations can become depleted or enriched. Alpha counting investigations are therefore necessary to accurately determine the alpha flux emission. Variations in total alpha activity (TAA) over time can be as large as 10 times [46].

In actual components the alpha emitters are typically distributed throughout each material. The distinct energy "lines" shown in Figure D.1 are usually not observed since emission can occur anywhere within the material and the fine spectrum is broadened as the alpha particles lose energy traveling to the material surface. The alpha spectrum from a thick source of ^{232}Th is shown in Figure D.2. The spectrum from a distributed source of ^{238,235}U will look very similar.

If the alpha source is confined to a thin layer so that all the alpha particle emission essentially occurs at or very near the surface a discrete spectrum is expected. Two examples of surface distributions are the residue

Annex D – The alpha particle environment (informative) (cont'd)

of alpha emitting impurities left after a wet-etch with certain phosphoric acids and the segregation of ^{210}Po to the surface of standard lead-based and tin-based solders. In this case, there will be a peak energy followed by a low energy tail as shown in Figure D.3.

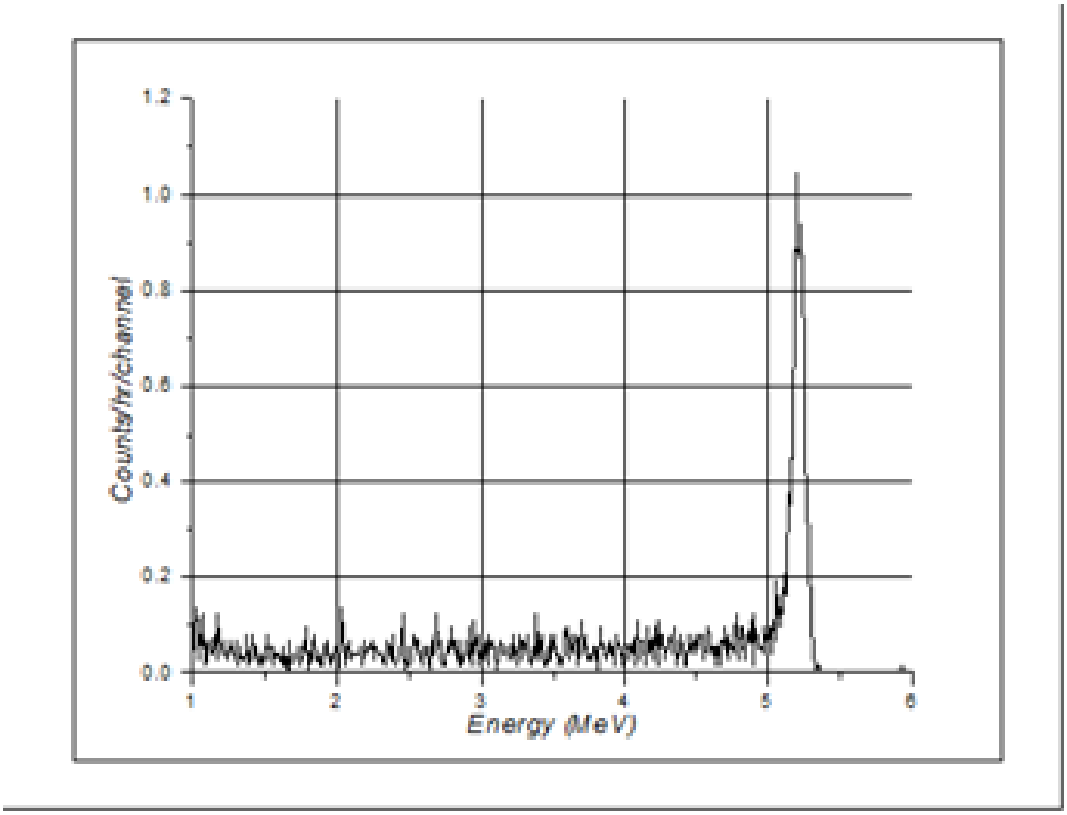

Figure D.3 — Alpha particle energy distribution from surface emission of ^{210}Po.

Annex D – The alpha particle environment (informative) (cont'd)

The probability that an alpha causes a soft error is based on its energy and on its trajectory. The wrong assumptions about the energy spectrum can lead to errors in estimating the SER from accelerated experiments. Alpha particles interact primarily by elastic coulombic scattering with the electrons surrounding nuclei, effectively freeing electrons from their material nuclei. This is also referred to as direct ionization. Significant quantities of electron-hole pairs are generated along the physical trajectory of the ion. For an alpha particle traveling in silicon, an average of 3.6 eV of energy is lost for every electron-hole pair created. The denser the material, the more quickly the alpha particle loses its energy since there is a higher density of charge with which to interact. The charge generation rate (energy loss) increases with the distance the alpha particle travels and reaches a maximum near the end of the alpha particle's path Bragg Peak). This non-linear response is due to the increased ionization efficiency as the velocity of the alpha particle is reduced. Knowing the energy spectrum of incident alpha particles is very important to correctly assess device SER. A curve of the stopping power (or linear energy transfer) and range of an alpha particle in silicon as a function of its energy is shown in Figure D.4. The alpha particle generates anywhere from 4 – 16 fC/μm.

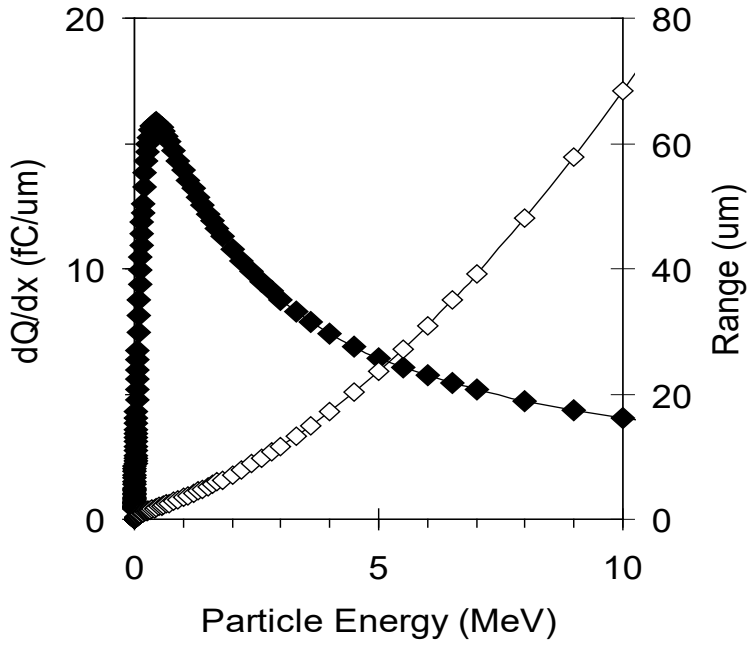

Figure D.4. Stopping power or linear energy transfer (solid diamonds) and range (open diamonds) of an alpha particle in silicon as a function of its energy calculated from SRIM [16]. The Bragg peak is the depth of the maximum charge deposition (~0.5MeV).

In a packaged semiconductor product the sources of alpha emitting impurities can be found in the packaging materials, the chip materials, materials used to attach the chip, and in the materials used during the fabrication process. Alpha particle surface emissions from some key production materials determined by alpha counting are summarized in Table D.1. The alpha emissivities are reported at the 90% confidence level. Depending on the grade and type of material, a large range of alpha emissivities was observed.

Annex D – The alpha particle environment (informative) (cont'd)

Table D.1 — Example of alpha emissivities of various materials. (Note – these emmissivities are examples of published measurements. Not all materials will fall in this range and will depend on their source of origin.)

Material	Emissivity (counts/khr-cm^2)
Fully Processed Wafers	< 0.4
30um thick Cu Metal	< 0.3
20um thick AlCu Metal	< 0.3
Mold compound	< 0.5 – < 24
Flip Chip Underfill	< 0.7 – < 4
Eutectic Pb-based Solders	< 0.9 – < 7200

In a well-controlled manufacturing environment the primary sources of alpha particles are the package materials (ceramic materials, mold compound, underfill, solder, etc.) and not the semiconductor manufacturing materials. However, cases of alpha contamination of semiconductor processing materials have been reported in the past – e.g., ^{85}Kr contamination during package integrity testing, ^{210}Po contamination from evaporator filaments and ^{210}Po contamination of nitric acid during bottle cleaning [47].

There are three ways to reduce alpha particle SER. The first is to use high purity materials and screen for alpha emission. Another is to keep packaging materials with the highest alpha emission separated from sensitive circuit components (e.g., "keep out" regions to separate sensitive SRAM circuits from solder bumps in flip chip packages). Another approach is to shield chips with films of various materials. Knowing the source and energy of the alpha emission is crucial since using a shield that is too thin can raise the SER above unshielded units by moving the peak of the energy deposition (Bragg Peak in Figure D.4) up into the active region.

Annex E – Neutron and Proton Test Facilities (informative)

E.1 Introduction

Most accelerated tests are performed at accelerator facilities which have been built for other applications, e.g., nuclear or high energy physics research at government laboratories or private facilities offering proton cancer treatment. Such facilities usually provide beams for chip testing on a cost recovery basis, which can range from a few percent to a significant fraction of their mission. Normally, the facility provides the beam and the dosimetry, and the user provides the test equipment. Sometimes, facilities collaborate with an outside company which will provide support with the dosimetry and/or test equipment, for a fee.

Radiation effects testing at these facilities covers a wide range of applications, from material damage studies to space effects studies. It is very important that the facility staff is aware of the requirements of the user in beam energy, dose and uniformity and can provide quality assurance that these requirements are met. It is the responsibility of the user to communicate those requirements well in advance of the experiment and to ask for assurance that they can be met. Accelerator facilities are large, complicated systems and on any given day, things can go wrong, so users should maintain flexibility and have some patience.

Sometimes facilities - particularly at government laboratories in the U.S. - require user agreements to be signed and estimated advance payment made before a test run can be scheduled. Ample time should be allowed for this paperwork to be completed, particularly the first time. Typically, university facilities are more flexible in this regard. Users should be aware that most of the time these facilities run 24 hours a day, sometimes 7 days/week. Sometimes the primary mission of the facility takes place during the day, and the availability of beams is limited to nights and weekends, e.g., at some proton therapy centers.

E.2 Facilities list

The major types of user facilities are described briefly in Tables E.2.1 through E.2.4. A spreadsheet of this information will be kept up to date at: www.seutest.com.

NOTE: Facilites managers should submit updates to www.jedec.org to keep www.seutest.com current.

E.2 Facilities list (cont'd)

Table E.2.1 List of thermal neutron facilities .

	FACILITY	url	LOCATION	Description
Thermal Neutron Sources				
	Breazeale Nuclear Reactor, Penn State	https://www.rsec.psu.edu/Neutron_Beam_Laboratory.aspx	Pennsylvania State University, Pennsylvania, USA	Beam Port#4 - 7" dia, thermal 100x > fast neutrons
	High-Flux Advanced Neutron Application Reactor (Hanaro) Ex-core Neutron-irradiation Facility (ENF)	https://hanaro.kaeri.re.kr:444/main.do	Daejeon, KOREA	
	Institut Laue–Langevin (ILL)	https://www.ill.eu/reactor-and-safety/high-flux-reactor/	Grenoble, FRANCE	
	Kytoto University Research Reactor Institute (KUR)	https://www.rri.kyoto-u.ac.jp/en/facilities/kur	Osaka, JAPAN	
	Laboratoire Léon Brillouin (LLB) at the Orphée Reactor	http://www-llb.cea.fr	Saclay, FRANCE	
	Low Energy Neutron Source (LENS)	http://www.indiana.edu/~lens/	Indiana University, Indiana, USA	Be Target - 5.6MeV neutron
	Lujan Center at Los Alamos Neutron Science Center (LANSCE)	https://lansce.lanl.gov/facilities/lujan/index.php	Los Alamos, NM, USA	Four moderators provide epi-thermal, thermal and cold neutrons to specialized beamlines.
	Material Life Science Experimental Facility (MLF), Japan Proton Accelerator Reseach Complex (J-PARC)	http://j-parc.jp/researcher/MatLife/en/instrumentation/ns3.html	Ibaraki, JAPAN	
	McClellan Nuclear Research Center (MNRC)	http://mnrc.ucdavis.edu/default.html	UC Davis, Davis, CA, USA	Training, Research, and Isotope Production General Atomics (TRIGA) reactor
	Massachusetts Institute of Technology Nuclear Reactor Laboratory (MITR)	https://nrl.mit.edu/reactor	Cambridge, MA, USA	
	TRIUMF Thermal Neutron Facility (TNF)	www.triumf.ca	Vancouver, Canada	
	University of Missouri Research Reactor Center (MURR)	www.murr.missouri.edu	Columbia, MO, USA	8.52E+08 n/cm2-s thermal neutron flux

E.2 Facilities list (cont'd)

Table E.2.2. List of mono-energetic, broad spectrum and quasi-mono energetic neutron facilities.

	FACILITY	url	LOCATION	Description
Mono-energetic Neutron Sources (1 - 14MeV)				
	Columbia University Center for Radiaological Research, Radiological Research Accelerator Facility (RARAF)	https://www.crr.columbia.edu/services/ion-beam-and-neutron-core-facility	New York, New York, USA	1.88 MeV neutron microbeam, 220keV - 15MeV mono-energetic neutrons
	GEnerator of NEutrons for Science and IrradiationS (GENESIS), Universite Genoble Alpes	http://lpsc.in2p3.fr/index.php/en/plateformes-technologiques/peren-energie-nucleaire	Grenoble, FRANCE	3 MeV D-D, 15 MeV D-T
	Physikalisch-Tchnische Bundesanstalt (PTB)	https://www.ptb.de/cms/en/ptb/fachabteilungen/abt6/fb-64/642-neutron-metrology/neutron-cross-sections.html	Bundesallee, Braunschweig DE	2.7 MeV and 15 MeV neutrons
	Texas A&M University (TAMU) AGN-201M	https://engineering.tamu.edu/nuclear/academics/laboratory-resources/agn-201m-reactor-laboratory.html	Austin, Texas, USA	14MeV
Broad Spectrum High Energy Neutron Sources				
	CERN-EU high energy Reference Field (CERF)	https://cerf-dev.web.cern.ch/	CERN, Switzerland	
	China Spallation Neutron Source (CSNS)	http://csns.ihep.ac.cn/english/	Dongguan, Guangdong Province, China	1.6GeV protons on W target, rapid cycling syncrotron (25Hz).
	ChipIR, ISIS Neutron and Muon Source	https://www.isis.stfc.ac.uk/Pages/ChipIR.aspx	Didcot, Oxfordshire, UK	800MeV protons on W target + Be reflector + scatterer
	Materials and Life Science Facility (MLF/J-PARC)	http://j-parc.jp/researcher/MatLife/en/instrumentation/ns.html	Ibaraki, Japan	1-400MeV
	Research Center for Nuclear Physics (RCNP), Osaka University	http://www.rcnp.osaka-u.ac.jp/index_en.html	Osaka, Japan	Is spallation source still available? Can't find on webpage.
	Swiss Spallation Neutron Source (SINQ)	https://www.psi.ch/sinq/	Paul Scherrer Institute (PSI)	10^{14} n/cm2/s
	Tri-University Meson Facility (TRIUMF)	http://www.triumf.ca/neutron-irradiation-facility	Vancouver, Canada	Thermal to 400MeV from 400MeV protons on aluminum target
	Weapons Neutron Research (WNR) at Los Alamos Neutron Science Center (LANSCE)	https://lansce.lanl.gov/facilities/wnr/index.php	Los Alamos, NM, USA	Target 4 - 800 MeV protons on W
Quasi-mono Energetic Neutron Sources				
	Cyclotron Radioisotope Research Center (CYRIC)	http://www.cyric.tohoku.ac.jp/english/index.html	Tohoku University, Japan	20-75MeV

E.2 Facilities list (cont'd)

Table E.2.3. List of High Energy Proton Facilities

	FACILITY	url	LOCATION	Description
Proton Sources - Cyclotron				
	California Proton Therapy Center	https://www.californiaprotons.com/	La Jolla, CA, USA	
	Center for Proton Therapy (ZPT), PROSCAN? at Paul Scherrer Institute (PSI)	https://www.texascenterforprotontherapy.com/	Paul Scherrer Institute (PSI)	
	Crocker Nuclear Laboratory (CNL)	http://cyclotron.crocker.ucdavis.edu/	Davis, CA, USA	4 to 63MeV
	Cyclotron Resource Center, Catholic University	http://www.cyc.ucl.ac.be/	Louvain-la-Neuve, Belgium	10MeV - 65MeV energies using beam degrader, +/-10% uniformity over 80mmx80mm, 50 to 2e8 protons/cm2s
	Hampton University Proton Therapy Institute (HUPTI)	http://www.hamptonproton.org/	Hampton, VA, USA	
	Hans-Meitner Institute	www.helmholtz-berlin.de/zentrum/historie/lise-meitner-campus/index_en.html		
	High Intensity Proton Accelerator (HIPA) at Proton Irradiation Facility (PIF)	https://www.psi.ch/gfa/	Paul Scherrer Institute (PSI)	590MeV protons
	Japan Proton Accelerator Research Complex (J-PARC)	http://www.j-parc.jp/Acc/en/index.html	Ibaraki, Japan	400 MeV linear accelerator (LINAC)
	Korea Multi-purpose Accelerator Complex (KOMAC)	https://komac.kaeri.re.kr/	Gyeongju, South Korea	linear accelerator (LINAC) - 100 MeV proton beam - Real time flux monitoring system
	Kyoto University Research Reactor Institute	Hiroki Tanaka, Kyoto University Research Reactor Institute (h-tanaka@rri.kyoto-u.ac.jp)	Osaka, Japan	http://ieeexplore.ieee.org/stamp/stamp.jsp?tp=&arnumber=6551089
	Laboratori Nazionali Legnaro (LNL-INFN)	www.lnl.infn.it/~neweb/index.php/en/introduction-to-the-lnl-accelerators		
	Lawrence Berkeley National Labs (LBNL)	www.lbl.gov	Berkeley, CA, USA	50MeV
	Mass General Francis H. Burr Proton Therapy (MGH)	www.massgeneral.org/radiationoncology/BurrProtonCenter.aspx	Boston, MA, USA	up to 222MeV
	Material Testing Reactor (MTR), the JulesHorowitz Reactor (JHR), is under construction at theCEA Cadarache (French Alternative Energies and AtomicEnergy Commission).	http://ieeexplore.ieee.org/stamp/stamp.jsp?tp=&arnumber=6759757		
	Northwestern Medicine Chicago Proton Center	https://www.chicagoprotoncenter.com/	Warrenville, IL, USA	
	ProCure Proton Therapy Center	https://www.procure.com/Oklahoma-Explore	Oklahoma City, OK, USA	
	Proton Beam Facility (PAULA) at The Svedberg Laboratory (TSL)	http://www.tsl.uu.se/irradiation-facilities-tsl/PAULA-proton-beam-facility/	Uppsala University, Sweden	20 - 180MeV, 1e11 1e12 proton/cm2-s
	Provision Center for Proton Therapy	https://provisionhealthcare.com/	Knoxville, TN, USA	
	Research Center for Nuclear Physics (RCNP), Osaka University	http://www.rcnp.osaka-u.ac.jp/index_en.html		100 - 392MeV. Looks like proton source available.
	Seattle Proton Therapy Center	https://www.seaprotontherapy.com/	Seattle, WA, USA	
	Texas A&M University (TAMU)	https://engineering.tamu.edu/nuclear/research/facilities/accelerator-laboratory.html	Austin, TX, USA	50MeV
	Texas Center for Proton Therapy	https://www.texascenterforprotontherapy.com/	Irving, TX, USA	
	Tri-University Meson Facility (TRIUMF)	http://www.triumf.ca/proton-irradiation-facility	Vancouver, Canada	BL2C - 5 to 120 MeV BL1B - 120 to 500 MeV
	University of Florida Health Proton Therapy Institute (UFHPTI)	https://www.floridaproton.org/	Jacksonville, FL, USA	
	University of Maryland Proton Treatment Center	http://www.mdproton.com/home	Baltimore, MD, USA	
	Weapons Neutron Research (WNR) at Los Alamos Neutron Science Center (LANSCE)	https://lansce.lanl.gov/facilities/wnr/index.php	Los Alamos, NM, USA	Target 2 (Blue Room) - direct 800 MeV proton exposure
Proton Sources - Syncrotron				
	NASA Space Radiation Lab (NSRL), Brookhaven National Laboratory	https://www.bnl.gov/nsrl/about.php	Brookhaven, NY, USA	Energies from 50 to 1500 MeV
	Slater Proton Treatment and Research Center at Loma Linda University Medical Center (LLUMC)	https://protons.com/why-choose-loma-linda/our-center	Loma Linda, CA, USA	

E.2 Facilities list (cont'd)

Table E.2.4. List of High Altitude Facilities, Underground Facilities and Terrestrial Neutron Monitoring Database.

High Altitude Facilities				
	Altitude SEE Test European Platform (ASTEP)	Website currently offline. Check https://en.wikipedia.org/wiki/Altitude_SEE_Test_European_Platform for updates.	Southern Alps, FRANCE	~2.6 km above sea level
	Magdalena Ridge Observatory (MRO)	www.mro.nmt.edu/	Magdalena Mountains, New Mexico, USA	~3.2 km above sea level
	Subaru Telescope	www.naoj.org	Peak of Mauna Kea, Hawaii, USA	~4.2 km above sea level
	White Mountain Research Center	https://www.wmrc.edu/applications/default.html	White Mountain, CA, USA	~3.9 km above sea level
	Yangbajing International Cosmic Ray Observatory	http://www.ircip.cn/bbx/999722-999726.html?id=26645&newsid=639942	Yangbajing (YBJ) Valley of Tibet, China	~4.3 km above sea level
Underground Facilites				
	Boulby Underground Laboratory	https://stfc.ukri.org/about-us/where-we-work/boulby-underground-laboratory/	Loftus, Saltburn-by-the-Sea, Cleveland, UK	Working potash, polyhalite and rock-salt mine ~1.1km underground
	Low Noise Underground Laboratory of Rustrel-Pays d' Apt (LSBB)	http://lsbb.unice.fr/	Rustrel, France	~0.5 km below the surface
	Modane Underground Laboratory (LSM, CEA-CNRS)	http://www-lsm.in2p3.fr/	Fréjus Tunnel, Modane France	~1.7 km under the peak of Fréjus mountain (4.8 km meters water equivalent)
	Oto Cosmo Observatory (Out of Service)	http://wwwkm.phys.sci.osaka-u.ac.jp/info/syoukai/oto-e.html	Oto-Tentsuji Tunnel, 100 km south of Osaka, Japan.	~0.8 km below the surface
	Sanford Underground Research Facility (SURF)	https://www.sanfordlab.org/facility	Lead, South Dakota, USA	Former site of the Homestake Gold Mine ~1.5 km below the surface
	Soudan Underground Laboratory	http://www.soudan.umn.edu/	Soudan, Minnesota, USA	Abandoned iron mine ~0.7 km below the surface
	Sudbury Neutrino Observatory (SNOLAB)	https://www.snolab.ca/	Sudbury, Ontario, Canada	~2 km below the surface in the Vale Creighton Mine
	Super-Kamiokande	http://www-sk.icrr.u-tokyo.ac.jp/sk/index-e.html	Mozumi Mine, Hida, Gifu Prefecture, JAPAN	Neutrino detector ~1 km below the surface
Neutron Monitor Database Websites				
	Neutron Monitor Database	http://www.nmdb.eu/	Around the world	Real-Time Database for high-resolution Neutron Monitor measurements and historical data

E.3 Heavy ion facilities

Heavy ion facilities are generally used for testing of parts destined for space orbit, where primary cosmic rays can cause significant damage to microelectronics. Heavy ion testing facilities are well established and could be an option for alpha tests over radioactive sources. These facilities are not included in the database at this time.

E.4 Proton facilities

The maximum and minimum flux and size of the beam which is available from any of the proton facilities depends on many factors, e.g., shielding, dosimetry, and radiation training of users (some facilities require additional training courses to run above certain levels). Most facilities are set up so that the part is run in air, which makes it easier to set up and allows the use of shorter cables. However, one should take great care that any radiation sensitive secondary equipment is shielded from the beam.

Proton dosimetry has been well established over the last 30 years by the therapy community and standards exist for calibration of ion chambers, the main means of real-time dosimetry in use. These have been summarized in a report by the International Atomic Energy Agency (IAEA) entitled, 'Absorbed Dose Determination in External Beam Radiotherapy: An International Code of Practice for Dosimetry based on Standards of Absorbed Dose to Water'. The user should consult with the facility's manager on beam calibration techniques and measurements.

E.5 Neutron facilities

Four types of neutron facilities are available:

1) Thermal neutrons, usually obtained from reactors, used for the studies described in **7**
2) (d,d) or (d,t) neutron sources, giving monoenergetic neutrons at 2.5 and 14 MeV, respectively, used for accelerated testing in combination with proton sources, as described in **6**,
3) spallation proton sources, which produce a neutron energy spectrum up to the energy of the proton source, also used for accelerated studies as described in **6**, and
4) quasi-monoenergetic neutrons of various energies, usually produced using protons on a Be or Li target, an alternative method described in **6**

Because neutrons have no charge, it is not possible to count the neutrons directly. Instead, secondary reactions which have high probability and are well understood must be used for dosimetry. The most appropriate material for dosimeters for neutrons is dependent on the neutron energy. For thermal neutrons, boron-containing material is efficient for capturing neutrons and can be used for real-time dosimetry. The most accurate method is activation foils, which are very well understood but must be counted offline after the irradiation. For fast neutrons, polyethylene, liquid-scintillator or other hydrogen-containing material is used and the proton recoils are measured. An old technique, which is still used extensively, is fission ion chambers. The fissionable material used, which could be uranium, bismuth or other heavy isotopes, determines the low energy threshold of sensitivity to neutrons. There is no standard for neutron dosimetry as there is for protons, and the dosimetry may not be as well understood as at proton facilities. The user should determine from the facility what the efficiency, accuracy and energy limits are of the dosimetry in use.

Annex F – Sources of measurement errors (informative)

This annex provides guidance in assessing the various sources of measurement errors in determining the fundamental quantities soft error cross-section (σ) and soft error rate (R):

$$\sigma = \frac{N}{\Phi} \tag{F.1}$$

$$R = \frac{N}{T} = \frac{\sigma \Phi}{T} \tag{F.2}$$

where N is the number of events, Φ is the alpha or neutron fluence per unit area and T is the measurement time interval.

F.1 Sources of errors in thermal and high energy neutron measurements (real-time and accelerated)

F.1.1 Measurement accuracy due to errors in fluence measurement - Φ

F.1.1.1 Accuracy of fluence

For accelerator or reactor facilities, the facilities manager should be consulted on the accuracy of the fluence. For example, how is variation of flux accounted for in the final fluence? Is the flux monitored real time and integrated at the end of the test? Or is an average flux assumed and multiplied by the test duration? In the case of real time testing, is the terrestrial flux assumed to be constant? Or are adjustments made for atmospheric pressure variation and solar activity?

F.1.1.2 Uniformity of fluence (large area devices and multiple devices side by side)

Depending on the beam configuration and device area (or if multiple devices are side by side), variations in the uniformity of the fluence will lead to differences in the measured cross-section and rate. The user should consult the facility manager on beam fluence variation over the area of devices tested.

F.1.2 Measurement accuracy due to uncertainty in number - N

F.1.2.1 Statistical variation

See annex C.

F.1.2.2 Undetected errors and masking effects

Not all soft error events will necessarily be observed. The number of events that go undetected will depend on the device design, test conditions and test algorithms. There is no way to generalize the measurement error introduced by not accounting for these undetected or masked upsets. However, the user should ensure that the testing uncovers as many errors as possible. If the user has a means of estimating these undetected errors (e.g., only half of memory can be tested, so errors from untested memory will go undetected), this should be noted in the final report.

F.1 Sources of errors in thermal and high energy neutron measurements (cont'd)

F.1.3 Measurement error due to uncertainty in time interval – T

This is not a significant source of measurement error because the time scale is large (minutes to hours for accelerated testing or days to months for real-time testing) and can be measured with better accuracy than fluence or soft error count discussed above.

F.1.4 Measurement errors due to secondary beam and energy effects

Equations F.1 and F.2 implicitly contain neutron energy dependence. Therefore, any mismatch in spectra between the test source and the reference spectrum will introduce errors.

F.1.4.1 Particle scattering in beamline

Secondary and scattered particles can be generated as a result of the beam interacting with materials in the beamline. The user should consult with the facility manger on characterization of these effects and if these secondary particles have sufficient energy to reach the device active area.

F.1.4.2 Fluence attenuation and secondary ion generation due to material in front of the active area

Several cases exist where the geometry of and material used in the test fixture (not the beamline) can impact incident beam energy *(spectrum shift)* and fluence *(beam attenuation due to scattering and absorbtion)* as well as generating secondary ions – e.g., heat sink materials and devices tested one in front of the other. For real time testing, building effects should be considered. The user should either 1) estimate the impact of fluence attenuation, energy shift and secondary ion generation using simulation (GEANT, FLUKA, etc.) or 2) count differences in the number of errors for each device (from front to back) and assess the impact of these effects. $1/r^2$ dependence should also be accounted for.

Note – For 2) above, the error counts must be high enough to discern differences between stacked devices that are not due to statistical counting variation. (see annex C).

F.1.4.3 Spallation source mismatch

The match between the reference spectrum and the various spallation sources will lead to measurement errors that depend on the energy dependence of the cross section. Unless the user makes independent measurments to determine this energy dependence, it is difficult to assess the impact of this mismatch.

F.1.4.4 Weibull fit

If mono-energetic or quasi-mono-energetic sources are used, fitting the data to a four parameter Weibull function can lead to errors. However, the user can use numerical integration techniques to assess the impact of the fit on Equation 6.10. [27].

F.1 Sources of errors in thermal and high energy neutron measurements (cont'd)

F.1.5 Propagation of errors

As discussed in **7.6.2** (see Equation 7.3), significant measurement errors can be encountered when using a high energy neutron source to measure the thermal neutron cross section in cases where the cross section measured with and without shielding is comparable (i.e., $N_{wo\ shield}/\Phi_{beam\ wo\ shield} \sim N_{w\ shield}/\Phi_{beam\ w\ shield}$). This can occur in cases where there is not a signicant thermal component in the beam or if the thermal cross section is significantly smaller than the high energy cross section. Considering the primary sources of errors as counting statistics and beam fluence, from Equation 7.3, these will be added in quadrature:

$$\delta\sigma_{th} = \sqrt{\delta\sigma_{wo\ shield}{}^2 + \delta\sigma_{w\ shield}{}^2}$$

$$= \sqrt{\sigma_{wo\ shield}{}^2\left(\frac{\delta N_{wo\ shield}{}^2}{N_{wo\ shield}{}^2} + \frac{\delta\Phi_{wo\ shield}{}^2}{\Phi_{wo\ shield}{}^2}\right) + \sigma_{w\ shield}{}^2\left(\frac{\delta N_{w\ shield}{}^2}{N_{w\ shield}{}^2} + \frac{\delta\Phi_{w\ shield}{}^2}{\Phi_{w\ shield}{}^2}\right)} \qquad (F.3)$$

$$\sim \sqrt{2}\,\delta\sigma_{wo\ shield}$$

in the case where $\sigma_{wo\ shield}$ and $\sigma_{w\ shield}$ are comparable (i.e., σ_{th} is small by comparison). The errors in both will also be comparable (i.e., $\delta\sigma_{wo\ shield} \sim \delta\sigma_{w\ shield}$). If $\delta\sigma_{wo\ shield} >> \sigma_{th}$, then the use of a high energy neutron source to measure thermal neutron cross section is not valid because $\delta\sigma_{th} >> \sigma_{th}$.

F.2 Sources of errors in alpha particle measurements

F.2.1 Alpha source flux calibration, energy spectrum and uniformity

The user should request information from the alpha source supplier on flux, energy spectrum and uniformity along with how the source should be maintained and calibrated. Uniformity of the source across the active area is critical and variation should be no more than +/-10%. If an encapsulant is used to protect the surface, it's impact on the energy spectrum should be assessed. If the surface is not protected, physical handling can cause change in flux over time. So precautions should be taken to not touch the surface. If something has happened to the surface, it should be sent back for recalibration.

F.2.2 Energy Spectrum Effects

The energy spectrum of the source used for accelerated measurements might be different than the actual package contaminants (e.g., ^{241}Am source vs ^{232}Th/^{238}U package contamination). The user should consider this impact and note in the final report. In addition, spectrum smoothing and attenuation effects can take place in a packaged part that would not be seen with a bare die and alpha source. There are no straightforward correction factors that can be applied in these cases. If the user chooses to undertake these calculations, they should be noted in the final report.

F.2.3 Geometrical Effects

Accelerated alpha soft error measurements use a uniform planar source separated by a physical gap from the active area. However, the real sources of alpha particles for the device might not be uniform (e.g., point source emission from Pb bumps in a flip chip package) and are in intimate contact with (or near) the active area. The user should consider these impacts and try to minimize as much as practically possible (e.g, minimize gap so attenuation of flux is minimal- see Figure 5.3 for source to bare die flux correction factor) and note in the final report. There are no straightforward correction factors that can be applied to cases where the package emissivty is nonuniform or is coming from different depths in the package. If the user chooses to undertake these calculations, they should be noted in the final report.

F.2.4 Measurement Accuracy Due to Uncertainty in Number - N

See annex F.1.2

F.2.5 Measurement Error Due to Uncertainty in Time Interval – T

This should not be a significant source of measurement error because the time scale for accelerated alpha soft error measurements are large (>>1hr) and can be measured with better accuracy than source flux or geometric factors discussed above.

Annex G – Recommendations for Final Report Content (informative)

As discussed in **3** through **7**, there are multiple radiation techniques required in order to measure the SEE characteristics due to alpha, thermal neutron and high energy neutron radiation. Once the user has determined and completed the entire test campaign (i.e., real time testing and/or accelerated alpha source testing, high energy neutron beam testing and thermal neutron testing), a final report should be produced that summarizes all the tests. All applicable SEE rates for the tested component should be individually reported (see Table G.2.A). If the user decides to eliminate some tests, the reasons should be noted in the final report. For example, a test campaign can include separate measurements of accelerated alpha, thermal neutron and high energy neutron cross sections. From this data, the total SER of a device at the reference standard can be calculated. Alternatively, a combination of real time SER and accelerated alpha source testing can be used to determine the soft error characteristics of a device in the reference spectrum, but the thermal and high energy contribution cannot be deconvolved if Cd or ^{10}B shielding is not used (see Sec 6.7). Either technique is acceptable and it is up to the user to determine the preferred approach. At a minimum, the device should be tested at nominal operating conditions (temperature, voltage and frequency) with normal angle of incidence for high energy neutrons. Additional characterization at different operating conditions and angle of incident radiation is optional. This section is intended to guide the user in assembling the various pieces of data collected into a format that can be easily communicated and demonstrate compliance to this standard.

G.1 Device and Test Equipment Electrical Charateristics

Table G.1 lists the general items that should be included in the final report with respect to the devices being tested. For any details that the user does not have access to or is considered confidential, the response should be “unknown” or “confidential”.

G.1 Device and Test Equipment Electrical Charateristics (cont'd)

Table G.1 — Device description, electrical tests and failure details that should be included in final report.

DUT description:	
	Sample size (number of devices tested)
	Vendor, Part # and Die rev (for commercial components) or Test Chip Description
	Process technology (feature size, # and type of metal levels, presence or absence of polyimide or other layers, etc.)
	Product (e.g., SRAM, DRAM, Microprocessor, test chip flip flop chain, etc.)
	On-chip error correction (type and coverage of ECC)
	Dimension of the active device area tested.
	Package (type, connection to chip, materials and geometries) with description of any modifications made for SER testing (e.g., etch back of encapsulant, etc.).
Electrical Test Description	
	Test duration
	Voltage (external supply, internal regulated, back bias voltages if applicable)
	Junction & ambient temperature during test
	Static or Dynamic test (core cycle time or frequency if dynamic) – special note must be made if the DUTs are run at a cycle time different than the intended end use
	Refresh rate (where applicable)
	Test patterns and data patterns, including dead-time calculation (see 3.3.3)
	Test Hardware (ATE commercial model and/or physical description if equipment is custom made)
	Description of test board (number of layers, number of devices, etc.)
	Description of types of errors that can be detected
	Duration of test time per device
	Shielding from radiation sources (if used) or building wall and ceiling description (for real time testing)
	Record any problems or unusual behavior
Failure Information	
	Periodicity of readouts/time of each failure
	Failing logical address/s
	Failing physical location/s
	NOTE: Electrical signature of each soft error including a description of the occurrence of SCU, MCU, MBU, SEL, and SEFI events. Estimating a failure rate without segregating the types of errors occurring (SEU, MBU, MCU, SEL, SEFI, etc.) can lead to erroneously high average failure rates. The effective failure rate of each unique failure signature must be calculated accordingly (e.g., Equation 6.1 and 6.2))
	Voltage, ECC on/off status, DUT power mode (i.e., standby, running traffic, etc.) and test/data pattern at the time of failure
	Identification of failures that are multiple-cell errors
	Electrical signature and source of hard errors (if observed)

G.2 Source Radiation Characteristics and Device Positioning

Table G.2.A and G.2.B list the items that should be included in the final report based upon the user determined source selection and test campaign.

Table G.2.A — Radiation source items that should be included in final report depending on which sources are used.

<table>
<tr><th>REAL TIME SER</th><th>ALPHA SER</th><th colspan="2">HIGH ENERGY NEUTRON SER</th><th>THERMAL NEUTRON SER</th></tr>
<tr><td>Location of devices under test: latitude, longitude and altitude</td><td>Source isotope(s) (e.g., ^{241}Am, ^{232}Th, etc.)</td><td colspan="2">Name, location, type and overall description of accelerator facility including beamline (if applicable)</td><td></td></tr>
<tr><td>Average of atmospheric conditions / range of calendar dates of data collection</td><td>Source manufacturer, serial number or other means of identification</td><td colspan="3">Description of source used to generate neutrons</td></tr>
<tr><td>Calendar date of each failure</td><td>Physical configuration of the source (e.g., diffusion bonded with gold over-layer, encapsulant material, etc.)</td><td colspan="3">Description of energy spectrum</td></tr>
<tr><td>General building description (e.g., number of floors, building material, windows, etc.) and location of DUTs within building</td><td>Source activity in Bq – implies integration over spherical emission volume</td><td colspan="3">Description of beam spot size, shape, uniformity and distribution (e.g., gaussian, uniform, etc.)</td></tr>
<tr><td rowspan="5">Either a measurement of the neutron flux at the ATE or an estimation showing clear details of the calculation (e.g., direct measurement over a particular energy range, calculations from annex A, etc.)</td><td rowspan="5">The last calibration date</td><td colspan="3">Description of measurement technique and correction factors used to determine flux at DUT (e.g., flux at DUT different than flux at detector due to solid angle effects) and relevant calibration information</td></tr>
<tr><td colspan="3">Description of method to determine fluence at each DUT (e.g., average of flux at start and end of test, real time flux integration, etc.)</td></tr>
<tr><td colspan="3">Description of special configurations or filters used (e.g., moderators, neutron guides, Cd shielding, etc.).</td></tr>
<tr><td colspan="2">Particles in beam and their energy other than high energy neutrons</td><td rowspan="2">Particles in beam and their energy (other than thermal neutrons)</td></tr>
<tr><td colspan="2">If complementary proton testing is used, note the correlation factor</td></tr>
</table>

Table G.2.B — Items that should be included in final report describing source and device orientation.

<table>
<tr><th>REAL TIME SER</th><th>ALPHA SER</th><th>HIGH ENERGY NEUTRON SER</th><th>THERMAL NEUTRON SER</th></tr>
<tr><td rowspan="6">Orientation of DUT to horizon and geometry of boards (i.e., planar or stacked)</td><td>Dimension and shape of source active area and device active area</td><td colspan="2">Beam angle of incidence with respect to the DUT</td></tr>
<tr><td>If available, the source energy spectrum (for thin foil sources with discrete energy peaks a simple list of peak energies will suffice while for sources with distributed spectra a plot is recommended)</td><td colspan="2">If multiple DUTs tested, decription of geometry with respect to the beam (e.g., stacked or side by side)</td></tr>
<tr><td>Alignment of source with respect to DUT active area tested</td><td colspan="2" rowspan="4">Describe any type of scattering/shadowing material in the neutron beam during the experiments needs to be described in detail (see 7.7.5)</td></tr>
<tr><td>A description of any shadowing which might affect the final result by obstructing some of the source flux</td></tr>
<tr><td>Source-to-die spacing</td></tr>
<tr><td>Estimate of the alpha flux reaching the active device surface</td></tr>
</table>

Note – Not all four test techniques are required. It is up to the user to determine the test requirements for a complete alpha and neutron soft error characterization.

G.3 SEU Cross Section and FIT Calculations

The final report should include the various tests done to arrive at a final soft error characterization at the reference spectrum level. This will include the alpha SEU due to material impurities as well as high energy and thermal neutron soft errors. Table G.3 summarizes what should be reported for real time or accelerated tests, measurement errors and the translation methodology to the reference spectrum.

G.3 SEU Cross Section and FIT Calculations (cont'd)

Table G.3 — Summary of soft error cross section or rate reporting.

<table>
<tr><th>ITEM</th><th>REAL TIME</th><th>ALPHA</th><th>HIGH ENERGY NEUTRON</th><th>THERMAL NEUTRON</th></tr>
<tr><td rowspan="4">Real Time or Accelerated Soft Error Cross Section or FIT</td><td>Calculation of real-time soft error cross section or FIT at test site for each type of event (e.g., cell upset, logic upset, latchup, etc.) using:</td><td>Calculation of accelerated alpha soft error cross section or FIT for each type of event (e.g., cell upset, logic upset, latchup, etc.)</td><td>Calculation of high energy neutron soft error cross section or FIT for each type of event (e.g., cell upset, logic upset, latchup, etc.) and for each electrical condition measured (e.g., voltage, ECC state, pattern, frequency, etc.) and each radiation test (e.g., single spallation source test, multiple mono-energetic or quasi-mono energetic sources).</td><td>Calculation of thermal neutron soft error cross section or FIT for each type of event (e.g., cell upset, logic upset, latchup, etc.) and for each electrical condition measured (e.g., voltage, ECC state, pattern, frequency, etc.) and each radiation test (i.e., with and without B or Cd shielding).</td></tr>
<tr><td rowspan="2">Description of the techniques used to calculate fluence at the DUT including building effects</td><td rowspan="2">Description of the techniques used to calculate fluence at the DUT including alpha attenuation through layers</td><td rowspan="2">Description of the techniques used to calculate fluence at the DUT including high energy neutron scattering effects</td><td>Description of the techniques used to calculate fluence at the DUT including thermal neutron absorbtion and scattering effects</td></tr>
<tr><td>For nuclear reactor facility tests: check pre and post device charateristic for gamma radiation damage.</td></tr>
<tr><td colspan="4">Statistical methods outlined in annex C if event count is small and the confidence intervals should be clearly stated in the final report).</td></tr>
<tr><td rowspan="4">Soft Error Cross Section or FIT at Reference Level (high energy 12.9 n/cm^{2}hr and thermal 6.6 n/cm^{2}hr)</td><td>Translation of real-time soft error FIT to reference spectrum</td><td>Translation of accelerated alpha soft error cross section or FIT to packaged product.</td><td>Translation of accelerated high energy neutron soft error cross section or FIT to reference spectrum.</td><td>Translation of accelerated thermal neutron soft error cross section or FIT to reference spectrum.</td></tr>
<tr><td rowspan="3">This will require estimation of high energy and thermal neutron and alpha particle components. The assumptions/ calculations should be stated clearly in the report (e.g., Is alpha cross section independently determined? What are scaling assumptions between high energy and thermal neutrons?)</td><td>Acceleration factor between alpha source and product package emissivity</td><td>For spallation sources, beam acceleration factor used.</td><td rowspan="3">Methods used to correct for cold, epithermal and high energy neutron contributions if appropriate (i.e., how closely does source represent terrestrial thermal neutron spectrum?)</td></tr>
<tr><td rowspan="2">Final report should clearly state any correction factors used to account for overlayer attenuation, package geometry and spectrum mismatch (e.g., ^{241}Am source vs ^{238}U package impurities).</td><td>For monoenergetic sources, report Weibull parameters and method used to calculate cross section or FIT</td></tr>
<tr><td>For complementing broad beam neutron test, method to arrive at correlation factor (see 6.6.2.5)</td></tr>
<tr><td colspan="4">Report any scaling factors between test chip and final product if appropriate</td></tr>
<tr><td colspan="5">NOTE Linearity check - for highly accelerated testing using alpha and neutron sources, the user should distinguish multiple errors (e.g., MCU) from a single event from multiple errors caused by multiple events (e.g., multiple SCUs). This can be accomplished by reducing source flux and increasing read-out frequency to reduce the probability of multiple events. The number of events should scale linearly with the source fluence. A good indication of operation in the non-linear regime is if there are errors every readout cycle. This indicates there can be a "collision" of events where two or more single events occur within the same readout cycle. As the probability of errors per readout cycle drops to $p < 1$, the probability of two independent single events scales down as p^2.</td></tr>
</table>

Annex H (informative) Differences between JESD89A and JESD89B

The following are changes made from JESD89A.

Introduction

Figure 1 added to diagram various single event terms used in the standard. Soft error remains as the primary term for JESD89B. Single event upset (SEU) more narrowly defined as a cell, flip-flop or latch-upset, so soft error replaces SEU throughout JESD89B.

1 Scope

List of related documents updated and extended to include other radiation effects.

2 Terms and definitions

New terms added to more precisely define soft error effects: bit, cell, reset soft error, single bit upset, single cell upset and single event hard error.

3 Test equipment and software requirements

3.1 Test plan - Section moved to beginning of Sec 3 as a better introduction. More guidance provided around planning a successful soft error test plan for first time users.

3.3 Test conditions - More details and guidance added to environmental conditions, static vs. dynamic testing.

3.4 Setup procedure (JESD89A) – This section has been eliminated because the information repeated in **4**, **5**, **6** and **7** under detailed testing procedures for each source.

3.5 General testing specification (JESD89A) – This section has been eliminated because the information repeated in **4**, **5**, **6** and **7** under detailed testing procedures for each source.

3.6 Data collection (JESD89A) – This section has been removed and the details required for the final report are added to annex G – Recommendations for Final Report Content.

3.4 Considerations for Soft Error Testing of Individual Circuit Elements (JESD89B) – This section is new and addresses soft error testing of individual building block circuits (i.e., test chips designed for soft error testing).

3.5 Considerations for Testing IC Products (JESD89B) - Examples of testing memory components has been added. 3.7 Considerations for testing non-memory components (JESD89A) has been eliminated as obsolete and other sections addressing random logic circuits, FPGAs and microprocessors have been re-numbered.

Annex H (informative) Differences between JESD89A and JESD89B (cont'd)

4 Real-time (unaccelerated and high-altitude) SER procedures

4.2.3 Test Hardware – Reference directly to BPSG for thermal neutron soft errors is eliminated and user is refereed to 7 Accelerated thermal neutron test procedures for updates on other sources of thermal neutron soft errors.

4.2.4 Test software – Added requirement the user must understand the details of embedded ECC capabilities of they are used.

4.4 Differences in real-time SER tests and actual end-user observed fail rates – Added more examples of how errors detected in RTSER set-up might go undetected in system operation.

4.5 Final Report (JESD89A) – Deleted. Details moved to annex G Recommendations for Final Report Content (JESD89B) where final report instructions for **4**, **5**, **6** and **7** have been consolidated.

5 Accelerated alpha-particle test procedures

5.1.1 Introduction – ^{210}Po contamination in lead and tin added as an additional source of soft errors.

5.3.1 Flip Chip Packages – new section

5.4.1 Alpha source selection – more details added on source selection, including ^{241}Am and ^{232}Th sources.

5.4.4 Alpha particle source flux (JESD89A) changed to **Alpha particle source intensity and uniformity (JESD89B)** – Details added on user checks for linearity of soft error measurements and source uniformity.

5.5 Basic test methodology (JESD89A) – eliminated as redundant information that is covered in new section **3.5.1** Memory components

5.6.1 General test specifications (JESD89A) – eliminated as redundant information to Sec 3 and annex G.

5.6.2 Basic alpha particle flux acceleration factor (JESD89A) – renumbered **5.5.1**

5.6.3 Geometry factor and shielding (JESD89A) – renumbered **5.5.2**

5.6.4 Extrapolating the failure rate to use conditions (JESD89A) – renumbered **5.5.3**

5.7.1 Rate of errors in accelerated tests (JESD89A) – eliminated as redundant information covered by linearity note in annex G.

5.7.2 Generalized noise issues (JESD89A) – eliminated as redundant information covered **3**

5.7.3 Total dose (JESD89A) – renumbered **5.6.1**

5.7.4 Package shadowing (JESD89A) – renumbered **5.6.2**

Annex H (informative) Differences between JESD89A and JESD89B (cont'd)

5.7.5 Single event latchup and single event functional interrupt – eliminated as redundant to note for Equation 5.2 and information provided in definitions for SEL and SEFI.

5.8 Final Report – eliminated as redundant information outlined in annex G.

6 Accelerated high-energy neutron test procedures

Note – Some sections were deleted and others moved forward, so section number refrencing below is with respect to JESD89B unless JESD89A is specifically called out.

Replaced "terrestrial cosmic ray" in JESD89A with "high-energy neutron" to more accurately define content of section and distinguish from thermal neutron testing in **7**.

General - Soft Error Cross Section and Soft Error Rate equations in **6** have been updated with subscript i to explicitly indicate different types of soft error events (e.g., i= SCU, MCU, SEL, SEFI, etc) that should not be mixed in the calculation.

6.1.5 Goal of test method – Changed reference level high-energy neutron flux above 10 MeV from NYC to a fixed number (3.596×10^{-3} cm^{-2} s^{-1} or 12.946 cm^{-2} h^{-1}). Details are covered in annex A.

6.3 Basic test methodology (JESD89A) - eliminated as redundant information that is covered in new section 3.5.1 Memory components

6.3 Angular Dependence Considerations – new section added based on learnings outlined in annex **A**

6.4 Basic test procedure (JESD89A) – eliminated as redundant information covered in **3**.

6.4.2 Beam Fluence – Examples added to help user determine how much fluence is needed to obtain desired soft error measurement accuracy.

6.4.3 Beam flux (JESD89A) – eliminated because guidelines for linearity are moved to **3** and different proton/neutron energies are covered in detail in **6.6.3**.

6.5.2.1 Monoenergetic proton beam: proton-induced soft error cross-sections at E_p – Notes added to alert user to proton energy loss in thick packages and loss of mono-energetic properties with beam degraders.

6.5.2.3 Quasi-monoenergetic neutron beam: neutron-induced SEU cross-sections at E_n - Figure 6.1 added as an example of quasi-monoenergetic neutron spectrum.

6.5.2.3.1 Iterative Unfolding Algorithm (New) – Algorithm equations added to calculate soft error cross section from quasi-monoenergetic neutrons.

6.5.2.3.2 Multiple Angle Neutron Irradiation (New) – Equation added to calculate soft error cross section from quasi-monoenergetic neutrons.

Annex H (informative) Differences between JESD89A and JESD89B (cont'd)

6.5.2.4 Spallation neutron beam: averaged neutron SEU cross-section over neutron spectrum – Figure 6.2 (formerly Figure. 6.1 in JESD89A) updated to include Chip IR and RCNP spectrum.

6.5.2.5 Complementing broad beam neutron soft error data – New section detailing technique used to develop correlation factor (CF) between broad spectrum neutron and monoenergetic proton soft errors.

6.5.3 Energy variation of soft error cross section – New Figure 6.4 (Figure 6.2 in JESD89A) added showing Weibull fit to SCU and SEL events.

6.5.4.2 Computation of fail rate from spallation soft error cross section - Integration of lower energy limit of beam fluence remains at 10 MeV for JESD89B even though iterature indicates finite neutron cross-section below 10MeV. However, errors introduced in acceleration factor due to mis-match of various spallation sources and the terrestrial neutron spectrum in the 1 – 10 MeV range would introduce larger errors [27].

6.6 Interferences - Scattering and secondary ion effects and thermal neutrons at the DUT – **7.4.5 Thermal neutron shielding -** moved from **7.7.5** (JESD89A) to **6.6** because it is applicable to high energy neutron sources that generate a large flux of thermal neutrons that can interfere with the soft error measurements.

6.7.1 Rate of errors in accelerated tests (JESD89A), 6.7.2 Generalized noise issues (JESD89A) and 6.7.3 Total dose (JESD89A) – removed as redundant and are included in **3** and annex G.

6.7.5 Proton range in thick packaging (JESD89A), 6.7.6 Single event latchup and single event functional interrupt (JESD89A) and 6.8 Final report (JESD89A) – these sections have been remove since they are redundant with **3** and annex G in JESD89B.

7 Accelerated thermal neutron test procedures

7.1.3 Safety Issues (JESD89A) – removed as redundant with **3**.

7.1.4 Guideline (JESD89A) – removed because **4**, **5** and **6** make it clear that complete soft error characterization requires various forms of alpha and neutron testing.

7.4.1 Thermal neutron source selection – Figure 7.1 added showing various thermal neutron sources. Cautions provided in using thermal neutron flux from high energy spallation sources.

7.4.4 Beam flux (JESD89A) - removed as redundant and are included in **3** and annex G.

7.4.5 Thermal neutron shielding (JESD89A) – moved to **6.6 Interferences - Scattering and secondary ion effects and thermal neutrons at the DUT.**

7.5 Basic test methodology (JESD89A) - eliminated as redundant information that is covered in new **3.5.1** Memory components.

Annex H (informative) Differences between JESD89A and JESD89B (cont'd)

7.5.2 Computation of fail rate from thermal neutron soft error cross section – JESD89B adds more proscriptive (and not relative) details on calculating and reporting of thermal neutron cross-section and soft error rate.

7.7 Interferences (JESD89A) – deleted as redundant to **3** and annex G.

Annex A - Determination of terrestrial neutron flux

Updated data to terrestrial neutron flux from JESD89A is insignificant (<2%). High energy and thermal neutron reference flux has moved from NYC to a fixed reference that will not change with shift magnetic pole. Information on angular distribution vs. neutron energy added to help user understand complex terrestrial neutron environment.

Annex D - The alpha particle environment

Figure D.2 change to log scale to help user visualize emission spectrum of ^{232}Th. Added Figure D.3 from surface emission of ^{210}Po.

Annex E – Neutron and proton test facilities

Updated to include new facilities and delete old facilities taken off line.

Annex F – Sources of measurement errors

New annex that details various sources of measurement errors.

Annex G - Recommendations for final report

New annex that consolidates recommendations for final report from **4**, **5**, **6** and **7**.

Annex J (informative) - Bibliographic References

[1] Seifert, N., and N. Tam, "Timing Vulnerability Factors of Sequentials", *IEEE Transactions on Device and Materials Reliability*, Vol. 4, No. 3, September 2004, pp. 516-522.

[2] Seifert, N., P. Shipley, M.D. Pant, V. Ambrose, and B.S. Gill, "Radiation-induced clock jitter and race". *41st Annual IEEE International Reliability Physics Symposium Proceedings*, 2005, pp. 215-222.

[3] Karnik, T., P. Hazucha, and J. Patel, "Characterization of soft errors caused by single event upsets in CMOS processes", Dependable and Secure Computing, *IEEE Transactions on Dependable and Secure Computing*, Vol. 1, No. 2, April-June 2004 pp.128–143.

[4] Gadlage, M.J.; R. D. Schrimpf, J. M, Benedetto, P.H. Eaton, and T. L. Turflinger, "Modeling and verification of single event transients in deep submicron technologies", *42nd Annual IEEE International Reliability Physics Symposium Proceedings*, 2004, pp. 673–674.

[5] Gill, B., N. Seifert and V. Zia, "Comparison of Alpha-particle and Neutron-induced Combinational and Sequential Logic Error Rates at the 32nm Technology Node", *Proceedings of the IEEE International Reliability Physics Symposium (IRPS)*, pp. 199-205, 2009.

[6] Mahatme, N. N., S. Jagannathan, T. D. Loveless, L. W. Massengill, B. L. Bhuva, S.-J. Wen, and R. Wong, "Comparison of combinational and sequential error rates for a deep submicron process," *IEEE Trans. Nucl. Sci.*, Vol. 58, No. 6, Dec. 2011, pp. 2719–2725.

[7] Narasimham, B., et al., "On-Chip Characterization of Single-Event Transient Pulsewidths", *IEEE Transactions on Device and Materials Reliability*, Vol. 6, No. 4, 2006, pp 542 – 549.

[8] Gill, Balkaran S., Chris Papachristou, Francis G. Wolff, Norbert Seifert, "Node sensitivity Analysis for Soft Errors in CMOS Logic", *IEEE International Test Conference*, Nov. 8, 2005, pp. 964-972.

[9] Zhu, Xiaowei Rob Baumann; Charles Pilch; Joe Zhou; Jason Jones; Claude Cirba, "Comparison of product failure rate to component soft error rate in a multi-core digital signal processor", *43nd Annual IEEE International Reliability Physics Symposium Proceedings*, April 2005, pp. 209-214.

[10] Autran, J. L., et al., Real-Time Soft-Error Testing of 40nm SRAMs, *IEEE International Reliability Physics Symposium*, 2012, pp 3C.5.1 - 3C.5.9).

[11] Wender, S. A., et al., "Neutron Beam Attenuation through Semiconductor Devices during SEU Testing", *57th Annual IEEE International Reliability Physics Symposium Proceedings*, April 2019, pp. 1–4.

[12] Wilkinson, J. D., et al, "Follow-up Multicenter Alpha Counting Comparison," *IEEE Trans. Nucl. Sci.*, vol 64, no. 4, pp 1516-1521, Aug 2014.

[13] McNally, B.D., et al., "Sources of Variability in Alpha Emissivity Measurements at LA and ULA Levels, a Multicenter Study", *Nucl. Inst. Meth in Phys. Res. A*, Vol 750, No. 21 June 2014 pp. 96-102.

[14] Tsoulfanidis, N., "Measurement and Detection of Radiation", second edition, Taylor & Francis 1995, pp. 273

[15] Baumann, R. C., Radaelli, D., "Determination of Geometry and Absorption Effects and Their Impact on the Accuracy of Alpha Particle Soft Error Rate Extrapolations", *IEEE Trans. Nucl. Sci.*, vol. 54, no.6, pp 2141-2148, Dec. 2007.

[16] https://www.srim.org

Annex J (informative) - Bibliographic References (cont'd)

[17] Tang, H. H. K., "Nuclear physics of cosmic ray interactions with semiconductor materials: Particle-induced soft errors from a physicist's perspective", *IBM J. Res. Develop*, Vol. 40, No. 1, pp. 91-108 (1996).

[18] Granlund, T., B. Granbom, and N. Olsson, "A Comparative Study Between Two Neutron Facilities Regarding SEU," *IEEE Trans. Nucl. Sci.*, Vol. 51,No. 5, OOctober 2004, p. 2922 – 2926.

[19] Lambert, D., et al., "Analysis of Quasi-monoenergetic neutron SEU cross sections for Terrestrial applications", *Proc. 2005 RADECS*, pp LN 5-1 to 5-6.

[20] Johansson, K., et al., "Energy-Resolved Neutron SEU Measurements from 22 to 160 MeV," *IEEE Trans. Nucl. Sci.*, Vol. 45, No. 6, Dec. 1998, pp. 2519-2526.

[21] IEC 62396 TS Ed. 1 (June, 2005), "PROCESS MANAGEMENT FOR AVIONICS INDUSTRY - Standard for the Accommodation of Atmospheric Radiation Effects via Single Event Effects within Avionics Electronic Equipment", International Electrotechnical Commission.

[22] Jahinuzzaman, S., N. Seifert, S. Sekwao, A. Neale; "On the Efficacy of Using Proton Beams For Estimating Neutron-Induced Soft Error Rates", in *Proc. IEEE Int. Rel. Phys. Symp.*, Monterey, CA, 2017, pp. SE-6.1-SE6.6.

[23] Seifert, N., et al., "Soft Error Susceptibilities of 22nm Tri-Gate Devices", *IEEE Trans. Nucl. Sci.*, vol. 59, no. 6, Dec. 2012, pp. 2666-2673.

[24] Lambert, D., et al., "Single Event Upsets Induced by a few MeV Neutrons in SRAMs and FPGAs", *IEEE Trans. Nucl. Sci., IEEE Radiation Effects Data Workshop (REDW)*, pp. 1-5, 2017.

[25] Alia, R. G., et. al., "SEL Hardness Assurance in a Mixed Radiation Field", *IEEE Trans. Nucl. Sci.*, Vol. 62, No. 6, Dec. 2015, pp.2555-2562.

[26] Petersen, E. L., et al., "Rate Prediction for Single Event Effects", *IEEE Trans. Nucl. Sci*., TNS-39, p. 1577 (1992).

[27] Quinn, H., et al., "The Effect of 1-10 MeV Neutrons on the JESD89 Test Standard", *IEEE Trans. Nucl. Sci.*, Vol. 66, No. 1, Jan. 2019,pp. 140 -147.

[28] IEC62396 TS "PROCESS MANAGEMENT FOR AVIONICS INDUSTRY – Standard for the accommodation of Atmospheric Radiation Effects via Single Event Effects within Avionics Electronic Equipment," International Electrotechnical Commission, 2005.

[29] Fleischer,R., "Cosmic ray interactions with boron: a possible source of soft errors" *IEEE Trans. Nucl. Sci.*, 30(5), p. 4013, Oct. 1983.

[30] Oldham, T. R., S. Murrill, and C.T. Self, "Single Event Upset of VLSI Memory Circuits Induced by Thermal Neutrons", HEART Conf., 1986.

[31] Knoll, Glen E., *Radiation Detection and Measurement*, Third Edition, ISBN: 0471073385.

[32] Fang, Y. P. and A. S. Oates, "Thermal Neutron-Induced Soft Errors in Advanced Memory and Logic Devices", *IEEE Trans Dev and Matl. Rel*., Vol. 14, No. 1, Mar 2014, pp 583-586.

[33] Baumann R. C. and E. B. Smith, "Neutron-induced 10B fission as a major source of soft errors in high density SRAMs," Elsevier Microelec. Reliability, vol. 41, no. 2, p.211, 2001.

[34] Gordon, M. S., P. Goldhagen, K. P. Rodbell, T. H. Zabel, H. H. K. Tang, J. M. Clem, and P. Bailey, "Measurement of the Flux and Energy Spectrum of Cosmic-Ray Induced Neutrons on the Ground," IEEE Transactions on Nuclear Science, vol. 51, no. 6, pp. 3427-3434, Dec. 2004.

Annex J (informative) - Bibliographic References (cont'd)

[35] Goldhagen,, P., "An Extended-Range Multisphere Neutron Spectrometer with High Sensitivity and Improved Resolution," *Nucl. Technol.* 175, pp. 81-88 (2011).

[36] Smart, D. F., and M. A. Shea, "Final Report: Vertical Geomagnetic Cutoff Rigidities for Epoch 2010" and "Table from IGRF 2010 field," Appendices A and G in K. Copeland, *CARI-7 Documentation: Geomagnetic Cutoff Rigidity Calculations and Tables for 1965-2010*, Federal Aviation Administration Office of Aerospace Medicine Report DOT/FAA/AM-19/4 (2019), https://www.faa.gov/data_research/research/med_humanfacs/oamtechreports/2010s/media/201904.pdf (in press).

[37] J. Clem and L. Dorman, "Neutron monitor response functions," *Space Sci. Rev.*, vol. 93, no. 1-2, pp. 335-363, 2000, and references therein.

[38] Belov, A., A. Struminsky, and V. Yanke, "Neutron Monitor Response Functions for Galactic and Solar Cosmic Rays", *1999 ISSI Workshop on Cosmic Rays and Earth*, poster presentation.

[39] Dirk, Lt. J. D., M. E. Nelson, J. F. Ziegler, A. Thompson and T. H. Zabel, "Terrestrial Thermal Neutrons", *IEEE Trans. Nucl. Sci*., vol. 50, no. 6., pp. 2060-2064, Dec. 2003.

[40] McKinney, G. W., H. J. Armstrong, M. R. James, J. M. Clem, and P. Goldhagen, "MCNP6 Cosmic-Source Option," Los Alamos National Laboratory Report LA-UR-12-00196 (2012), available at https://mcnp.lanl.gov/pdf_files/la-ur-12-00196.pdf .

[41] McMath, G. E., G. W. McKinney, and T. A. Wilcox, "MCNP6 Cosmic & Terrestrial Background Particle Fluxes – Release 4," Los Alamos National Laboratory Report LA-UR-14-20090 (2014), available at https://mcnp.lanl.gov/pdf_files/la-ur-14-20090.pdf .

[42] https://mcnp.lanl.gov/

[43] http://www.fluka.org/fluka.php

[44] https://geant4.web.cern.ch/

[45] https://phits.jaea.go.jp/

[46] Kaouache, A., et. al., "An Analytical Model to Quantify Decay Chain Disequilibrium–Application to the Thorium Decay Chain", *IEEE Trans Nucl Sci*., Vol. 61, No. 3, Jun 2014, pp 1414-1419.]

[47] Ziegler, J. F., et al., "IBM experiments in soft fails in computer electronics (1978-1994)", *IBM J. Res. Develop.*, Vol. 40, No. 1, Jan, 1996, pp 3-18.

Standard Improvement Form **JEDEC** _____

The purpose of this form is to provide the Technical Committees of JEDEC with input from the industry regarding usage of the subject standard. Individuals or companies are invited to submit comments to JEDEC. All comments will be collected and dispersed to the appropriate committee(s).

If you can provide input, please complete this form and return to:

JEDEC
Attn: Publications Department
3103 North 10th stree, Suite 240
Arlington, VA 22201

Fax: 703.907.7583

1. I recommend changes to the following:

☐ Requirement, clause number _____

☐ Test method number _____ Clause number _____

The referenced clause number has proven to be:

☐ Unclear ☐ Too Rigid ☐ In Error

☐ Other _____

2. Recommendations for correction:

_____

_____

_____

_____

3. Other suggestions for document improvement:

_____

_____

_____

_____

Submitted by

Name: _____ Phone: _____

Company: _____ E-mail: _____

Address: _____

City/State/Zip: _____ Date: _____


JEDEC®